ROLE OF RENAL LYMPHATICS IN BLOOD PRESSURE REGULATION DURING HYPERTENSION

A Dissertation

by

DAKSHNAPRIYA BALASUBBRAMANIAN

Submitted to the Office of Graduate and Professional Studies of
Texas A&M University
in partial fulfillment of the requirements for the degree of

DOCTOR OF PHILOSOPHY

Chair of Committee, Brett M. Mitchell
Co-Chair of Committee, Joseph M. Rutkowski
Committee Members, Mariappan Muthuchamy
Cristine L. Heaps
Head of Program, Carol Vargas

May 2020

Major Subject: Medical Sciences

ABSTRACT

Hypertension is the leading contributor for all-cause mortality and morbidity worldwide and is a major risk factor for cardiovascular diseases, stroke, chronic kidney disease, and cognitive impairment. Renal immune cell infiltration and inflammation are well known to contribute to the pathogenesis of hypertension. The lymphatic system plays a crucial role in maintaining body fluid homeostasis and governs immune responses. However, the involvement of the renal lymphatic system in renal inflammation during hypertension is unknown. In the present study, we asked whether renal lymphatic vessels are altered during angiotensin II-induced hypertension. We hypothesized that renal lymphatic vessel density will be increased in angiotensin II-induced hypertension. To test our hypothesis, we investigated male and female mice with angiotensin II-induced hypertension. Results demonstrate that renal lymphatic vessel density is increased in male and female mice with angiotensin II-induced hypertension in association with renal inflammation. Our results also demonstrate that genetic augmentation of renal lymphatic vessel density reduces renal immune cell accumulation and prevents the development of angiotensin II-induced hypertension in male and female mice. Results from our *in vitro* studies demonstrate that angiotensin II activates immune cells to secrete lymphangiogenic and pro-inflammatory factors that exert proliferative and inflammatory effects on lymphatic endothelial cells. Using a nitric oxide inhibition-induced model of hypertension, we demonstrate that therapeutic augmentation of

renal lymphatic expansion after hypertension is established attenuates blood pressure. Importantly, we demonstrate that this reduction in blood pressure was not associated with a reduction in renal immune cell accumulation, but was associated with increased natriuresis. A chronic high salt diet also induced an enhanced natriuretic response and lowered blood pressure in mice with augmented renal lymphatic vessel density. Our results thus establish a novel role for renal lymphatics in sodium homeostasis and blood pressure regulation during conditions of sodium retention such as hypertension and chronic high salt intake. Therapeutic renal lymphatic expansion also attenuated blood pressure in mice with angiotensin II-dependent and salt-sensitive hypertension. Thus, this study demonstrates the role of renal lymphatic vessels in blood pressure regulation and highlights the novel therapeutic potential of renal lymphatic vessels in controlling blood pressure during hypertension.

DEDICATION

This dissertation is dedicated to my family, who have been my support throughout. I express my deepest gratitude and love for my parents, Balasubramanian and Devi, and my husband, Avinash. It is with their unconditional support that I have been able to make progress in my career and my life, and I am forever indebted to them.

ACKNOWLEDGEMENTS

I would like to acknowledge my mentor and chair of my committee, Dr. Brett Mitchell, for his invaluable guidance and support. He has supported me through my tough phase of transition, and has helped me establish a professional career. Apart from inculcating the skills needed to do good research, Dr. Mitchell has trained me in manuscript writing, conference presentations, and mentoring trainees, and has always prioritized my professional advancement. In the short period of time that I spent in his lab, Dr. Mitchell has been very thoughtful in training me for a successful professional career, and I express my deepest gratitude for all his guidance, for they will follow me always.

I would also like to acknowledge the co-chair of my committee, Dr. Joseph Rutkowski for his extraordinary guidance throughout my time in the lab. Dr. Rutkowski has given me the opportunity to learn several things from him, and has never shied away from helping trainees and offering them professional advice. I thank Dr. Rutkowski for his time spent in conversations, and they have been immensely helpful, motivating, and thought-provoking. I am extremely grateful for all the knowledge and training poured into me for they will guide me always.

I would like to thank members of my committee, Dr. Mariappan Muthuchamy and Dr. Cristine Heaps. Since my transition into the lab, they have been extremely understanding of my situation, and have been very supportive and encouraging. I thank them for the constructive feedback they have offered over the years, and hope to inculcate the skills I learnt from them in my career.

Finally, I would like to thank my co-workers Catalina Lopez-Gelston, Andrea Reyna, and Bethany Goodlett for their immense help, patience, and encouragement, which I deeply appreciate. I also thank all members of the department of Medical Physiology for their kind support.

CONTRIBUTORS AND FUNDING SOURCES

It is with deep gratitude and appreciation that I acknowledge the professional guidance of my committee chair Dr. Brett Mitchell, and co-chair Dr. Joseph Rutkowski. I would also like to extend my thanks to members of my dissertation committee, Dr. Mariappan Muthuchamy and Dr. Cristine Heaps. I also thank the Department of Medical Physiology, and the College of Medicine at Texas A&M Health Science Center for supporting my work.

This work was supported by my American Heart Association Predoctoral Fellowship (18PRE33990461), an American Heart Association Transformational Project Award (18TPA34170266) and a National Institute of Diabetes and Digestive and Kidney Diseases Grant (DK120493) to Dr. Brett Mitchell, and an American Heart Association Grant in Aid (17GRNT33671220) to Dr. Joseph Rutkowski.

NOMENCLATURE

A2HTN: Angiotensin II-induced hypertension

ACE: Angiotensin converting enzyme

AGTR: Angiotensin receptor

ANG II: Angiotensin II

ANP: Atrial natriuretic peptide

BP: Blood pressure

CCL19: Chemokine ligand 19

CCL21: Chemokine ligand 21

CCR7: C-C chemokine receptor type 7

Cdh16: Cadherin 16

ClCr: Creatinine clearance

CM: Conditioned media

CXCL10: C-X-C motif chemokine 10

DC: Dendritic cell

DOX: Doxycycline

ENaC: Epithelial Na_+ channel

FENA: Fractional excretion of Na_+

Fn1: Fibronectin

GFR: Glomerular filtration rate

ICAM-1: Intercellular adhesion molecule 1

IFNY: Interferon gamma

IL-1β: Interleukin 1 beta

IL-6: Interleukin 6

IL-17: Interleukin 17

KidVD: Kidney-specific overexpression of VEGF-D

KSP: Kidney specific protein

L-NAME: L-nitro-arginine methyl ester

Lcn2: Lipocalin 2

LEC: Lymphatic endothelial cell

LYVE-1: Lymphatic endothelial hyaluronan receptor-1

Mcp1: Monocyte chemoattractant protein-1

NCC: Sodium-chloride cotransporter

NHE3: Sodium-hydrogen exchanger 3

NKCC2: Sodium-potassium-chloride cotransporter 2

NO: Nitric oxide

NOS: Nitric oxide synthase

Pdpn: Podoplanin

RAS: Renin-angiotensin system

ROS: Reactive oxygen species

rtTA: reverse tetracycline-controlled transactivator

SBP: Systolic blood pressure

SHR: Spontaneously hypertensive rat

TGFß: Transforming growth factor beta

Th17: T helper 17

TNFα: Tumor necrosis factor alpha

VCAM-1: Vascular cell adhesion molecule 1

VEGF: Vascular endothelial growth factor

VEGFR: Vascular endothelial growth factor receptor

TABLE OF CONTENTS

Page

LIST OF FIGURES

LIST OF TABLES

TABLE Page

1. INTRODUCTION AND LITERATURE REVIEW*

1.1 Hypertension

An increasing prevalence of hypertension in children and adults is a significant public health issue. A major concern in hypertensive disease, and what makes its investigation necessary, is target organ damage. Hypertension actively contributes to the development of heart, kidney, brain, eye, and peripheral vascular diseases. Endothelial cell activation by inflammatory factors and attenuated endothelium-dependent vasodilation are underlying events in the pathogenesis of hypertension (Sprague and Khalil, 2009) . Blood vessels undergo remodeling wherein the lumen diameter decreases and the ratio of medial to intimal thickness increases. Chronic hypertension increases the workload on the heart, which eventually undergoes hypertrophy and fibrosis leading to increased wall stiffness and dysfunction (Drazner, 2011). The systemic elevated blood pressure load eventually reaches the renal microvasculature leading to nephrosclerosis and renal damage. Changes in the microvascular structure of the cerebral circulation are associated with an increased risk for death, ischemic stroke, and cognitive decline (Gąsecki et al., 2013).

1.2 Angiotensin II-induced hypertension

The renin-angiotensin-system (RAS) is implicated in the pathogenesis of over 70% of patients with essential hypertension. Angiotensin II is the main effector molecule of the RAS. It is an octapeptide generated from its substrate angiotensinogen through a series of enzymatic cleavages. Angiotensinogen is produced mainly from the liver, which is cleaved by renin produced from the kidney to generate angiotensin I. Angiotensin converting enzyme (ACE) then acts on angiotensin I and converts it into angiotensin II. Other enzymes such as chymase can also produce angiotensin II from angiotensin I. Angiotensin II can be further cleaved by ACE2 to generate angiotensin 1-7. Angiotensin II exerts its actions by binding to one of two G-protein coupled receptors, angiotensin II receptor type 1 (AT1R) and type 2 (AT2R). AT1R is present in several tissues including vascular smooth muscle, heart, brain, kidney, adrenal gland, and adipose tissue. AT2R is present mainly in fetal tissues and decreased through development, and its expression in adults is confined mainly to the heart, blood vessels, kidney and liver. Most of the hypertensive actions of angiotensin II are induced by its actions through AT1R, whereas, at the tissue level AT2R opposes the actions of AT1R. For example, angiotensin II binding through AT1R induces vasoconstriction, cardiac hypertrophy, fibrosis, and inflammation, whereas signaling through AT2R induces vasodilation, is anti-fibrotic, and anti-inflammatory (Forrester et al., 2018). In addition to these peptides and receptors, more recent research has identified novel members of the angiotensin signaling

pathway, including angiotensin 1-7, which exerts its action by binding to the G-protein coupled receptor Mas, and is primarily antagonistic to signaling through AT1R (Karnik et al., 2017) (Fig 1.1).

Figure 1.1 Angiotensin peptides and receptors in RAS signaling. Angiotensin I is cleaved by angiotensin converting enzyme (ACE) to angiotensin II that can bind both AT1R and AT2R. Angiotensin I can also be cleaved into angiotensin (1–9) which can bind to AT2R. Angiotensin II can further diverge into either angiotensin (1–7) through ACE 2 or angiotensin III through an aminopeptidase. Angiotensin (1–7) has been identified to bind to AT2R, Mas receptor, and the MrgD receptor. Angiotensin (1–7) can also form alamandine that binds to the MrgD receptor. Angiotensin III binds to AT1R and AT2R. Angiotensin III can be further cleaved into angiotensin IV that binds to AT4R. Figure adapted from (Forrester et al., 2018).

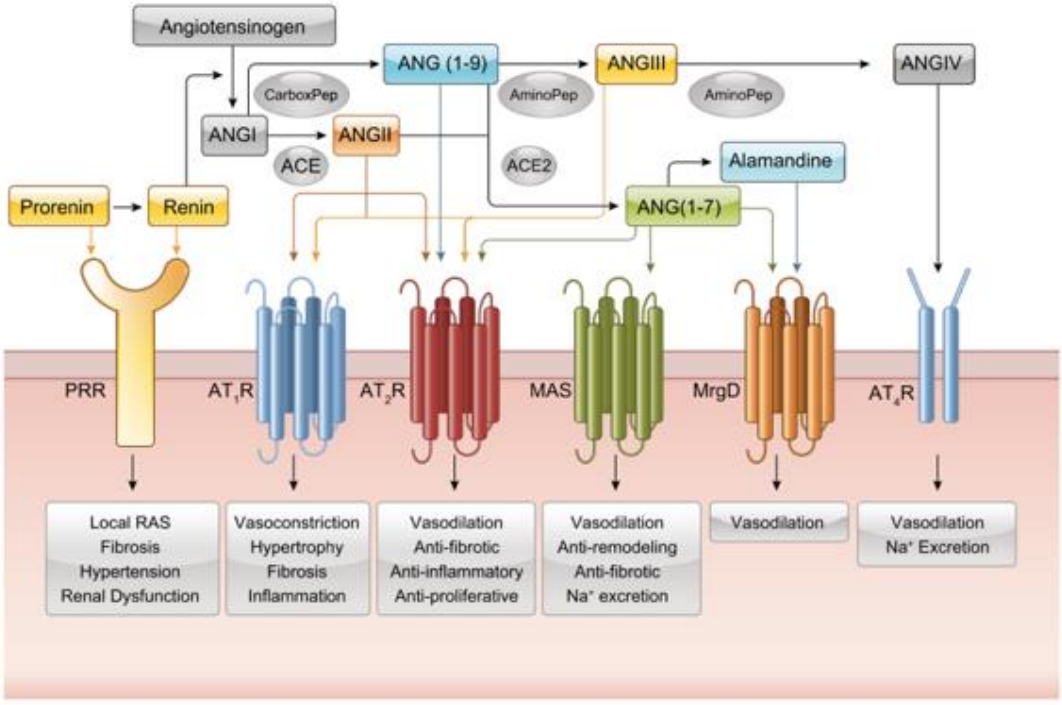

The renal control of sodium and water excretion by angiotensin II is critical to the regulation of salt and water balance, and hence blood pressure; dysregulation of RAS signaling, particularly within the kidney, thus disrupts this

balance and leads to the development of hypertension (Crowley and Coffman, 2014; Sparks et al., 2014). Within the kidney, angiotensin receptors are expressed in majority of cell types, including the blood vessels, as well as in the podocytes and mesangial cells of the glomerulus, and tubular epithelial cells and hence exert a broad impact on renal function. Angiotensin II induces vasoconstriction of the afferent and efferent arteriole, thus reducing renal blood flow and favoring sodium reabsorption. By binding to AT1R within the adrenal gland, angiotensin II stimulates aldosterone secretion that further promotes sodium reabsorption. Angiotensin II also directly stimulates sodium and water reabsorption in several parts of the nephron. Within the proximal tubule, the actions of angiotensin II have been long-recognized to induce trafficking and activation of various sodium transporters, including sodium hydrogen ion exchanger 3 (NHE3) and sodium phosphate co-transporter 2 (NaPi2) (Riquier-Brison et al., 2010). Consistent with these studies, cell-specific deletion of AT1R from the proximal tubule lowers blood pressure at baseline and attenuates angiotensin II-induced hypertension (Gurley et al., 2011). Within the thick ascending limb, angiotensin II increases renal phosphorylation of sodium/potassium/chloride co-transporter 2 (NKCC2) and STE20/SPS1-related, proline alanine-rich kinase (SPAK), thus increasing sodium reabsorption (Kamat et al., 2015). In general, lysine deficient protein kinases (WNK) participate in the molecular pathway involving angiotensin II and aldosterone in renal sodium and potassium transport, and angiotensin II activates or prevents the degradation of WNK kinases (Shibata et al., 2014). In the distal

convoluted tubule, angiotensin II promotes sodium chloride co-transporter (NCC)-dependent sodium transport through WNK4 and SPAK/OSR-1 dependent signaling. Within the collecting duct, epithelial sodium channel (ENaC) is activated by angiotensin II and aldosterone (Mamenko et al., 2013). In addition to such direct mechanisms, indirect mechanisms also contribute to increased sodium reabsorption. For example, interleukin 1 (IL-1) receptor activation during angiotensin II-induced hypertension augments NKCC2 activity and hypertension. Besides its role in blood pressure regulation, angiotensin II exerts pro-inflammatory and pro-fibrotic effects within the kidney, and through these actions, angiotensin II significantly contributes to the progression of chronic kidney injury and end-stage renal disease. Angiotensin II signaling via the TGFβ pathway, which leads to epithelial-mesenchymal cell transition, primarily contributes to renal fibrosis, as with vascular and cardiac fibrosis. Angiotensin II-induced fibrosis is also mediated through CTGF, COX-2, osteopontin, and various inflammatory mediators such as IL-6, VCAM-1, and TNFα. These mediators induce the synthesis of extracellular matrix proteins, thus promoting renal fibrosis (Forrester et al., 2018).

An important concept regarding the actions of the RAS is the existence of a tissue RAS. Several tissues including the kidney and brain express all components necessary for the local synthesis of angiotensin II. The role of intrarenal RAS in hypertension has been particularly investigated in great detail. The levels of angiotensin II peptides in the kidney and the proximal tubular fluid

compartment are much higher than in the plasma, suggesting that angiotensin II might be produced intracellularly and released into the proximal tubular fluid (Navar, 2014). The role of the intrarenal RAS in blood pressure regulation has been demonstrated by studies utilizing knockout mouse models of RAS components. Studies using cross-transplantation of kidneys between wild-type and global AT1 knock-out mice revealed the importance of AT1 receptors in the kidney for the development of hypertension and cardiac hypertrophy in response to angiotensin II infusion (Crowley et al., 2005). In ACE 2/2 mutant mice, where circulating ACE levels are elevated but renal ACE levels are reduced, basal blood pressure was significantly lower. Renal ACE has also been shown to be required for the development of angiotensin II-induced, L-NAME-induced, and salt-sensitive hypertension, and mice lacking renal ACE have significantly blunted hypertension (Gonzalez-Villalobos et al., 2013; Giani et al., 2014a, 2015a). More recently, the functional consequences of intracellular angiotensin II in hypertension have been investigated. Several studies have reported the direct effects of intracellular angiotensin II in cultured vascular smooth muscle cells, proximal tubular cells, and freshly isolated renal cortical nuclei. In cultured smooth muscle cells, direct injection of angiotensin II induced cytosolic and/or nuclear calcium mobilization (Zhuo et al., 2006). In freshly isolated renal cortical nuclei, angiotensin II directly stimulated NHE3, TGFß and MCP-1 (Li and Zhuo, 2008). Furthermore, overexpression of angiotensin II fusion protein increased NHE3 expression in proximal tubular cells (Li et al., 2012). Together, these studies

suggest that intracellular angiotensin II contribute to cardiovascular and renal pathology and hypertension (Li et al., 2018).

In addition to the central role of the renal RAS in the development of hypertension, vascular and cardiac RAS dysregulation also contribute significantly to the pathogenesis of hypertension. Within the vascular system angiotensin II, through its AT1R receptor, induces vasoconstriction, endothelial dysfunction, inflammation, remodeling, and proliferation. Angiotensin II signaling activates G protein-coupled pathways which converge in myosin light chain (MLC) phosphorylation leading to vasoconstriction. Angiotensin II also increases vascular expression of Ca2+ channel subunits. Angiotensin II increases NADPH oxidase activity within the vessel wall and induces the production of reactive oxygen species (ROS) including superoxide and hydrogen peroxide. These ROS in turn activate multiple signaling pathways involving MAPK, tyrosine kinases, calcium channels, and redox-sensitive transcription factors, culminating in vasoconstriction, cell proliferation, expression of pro-inflammatory genes, and synthesis of extracellular matrix proteins. Through the excess production of collagen and other extracellular matrix proteins, angiotensin II can stimulate vascular fibrosis. In endothelial cells, angiotensin II activates the NF-kB cascade and induces the expression of endothelial adhesion molecules including P-selectins, ICAM-1, VCAM-1, and integrins. Angiotensin II also activates toll-like receptor signaling in vascular smooth muscle cells that induces oxidative damage and inflammation (Benigni et al., 2010; Giani et al., 2014b; Carey, 2015;

Nishiyama and Kobori, 2018). Vascular AT1R receptors were also recently shown to regulate renal blood flow and urinary sodium excretion (Sparks et al., 2015). Angiotensin II signaling within the heart also induces cardiac hypertrophy and fibrosis.

Within the central nervous system (CNS), the brain RAS regulates blood pressure through its effects on the sympathetic nervous system and fluid homeostasis. AT1R is highly expressed in neurons of many nuclei regulating fluid intake and blood pressure. Among these, the subfornical organ (SFO) has long been known to be critical in blood pressure regulation. Deletion of AT1R in the SFO blunts the pressor response induced by a DOCA-salt challenge. However, the selective activation of angiotensin II production in the SFO is insufficient to increase blood pressure. AT1R-expressing astrocytes have also been identified in mediating an increase in BP by inducing sympathoexcitation. Within the brain, angiotensin II induces the production of ROS and oxidative stress, endoplasmic reticular stress, and inflammation, all of which contribute to hypertension. Angiotensin II-induced NF-kB transcription and cytokine production have been strongly linked to inflammation in the microglial cells within the brain (Shi et al., 2010).

1.3 Salt-sensitive hypertension

The basic renal-body fluid feedback control mechanism of BP regulation was proposed by Guyton and Coleman in the 1960s and dictates that the extracellular fluid volume (ECFV) is determined by the balance between intake

and renal excretion of sodium and water. An increased salt intake, for example, increases ECFV and eventually blood volume, leading to an increase in cardiac output. An increase in cardiac output leads an increase in arterial pressure, and this increase in blood pressure increases sodium excretion, a phenomenon termed pressure-natriuresis. When BP increases, sodium excretion increases and this reduces ECFV until blood pressure normalizes. The pressure-natriuresis feedback control plays a dominant role in long-term blood pressure regulation, and in several models of chronic hypertension, the pressure-natriuresis curve is shifted to the right, requiring a higher blood pressure to achieve sodium excretion. In salt-resistant subjects, multiple renal and neurohumoral adjustments permit increased salt excretion during increased salt intake with minimal changes in blood pressure. However, in salt-sensitive subjects, an elevated blood pressure is required to maintain increased salt excretion to match sodium intake through pressure-natriuresis (Hall, 2016).

Given the central role of renal sodium excretion in blood pressure regulation, disturbances that reduce the kidney's ability to excrete sodium increase blood pressure and could lead to the development of salt-sensitive hypertension. Intrarenal factors such as a reduction in glomerular filtration or increased tubular reabsorption could decrease sodium excretion. Studies have demonstrated that the local RAS in the kidney was augmented by salt loading in Dahl salt sensitive rats, despite reduction in circulating RAS components, but was unchanged in Dahl resistant rats (Kobori et al., 2003). Hence, an inappropriate

Figure 1.2 Renal body-fluid feedback regulation: Basic renal–body fluid feedback mechanism for long-term blood pressure regulation. Renal pressure-natriuresis is characterized by the effect of arterial pressure on urinary sodium excretion. The dashed pressure-natriuresis indicate impaired pressure-natriuresis during hypertension. Increased arterial pressure may cause secondary increases in total peripheral resistance via pressure- or flow-dependent autoregulation in various tissues. Figure adapted from (Hall, 2016).

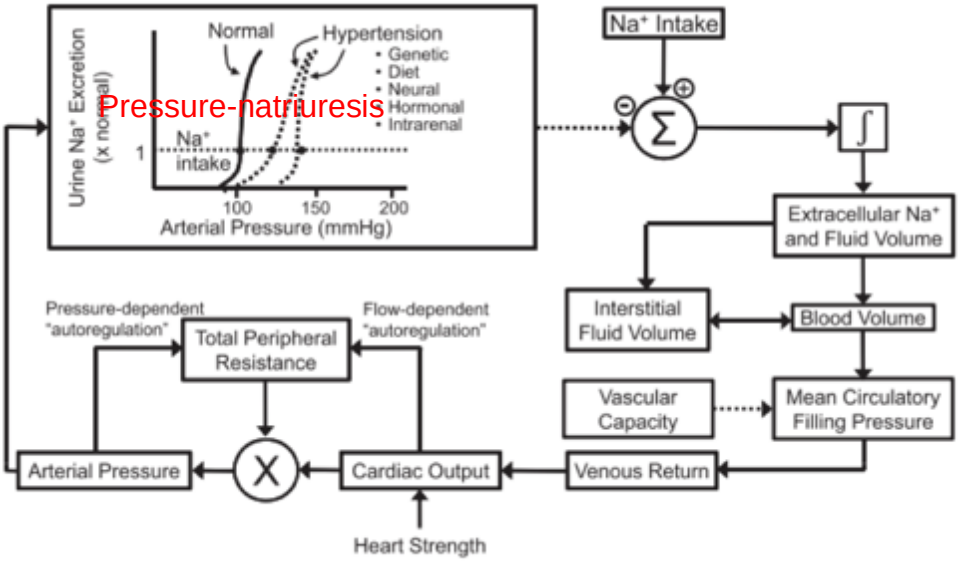

increase in renal angiotensin II on a high-salt diet may contribute to the development of salt-sensitive hypertension in Dahl salt sensitive rats. Increased salt intake increases sympathetic nervous system (SNS) activity especially in the kidney, and salt sensitive hypertension patients have increased levels of plasma norepinephrine (Gill et al., 1988). Increased renal sympathetic nerve activity could lead to increased renin secretion, increased tubular reabsorption, and reduced renal blood flow, all of which contribute to decreased sodium excretion. Another mechanism by which salt induces hypertension might be through the activation of immune cells. Several reports suggest that salt drives inflammation; sodium accumulates in cutaneous wounds and drives macrophage activation to facilitate

wound healing (Jantsch et al., 2015). Mouse and human macrophages cultured in an additional 51mM NaCl produced more inflammatory and less anti-inflammatory cytokines than macrophages cultured in normal salt (Zhang et al., 2015). Besides macrophages, circulating monocytes are increased in patients on a high salt diet of 12g/day (Yi et al., 2015). Moreover, an increase in inflammatory cytokines such as IL-6 and IL-23 and a decrease in the anti-inflammatory cytokine IL-10 was observed in the blood of patients fed a high-salt diet. Salt could also amplify T helper 17 (Th17) cell polarization and pro-inflammatory interleukin-17 (IL-17) production. Thus high-salt microenvironments in hypertension can lead to activation of T cells, macrophages, and dendritic cells and lead to renal and vascular inflammation (Foss et al., 2017). Salt is also proposed to act via endothelial specific mechanisms leading to endothelial inflammation. Increased salt intake leads to expansion of extracellular fluid (ECF) volume, leading to increased cardiac output. The endothelium responds by releasing nitric oxide (NO) and leading to overall vasodilation. A decrease in renal vascular resistance facilitates natriuresis and lowers blood pressure. However, increased salt intake also promotes the production of vascular TGFß that inhibits NO by increasing endothelial NADPH oxidase 4 (NOX4). Thus, NO bioavailability is reduced and blood pressure is increased (Feng et al., 2017). In addition to the above-mentioned mechanism of blood pressure regulation, studies by Titze and colleagues have shown that skin and skeletal muscles of hypertensive patients are involved in sodium storage more so than the plasma, and that blood pressure

correlates with skin and muscle sodium storage in humans (Nikpey et al., 2017; Wiig et al., 2018). Thus, extra-renal mechanisms of sodium storage exist and are under study.

1.4 Nitric oxide-inhibition-induced hypertension

The discovery in 1987 that endothelium-derived NO mediates the vasodilatory effect of certain endothelium-dependent agonists inaugurated the current field of NO biology. It is now recognized that NO plays essential roles in many diverse physiological processes and in some pathophysiologic events. NO exerts a tonic influence mainly on the renal medullary circulation. Acute systemic NO synthase (NOS) inhibition induces severe renal vasoconstriction along with marked reduction of renal blood flow and a reduction in glomerular filtration rate (GFR). NO is also an important contributor to tubuloglomerular feedback (TGF) responses. NO attenuates the afferent arteriole constriction induced by TGF. NO also affects tubular sodium transport by regulating sodium transporters within the nephron, and also by mediating pressure-induced natriuresis (Majid, 2002). The acute withdrawal of the tonic vasodilatory effect of NO could be responsible for acute hypertension, however, chronic hypertension might not be maintained solely because of the inactivation of the NO pathway. There is now considerable evidence that both angiotensin II and the SNS contribute to the hypertension induced by chronic NOS inhibition. Ribeiro et al showed that concomitant chronic administration of the angiotensin II receptor antagonist losartan to rats chronically treated with the nitric oxide synthase inhibitor, L-nitro-arginine methyl ester (L-

NAME), prevented both the hypertension and the renal injury associated with this model, suggesting a key participation of the RAS in these events (Ribeiro et al., 1992). Renal ACE was shown to be necessary for mediating the hypertensive effects of NOS inhibition (Giani et al., 2014a). Increased central sympathetic drive may be involved in chronic NOS inhibition induced hypertension, as sympathectomy by daily injections of ganglionic blockers attenuated L-NAME induced hypertension (Sander et al., 1995). The level of dietary salt intake also profoundly influences the severity of L-NAME hypertension. Administration of a high-salt diet to rats on chronic L-NAME treatment aggravated the hypertension and renal injury. Conversely, restricting dietary salt intake prevented the development of L-NAME hypertension (Jover and Mimran, 2001; Evans et al., 2005).

Over the years a better understanding of the pathophysiology of hypertensive end-organ damage has been attained which aids the design of better therapeutics. However, the incidence of hypertension continues to rise globally, indicating the need to revisit current treatment options. Hypertension and cardiovascular disease have gained appreciation as a low-grade inflammatory disease and studies on human hypertension support this association (Solak et al., 2016). Aberrant immune system activation and inflammation is now recognized to have a mechanistic role in the progression of hypertension and should pave the way for designing more effective therapeutics to attenuate end-organ damage in hypertensive patients (Miguel et al., 2011; Lopez Gelston and Mitchell, 2017).

1.5 Immune system activation in hypertension

The contribution of both the innate and adaptive immune systems in the pathogenesis of hypertension has been recognized for the past 50 years. Pioneering studies by Grollman and White showed that immunosuppression blunted hypertension in rats with partial renal infarction (White and Grollman, 1964),(Okuda and Grollman, 1967) and that the transfer of lymphocytes from lymph nodes of rats with renal infarction triggered the elevation of blood pressure in normal recipient rats (Okuda and Grollman, 1967). Subsequently, studies by Finn Olsen in 1970 reported the presence of inflammatory cells in the vasculature of angiotensin II-infused rats (Olsen, 1970). In another study, it was demonstrated that thymectiomized or athymic nude mice with renal infarction did not maintain hypertension (Svendsen, 1976). Transplant of the thymus from Wistar-Kyoto rats to Spontaneously Hypertensive Rats (SHRs) lowered blood pressure (Bendich et al., 1981), and similar results were obtained by treatment with anti-thymocyte drugs or the immunosuppressive drug cyclophosphamide (Dzielak, 1991). Studies also demonstrated that transfer of splenocytes from deoxycorticosterone acetate (DOCA)-salt hypertensive rats to normal recipient rats triggered hypertensive responses in the recipient rats (Olsen, 1980).

Following evidence of immune system activation in hypertension, immunosuppression became a popular tool of choice to lower blood pressure in experimental models of hypertension. Administration of the immunosuppressive agent mycophenolate mofetil blunts the development of several forms of

hypertension including salt-induced hypertension after angiotensin II infusion (Turbe, 2001), SHRs (Rodriguez-Iturbe et al., 2002), salt-induced hypertension after NOS inhibition (Quiroz et al., 2001), Dahl salt-sensitive rats (Mattson et al., 2006), and in hypertensive patients (Herrera et al., 2006). All of these studies had demonstrated renal injury associated with increased blood pressure, and treatments that reduced renal inflammation and injury lowered blood pressure.

Inflammation in the cardiovascular system and the brain are also important events that contribute to the pathogenesis of hypertension. Immune cells accumulate in the adventitia and perivascular adipose tissue (PVAT) of the larger vessels and of the smaller resistance vessels during hypertension. PVAT can then release factors that modulate the tone of these vessels and can also secrete factors leading to inflammation (Guzik et al., 2007). Several forms of hypertension are associated with increased vascular wall expression of chemokines like MCP-1 and adhesion molecules including VCAM-1 and ICAM-1 (Ebrahimian et al., 2011). Another important target of activated immune cells in hypertension is the heart. Activation of T cells found in the heart of angiotensin II infused hypertensive mice caused cardiac inflammation, hypertrophy, and fibrosis (Kvakan et al., 2009). Blood pressure regulation is also governed by central mechanisms, in part, through innervation of the blood vessels and the kidney. Strong evidence for the involvement of the CNS is demonstrated by the study showing that renal denervation abrogates hypertension in humans (Schlaich et al., 2009). Intra-cerebroventricular administration of the anti-inflammatory antibiotic minocycline

reduces levels of TNFα, IL-1ß, and IL-6 in the paraventricular nucleus and reduced angiotensin II-dependent hypertension (Shi et al., 2010).

The immune system involves both the innate immune system consisting of macrophages, DCs, mast cells, granulocytes, and others, and the adaptive immune system consisting of T and B lymphocytes. Components from both classes of the immune system are implicated in hypertension (Norlander et al., 2018). In 2007, Guzik et al (Guzik et al., 2007) conducted a study that dissected the role of T and B lymphocytes in hypertension. They demonstrated that angiotensin II-induced hypertension was blunted in Rag1 -/- mice that are deficient in T and B lymphocytes. Vascular superoxide production and endothelial dysfunction were also blunted in these mice. Adoptive transfer of T but not B lymphocytes restored hypertension, indicating the importance of T cells in the maintenance of hypertension. T cells are required for the development of DOCA salt-induced and norepinephrine-induced hypertension (Marvar et al., 2010). Similarly, Crowley et al demonstrated that severe combined immune deficiency (SCID) mice deficient in lymphocytes are protected against hypertension. The lymphocyte-deficient mice displayed diminished cardiac damage and renal injury in response to angiotensin II infusion. Mattson et al used Dahl salt-sensitive rats with deleted Rag1 gene to demonstrate that these rats have attenuated blood pressure, kidney damage, and albuminuria (Mattson et al., 2013). Mice lacking the macrophage colony-stimulating factor, also called osteopetrotic mice (op/op) have blunted hypertensive responses to chronic angiotensin II infusion.

Endothelial dysfunction, vascular remodeling, and oxidative stress associated with wild type controls were reduced in these op/op mice (De Ciuceis et al., 2005). Deletion of monocytes using diphtheria toxin prevented hypertension and reduced the expression of markers of aortic inflammation (Wenzel et al., 2011). Harwani et al demonstrated that the cholinergic agonist nicotine promoted the development of pro-inflammatory responses in splenic macrophages from SHRs and also induced Toll-like receptor-mediated cytokine release (Harwani et al., 2012). Most recent studies have also demonstrated the involvement of the gut microbiome in hypertension. Karbach et al reported that germ-free mice had reduced blood pressure and reduced leukocyte infiltration in the kidney and vasculature in response to angiotensin II infusion (Karbach et al., 2016).

1.6 Cytokines and antigens in hypertension

In generalized terms, Th1 cells secrete pro-inflammatory cytokines and Th2 cells secrete anti-inflammatory cytokines. Th1 cytokines mediate the pathogenic effects leading to end-organ damage and evidence exists for elevated levels of these cytokines in hypertensive models (Trott and Harrison, 2014). Once localized in the target organs, immune cells release inflammatory cytokines such as TNFα, IL-1ß, IL-6, IL-17, and IFNϒ. Direct infusion of IL-17, for example, has been reported to induce hypertension and endothelial dysfunction in mice (Nguyen et al., 2013a). IL-17 -/- mice exhibited an initial increase in blood pressure as wild type mice in response to angiotensin II; however, blood pressure dropped in IL-17 -/- mice after a week (Madhur et al., 2010). Increases in vascular oxidative

stress and endothelial dysfunction were also blunted in IL-17 -/- mice. IL-6 promotes the polarization of T cells towards Th17 cells that secrete IL-17. IL-6 -/- mice display blunted responses to angiotensin II infusion (Lee et al., 2006). Etanercept, a TNFα antagonist, prevents vascular dysfunction and the development of hypertension (Guzik et al., 2007). Following angiotensin II infusion, IFNϒ is elevated in the kidneys of hypertensive mice and inhibition of IFNϒ prevents end-organ damage induced by angiotensin II infusion (Garcia et al., 2012). Accordingly, adoptive transfer of anti-inflammatory regulatory T cells did not affect hypertension but attenuated cardiac hypertrophy, fibrosis, and inflammation induced by chronic angiotensin II infusion (Kvakan et al., 2009). IL-10 is an anti-inflammatory cytokine that stimulates the differentiation of regulatory T cells and is produced by the same cells; studies have reported that carotid arteries from IL-10 -/- mice have marked endothelial dysfunction in response to angiotensin II. Vascular superoxide production is also increased in IL-10 -/- mice (Kassan et al., 2013).

The complete mechanisms by which inflammatory cytokines mediate end organ damage are not well understood. In the kidneys, accumulation of inflammatory cytokines leads to loss of peritubular capillaries resulting in medullary hypoxia, and increased oxidative stress (Rodriguez-Iturbe et al., 2013). The infiltrating lymphocytes also express angiotensin II, and increased renal interstitial angiotensin II and oxidative stress are factors well known to impair pressure natriuresis thereby affecting renal function. Inflammation and oxidative

stress are inextricably linked and the generation of ROS reduces the bioavailability of NO. Chabrashvilli et al demonstrated that mRNA levels of the components of NADPH oxidase increased in the kidneys of SHRs prior to the development of hypertension (Chabrashvili et al., 2002). The SHR kidney has an exaggerated TGF response, which may be due to the diminished availability of NO. In the vasculature, inflammatory cytokines released around blood vessels can alter the rates of synthesis and degradation of vasoconstrictors and vasodilators, including NO. TNFα inhibits the endothelial NOS promoter and reduces the capacity of the endothelium to produce NO leading to impairment of vasodilatory responses. Accordingly, inhibiting TNFα restored endothelium-dependent vasodilation. IL-17 has also been demonstrated to cause inhibition of endothelial NOS activity, thereby increasing vascular tone and leading to endothelial dysfunction (Nguyen et al., 2013a). Vascular collagen deposition and aortic stiffening happen as a consequence of increased oxidative stress (Wu et al., 2014). IFNϒ has been reported to induce the expression of angiotensinogen in renal proximal tubular cells (Satou et al., 2018), which when converted to angiotensin II promotes sodium reabsorption in the nephron.

What activates the immune system in hypertension and causes the infiltration of immune cells in target organs is a more recent subject of investigation. The concept of self-antigens promoting hypertension was introduced following the discovery of agonistic antibodies to adrenergic and angiotensin receptors. Endogenous antigens like heat shock proteins and gamma

ketoaldehydes (isoketals) generated by the lipid peroxidation of arachidonic acid are increased in the kidneys of hypertensive animals (Kirabo et al., 2014). Isoketals can react with intracellular proteins and form protein adducts which could then be taken up by DCs and presented to MHC type I receptors thus activating the immune system. The production of isoketals also promotes the production of cytokines like IL-1ß, IL-6, and IL-23 by DCs, which further affect the polarization of T cells (Kirabo et al., 2014). Studies have also examined the effects of antigen recognition by specifically blocking the interaction between DC CD80 and CD86 with the T cell receptor CD28; this reduced vascular T cell accumulation and prevented hypertension (Vinh et al., 2010). Seminal work by Zimmerman et al reported that hypertension is caused in part by increased sympathetic outflow following elevated levels of ROS in the subfornical organ (SFO) of the brain in response to angiotensin II infusion. Adenoviral overexpression of cytoplasmic superoxide dismutase in the SFO reduced ROS and lowered blood pressure as potently as direct intracerebroventricular infusion of losartan, highlighting the crucial role of CNS inflammation in hypertension (Zimmerman et al., 2004). Collectively, mounting evidence has changed the previously existing notion that immune cell infiltration and inflammation are a consequence of hypertension and suggest that the inflammation in the kidneys and other organs are rather central to the development of hypertension.

1.7 Renal sodium transport in hypertension

Although all segments of the nephron contribute to the reabsorption of Na+

(with the exception of the thin descending loop of Henle), approximately 65% of total Na+ filtered is reabsorbed by the proximal tubule. The thick ascending loop reabsorbs another 25-30% of the filtered Na^+, and the cortical and medullar collecting ducts reabsorb 5-10% of filtered Na. The reabsorption of Na is an active, energy-consuming process, driven by the basolateral Na^+ K^+ ATPase. Active translocation of Na^+ creates driving forces for Na^+-dependent co-transport and ion exchange. Within the nephron, different Na^+ transporters are located in different parts, and regulation the reabsorption of Na^+.

In the proximal tubule, apical Na^+/H+ exchanger 3 (NHE3) mediates the reabsorption of Na^+, as well as NaHCO3. The loop of Henle is a heterogenous segment, consisting of the thin descending limbs, the thin ascending limbs, and the thick ascending limb. The thin descending limb has a very low Na^+ permeability, and in contrast, is highly permeable to water. Relative to the thin descending limb, the thin ascending limb has higher Na^+ permeability. Since the Na^+K^+ ATPase levels are very low, Na^+ reabsorption is assumed to be a passive process in this segment. In contrast, the thick ascending limb is a major Na^+-reabsorbing segment. Na^+ transport is mainly mediated through the $Na^+/K^+/2Cl^-$ cotransporter 2 (NKCC2), and partly through NHE3. Na^+ uptake in the macula densa is also mediated by NKCC2, where it is coupled to the generation of a vasoconstrictor signal to the afferent arteriole and regulates the tubuloglomerular feedback response. In the early distal convoluted tubule, NaCl cotransporter (NCC) is the main mediator of Na^+ reabsorption, whereas in the late distal

convoluted tubule and the collecting duct, the epithelial Na^+ channel (ENaC) is responsible for Na^+ reabsorption (Palmer and Schnermann, 2015) (Fig 1.3).

As mentioned earlier, blood pressure is a product of cardiac output and total peripheral resistance and as such, blood pressure can be increased by raising one of the two factors. A rise in effective circulating volume raises cardiac output and hence blood pressure. According to Guyton's hypothesis, the long-term regulation of circulating volume depends on fractional renal Na^+ absorption. The kidney maintains Na^+ and volume homeostasis in the body by mediating pressure-natriuresis and involves the regulation the various Na^+ transporters. Guyton stated that the kidney possesses the capacity to normalize blood pressure in the face of excess circulating volume through pressure-natriuresis, and thus, hypertension could be characterized as a failure to sufficiently carry out natriuresis. Indeed, evidence for impaired Na^+ excretion exists in several models of hypertension induced by varying stimuli such as angiotensin II infusion, high-salt diet, inhibition of NO production, and elevated renal sympathetic nerve activity. In these models, the sodium transporters have been shown to be regulated by intrarenal angiotensin II, inflammation, and immune cell infiltration. Chronic hypertension is reflected by a balance between the effects of the hypertensive stimuli vs. the elevated blood pressure itself. It was demonstrated that angiotensin II hypertension increases transporters' abundance and activation from the cortical thick limb to the medullary collecting duct (NKCC2, NCC, ENaC, and regulatory kinase SPAK), and that this stimulation is balanced by a

compensatory inhibition of transporters from proximal tubule through medullary

Figure 1.3 Distribution of renal sodium transporters: Anatomic arrangement of renal cortex and renal medulla in a kidney cross-section with adjacent drawing of a single nephron indicating locations of sodium transporters. Cortical sodium–hydrogen exchanger isoform 3 (NHE3) and sodium–phosphate cotransporter isoform 2 (NaPi2) are primarily restricted to the proximal tubule, where majority of the filtered sodium is reabosrbed. Sodium–potassium-2 chloride cotransporter (NKCC2; target of loop diuretics) is expressed in both medulla and cortex all along the thick ascending limb. Sodium chloride cotransporter (NCC; target of thiazide diuretics) is localized to the cortical distal convoluted tubule and SPAK (kinase that activates NKCC2 and NCC) is expressed in both cortex and medulla from thick ascending limb through distal convoluted tubules. ENaC (target of potassium sparing diuretics) α, β, and γ subunits are expressed in the cortex from late distal convoluted tubule through to principal cells of the cortical collecting duct, as well as in the medullary collecting ducts. Figure adapted from (McDonough and Nguyen, 2015).

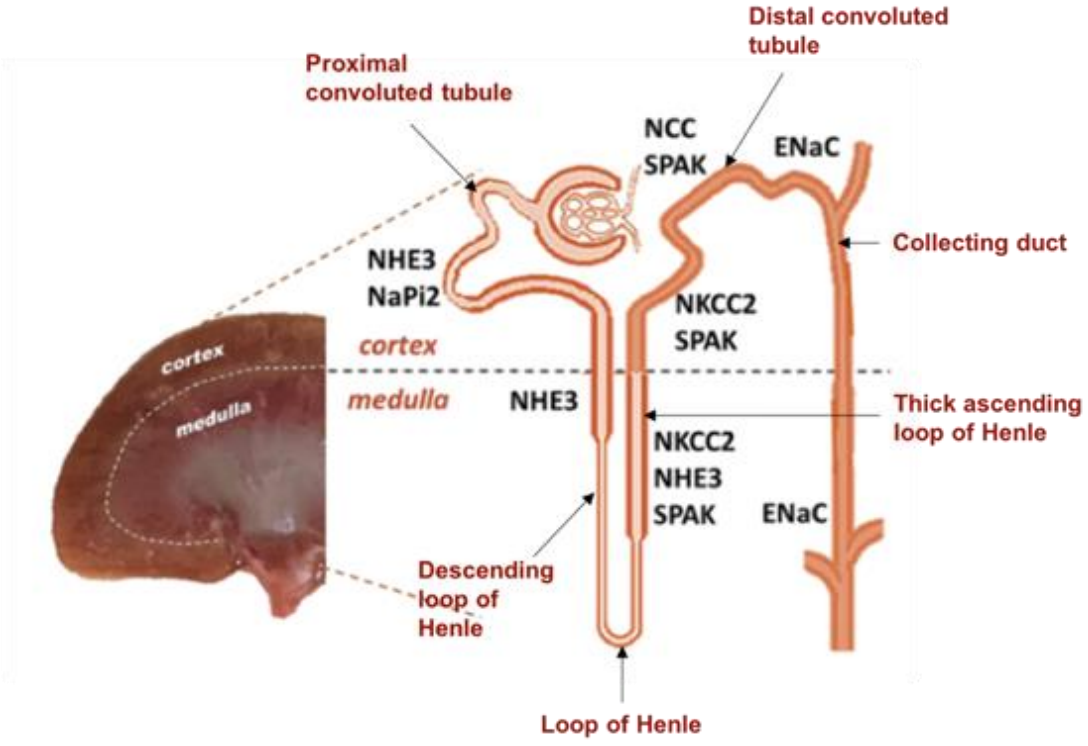

thick limb (cortical NHE3 and medullary: NHE3, NKCC2, Na-K-ATPase, SPAK), presumably driven by elevated blood pressure. Thus, there is a distal stimulation

counteracted by a proximal inhibition of transporters during angiotensin II hypertension. The exact signals mediating these regulatory mechanisms in hypertension are still being investigated. Some of the proposed mediators may include cytochrome P-450 metabolites, NO, and players of the RAS (McDonough and Nguyen, 2015; Palmer and Schnermann, 2015).

1.8 The lymphatic system

Lymphatic vessels transport immune cells and soluble antigens out of the peripheral interstitium to the draining lymph nodes, where further acquired immune responses are initiated. Soluble antigens reach the lymph nodes faster than they reach antigen presenting cells (APCs) like DCs, and are thought to prime the lymph node for the arrival of APCs (Randolph et al., 2017). By also taking up fluid extravasated from the blood vasculature lymphatic vessels regulate tissue fluid homeostasis (Levick and Michel, 2010; Aspelund et al., 2016). Lymphatic capillaries, also called initial lymphatic vessels, are blind-ended structures present in nearly all tissues. They consist of a single layer of oak leaf-shaped lymphatic endothelial cells (LECs) that connect to the surrounding extracellular matrix by thin fibrillar structures called anchoring filaments that permit expansion of these vessels with increased interstitial fluid pressure. The capillaries lack mural cell coverage, have little basement membrane coverage, and button-like cell-cell junctions (Trzewik et al., 2001; Baluk et al., 2007). As such, lymphatic capillaries are the preferred route for uptake of fluid and macromolecules in what is generally assumed to be a nonselective process

[although mechanisms for selective uptake may exist (Triacca et al., 2017)]. Lymphatic vessels are not passive conduits for the transport of antigens and leukocytes, but rather the process is actively regulated by LECs (Card et al., 2014). LECs express an array of chemokines and most notably, and nearly LEC-specific, are CCL21 and CCL19. The receptor for these chemokines, CCR7, is expressed on DCs and other leukocytes, and this ligand-receptor interaction aids the recruitment of immune cells into and through the lymphatic vessels to the lymph nodes (Förster et al., 2008; Card et al., 2014). Recent studies have also reported that LECs can themselves participate in induction of peripheral immune tolerance through antigen archiving and presentation through MHC class I and class II molecules (Cohen et al., 2010; Dubrot et al., 2014; Tamburini et al., 2014). LECs have also recently demonstrated direct interactions with DCs and T cells altering their maturation, differentiation, and cytokine repertoires [elegantly reviewed in (Maisel et al., 2017)]. Under homeostatic conditions, LECs were shown to participate in active antigen scavenging and cross present foreign antigens to CD8+ T cells, indicating a patrolling role for LECs during steady state (Hirosue et al., 2014). LECs upregulated the expression of MHC class I and programmed death (PD)-1 ligand PD-L1. As a consequence of this priming, CD8+ T cells differentiate into memory T cells, preferentially home to lymph nodes and mount a rapid and robust response following antigenic challenge (Vokali et al., 2020). Moreover, in conditions of melanoma and inflammation, IFNγ expressed by CD8+ T cells induces PD-L1 expression in LECs, which limits T cell

accumulation. Blocking IFNγ expression in LECs failed to induce PD-L1 expression, thus improving T cell responses within the tumor (Lane et al., 2018). Indeed, the respiratory and gastrointestinal systems, which are readily exposed to foreign antigens, have a dense network of lymphatic vessels stressing its importance in immune surveillance and defense mechanisms (Aspelund et al., 2016).

Lymphatic capillaries coalesce into larger collecting vessels, which unlike the capillaries have tight zipper-like junctions with a continuous basement membrane (Wiig and Swartz, 2012). The collecting vessels have intraluminal valves and possess muscle cell coverage. The inter-endothelial flaps in the capillaries and the intraluminal valves in the collecting vessels are responsible for the unidirectional transport of lymph. Unlike the extrinsic contraction of veins, lymphatic muscle cells provide an intrinsic pump to propel fluid along against a gradually increasing pressure before returning lymph to the blood circulation (Zawieja and Ph, 2009; Wiig and Swartz, 2012). Backflow within the vessels is minimized by the presence of unidirectional valves.

The lymphatic muscle cells are a unique class of muscle cells, possessing components of both smooth and striated muscle cells (Muthuchamy et al., 2003). Similar to vascular smooth muscle, the lymphatic muscle cell possesses basal myogenic tone and displays myogenic responses to pressure changes (Davis et al., 2009). Lymphatic muscle contraction is regulated by the amount of myosin light chain phosphorylation. However, lymphatic muscles also exhibit rapid phasic

contractile activity. Lymphatic muscle cells enable lymphatic vessels to respond to the various hydrodynamic forces that exist in different regions in the body. Thus, peripheral lymphatic vessels such as the femoral vessels exhibit high pumping activity, whereas, visceral lymphatic vessels such as the cervical and thoracic vessels exhibit low pumping activity (Chakraborty et al., 2015a). Lymphatic pumping is modulated by intrinsic factors such as preload and afterload, as well as external factors such as NO, prostaglandins, histamine, and neurotransmitters (Gasheva et al., 2013). Lymphatic vessels adapt to changes in preload and afterload, and this enables them to maintain a sufficient output flow under varying conditions. Increasing the filling pressures enhances lymph pump output over a certain range, which is similar to the Frank-Starling relationship in the heart, and reaches a plateau at higher pressures (Gashiev et al., 2004). Similarly, the lymphatic pump adapts to elevated outflow pressures such as those resulting from an increased central venous pressure. Although under studied, lymphatic contractions are also affected by neural modulation. It has been demonstrated that lymphatic contraction tone, amplitude, and frequency are increased with α-adrenergic stimulation, and that this effect is counteracted by ß -adrenergic activation (Von Der Weid, 1998). Serotonin, calcitonin gene-related peptide, and vasoactive peptide have also been reported to affect lymphatic contractile function. Substance P (SP) released during inflammation has been reported to induce tonic contraction in mesenteric lymphatic vessels. SP also activates inflammatory pathways in lymphatic muscle cells through the activation of pro-

inflammatory p38/pERK pathways (Chakraborty et al., 2011). Similarly, an acute induction of inflammation by LPS has been shown to cease flow in mesenteric lymphatics (Chakraborty et al., 2015b) and similar effects have been observed with other cytokines such as TNFα, IL-1ß, and IL-6. It has been demonstrated that inducible NOS (iNOS)-expressing immune cells, under inflammatory conditions, attenuate lymphatic contraction in mouse popliteal lymphatics (Liao et al., 2011). iNOS-derived NO may also cause chronic relaxation of the lymphatic muscle cells, thus reducing contractile strength. Thus, lymphatic contractility, lymph flow, and inflammation are closely related processes and changes in one of these factors greatly influence outcomes during disease conditions. Given these important roles of the lymphatic vessels, defects in function disrupt fluid and immune homeostasis causing edema and inflammatory diseases. Collecting lymphatic vessel remodeling is observed in metabolic syndrome, a chronic inflammatory disease, thereby affecting the intrinsic contractility required to maintain proper flow (Zawieja et al., 2012). Studies have also shown that adipose tissue expansion in mice fed a high fat diet leads to impairment of lymphatic contractility (Blum et al., 2014). Insufficient lymphatic function also leads to lymphedema, characterized by fluid accumulation and chronic swelling of the limbs. Thus, it is evident that several factors regulate the contractile functions of lymphatic factors, and dysregulation of lymph flow could have a significant impact in pathological conditions.

1.9 Inflammation-associated lymphangiogenesis

Inflammation is a complex biological process that occurs as a protective mechanism against harmful agents and tissue remodeling. Inflammation is associated with migration and activation of leukocytes, increased vascular permeability, and an accumulation of excess interstitial fluid. To relieve the tissue of this hostile microenvironment, excess fluid, cells, and antigens must be cleared and hence an increased demand for lymphatic drainage. To keep up with this need, lymphangiogenesis occurs at the site of persistent inflammation given that lymphatics are structurally suited to be the physiological route for removal of increased antigens, fluid, cytokines, and macromolecules from the site of inflammation. The process has been termed inflammation-associated lymphangiogenesis (IAL) (Medzhitov, 2010; Lim et al., 2013; Kim et al., 2014). The rate at which these new vessels grow and the nature of these new vessels are highly tissue- and stimulus-specific. IAL has been observed in inflammatory conditions in several organs including the skin, intestine, heart, kidney, and airway tract, and the consequences of IAL varies with the disease state and type of tissue in question [excellently reviewed in (Kim et al., 2014; Abouelkheir et al., 2017)]

In the search for the mechanisms of such postnatal lymphangiogenesis, several mediators of IAL have been found in different inflammatory diseases (Tan et al., 2014; Maisel et al., 2017), however the most common of these are the potent lymphangiogenic vascular endothelial growth factors (VEGFs) VEGF-C and VEGF-D. VEGF-C/D signal through the VEGFR-3 receptor. The sources of

such mediators may either be leukocytes or stromal cells. Macrophages in particular have been demonstrated to be sources of VEGF-C in several cases. In a mouse model of tail lymphedema, CD68+ macrophages were reported to be sources of VEGF-C (Gousopoulos et al., 2017), and depletion of macrophages reduced IAL in a mouse model of acute colitis. DCs and neutrophils have also emerged as sources of lymphangiogenic signals (Baluk et al., 2005). Besides leukocytes, epithelial cells (Wuest and Carr, 2010), keratinocytes (Halin et al., 2007), and fibroblastic reticular cells (Chyou et al., 2008) have also been reported to be VEGF-C sources in inflammation. In the kidney, VEGF-C staining was observed in tubular epithelial cells during unilateral ureteral obstruction (UUO) (Lee et al., 2012). Other inflammatory stimuli like LPS (Kang et al., 2009), lymphotoxin (LTa and LTb), and inflammatory cytokines like IL-17 and IL-8 (Choi et al., 2013) can also mediate IAL. Some cytokines like IFNϒ exhibit inhibitory effects on IAL, and TGFß has been implicated in both stimulation and inhibition of lymphangiogenesis in disease states (Zampell et al., 2012; Kinashi et al., 2013a). Inhibition of TGFß induces lymphangiogenesis in a mouse model of chronic peritonitis (Oka et al., 2008) and also improves lymphatic function in a model of lymphedema (Avraham et al., 2010), whereas in a model of peritoneal fibrosis, inhibiting the TGFß receptor suppressed lymphangiogenesis (Kinashi et al., 2013b). Thus, the outcome of IAL is dependent on the balance of pro- and anti-lymphangiogenic factors and cytokines (Zampell et al., 2012). The new lymphatic vessels that are formed may proliferate from existing vessels (Wirzenius et al.,

2007), sprout as new vessels (Kataru et al., 2009; Flister et al., 2010), or form from the trans-differentiation of bone marrow-derived cells (Maruyama et al., 2005; Kerjaschki et al., 2006). Interestingly, this seems to depend on the type of lymphangiogenic stimulus. Although controversial, evidence exists for the trans-differentiation of macrophages into LECs in LPS-induced peritonitis (Hall et al., 2012) and corneal inflammation (Maruyama et al., 2005). Moreover, activated murine peritoneal CD11b+ macrophages in vitro were reported to form tube-like structures and express LEC-specific markers (Maruyama et al., 2005).

1.10 Is inflammation-associated lymphangiogenesis good or bad?

Whether IAL serves to resolve or exacerbate inflammation remains a matter of debate. In the skin, IAL has been demonstrated to have functional implications in both acute and chronic inflammation. In acute models of skin inflammation, blocking IAL by the inhibition of VEGFR-3 signaling increased inflammation (Kajiya and Detmar, 2006) and conversely, overexpression of VEGF-C induced lymphangiogenesis and limited inflammation in chronic inflammatory conditions (Huggenberger et al., 2011). It has also been demonstrated that in contact hypersensitivity, lymphatic vessels are necessary for the regulation of long-term immune responses and fluid balance. Upon initial contact K14-VEGFR3-Ig mice, which lack dermal lymphatic vessels, not only develop greater swelling, but also fail to tolerize to hypersensitization upon subsequent challenges (Thomas et al., 2012). In the gut, alteration to the lymphatics results in changes not only to immune function but also to lipid

transport. Deficiencies in the structure or function of lacteals tamper with lipid absorption and lead to the leakage of lymph. Proliferation of lymphatic vessels is associated with chronic inflammatory bowel diseases like Crohn's, ileitis, and colitis, and IAL is unlikely to improve lymphatic drainage as edema and lack of DC migration to the draining lymph nodes is evident in such cases (Acedo et al., 2011; Abouelkheir et al., 2017). In airway inflammation, infection leads to robust lymphangiogenesis and blocking IAL during infection resulted in increased mucosal edema (Aurora et al., 2005; Baluk et al., 2005). Conversely, stimulating IAL also increased edema in severe pulmonary lymphangiectasia (Yao et al., 2014). In rat cardiac allografts, newly formed lymphatic vessels participated in trafficking of immune cells, and presumably donor antigen, to the secondary lymphoid organs; inhibiting VEGFR-3 using adenoviral VEGFR3-Ig was reported to increase cardiac allograft survival. Interestingly, this was not linked to reduced lymphangiogenesis, but rather reduced CCL21 production and entry of CD8+ T cells in the allograft (Edwards et al., 2018). Thus, the functional implications of IAL are highly disease- and tissue-specific.

Besides the macroscopic expansion, inflammation also affects lymphatic vessels at the cellular level. Under steady state, the expression of adhesion molecules like ICAM-1, VCAM-1, and LCAM by LECs is quite low, whereas their expression is dramatically upregulated by increased flow and inflammatory signaling presumably to facilitate the migration of DCs (Johnson et al., 2006; Maddaluno et al., 2009; Miteva et al., 2010; Halin et al., 2011). Exposure of LECs

to TNFα in vitro upregulates the expression of CCL21 and the upregulation of CCL21 has also been demonstrated in vivo under inflammatory conditions (Johnson and Jackson, 2010; Miteva et al., 2010; Halin et al., 2011). Besides CCL21, CXCL12 and CX3CL1 are other chemokines implicated in DC migration that are also upregulated during inflammation (Johnson et al., 2006; Pegu et al., 2008). In response to inflammation, LECs also increase the expression of molecules that help remove inflammatory chemokines. For example, the chemokine-scavenging receptor D6 is upregulated under inflammatory contexts, and in the absence of D6 myelomonocytic cells accumulated around lymphatics vessels and impeded lymph flow (Lee et al., 2011; McKimmie et al., 2013). Inflammation also modulates lymphatic pumping activity. Systemic or intradermal injection of inflammatory cytokines IL-6, TNFα, and IL-1ß decreased lymphatic pumping frequency and lymph flow velocity in vivo (Aldrich and Sevick-Muraca, 2013) (Aldrich and Sevick-Muraca, 2013). However, SP, a neuropeptide secreted by inflammatory cells, increases the pumping frequency of rat mesenteric vessels (Davis et al., 2008). How inflammation affects lymphatics and vice-versa has been and continues to be investigated in great detail.

1.11 Lymphatics and hypertension

In 2009, a previously uncovered role for lymphatic vessels and lymphangiogenesis was described by Titze and his colleagues in the context of interstitial sodium homeostasis (Machnik et al., 2009). This study demonstrated that the skin interstitium could act as a reservoir for sodium in order to buffer the

effects of sodium overload on blood pressure. In response to a high-salt challenge, the investigators identified that dermal lymphangiogenesis is associated with sodium accumulation in the skin interstitium. The resulting hypertonicity from sodium accumulation activates the transcription factor, tonicity-responsive enhancer binding protein (TonEBP) in infiltrating macrophages. TonEBP binds to the gene encoding VEGF-C and causes macrophages to secrete VEGF-C, thereby leading to a robust expansion of the dermal lymphatic network. The lymphatic expansion was dependent on TonEBP secretion from the macrophages; macrophage depletion prevented dermal lymphatic hyperplasia and worsened sodium-dependent hypertension. Blockade of VEGF-C signaling had similar effects in these mice (Wiig et al., 2013). This study not only uncovered a novel role for dermal lymphatic vessels, but also demonstrated the extrarenal regulation of sodium homeostasis and blood pressure control by the skin interstitium.

In another study, TonEBP-mediated cardiac lymphangiogenesis and macrophage infiltration was observed in the left ventricles of SHRs that were fed a high-salt diet (Yang et al., 2014, 2017). Retrovirus-induced overexpression of VEGF-C led to enhanced lymphangiogenesis, reduced myocardial fibrosis, macrophage infiltration, decreased blood pressure, and preserved myocardial function. The opposite effects were observed after blocking VEGF-C, where diminished lymphangiogenesis was accompanied by increased macrophage infiltration and pronounced left ventricular remodeling (Yang et al., 2014).

1.12 Renal lymphatics and hypertension

Renal lymphatics follow the topography of the renal vasculature. They begin in the cortex as intralobular lymphatics, which are blind-ended tubes located closely to the renal tubules. These vessels join the interlobular lymphatics, which then connect to the larger arcuate and interlobar lymphatics, and drain through the hilar lymphatics. The presence of medullary lymphatics is debated, with studies reporting the absence of presence of lymphatics in the medulla in dogs, rabbits, and pigs. Similarly, in humans, studies have detected renal medullary lymphatics in four out of ten cases of normal renal tissue, however, these vessels were present near the cortex and not in the central region of the medulla. Lymphatic vessels have also been reported to be present closely associated with the glomerulus, but not penetrating the glomerulus. Renal lymph forms as a result of both capillary filtration and tubular reabsorption, and is drained by the cortical lymphatic vessels out through the hilus. Interstitial fluid volume and intra-renal venous pressure are the main drivers of renal lymph formation. In addition to the venous and ureteral drainage, the lymphatic system contributes to the drainage of renal fluid, and these systems act reciprocally. Obstruction of both the upper ureter and renal vein results in an increased renal lymph pressure and flow, and conversely, ligating the lymphatic vessels results in increased urine flow (Russell et al., 2019).

Figure 1.4 Schematic diagram of a human renal lobe: Blind-ended lymphatic capillaries begin in the substance of a renal lobule as intralobular lymphatics, which in turn become interlobular lymphatics. From here, lymph can flow either toward the capsule or toward the hilum. Valves are present at the level of the capsule and arcuate vessels to prevent backflow. Intra-renal arteries are depicted in red and intra-renal veins in blue. Figure and figure legend adapted from (Russell et al., 2019).

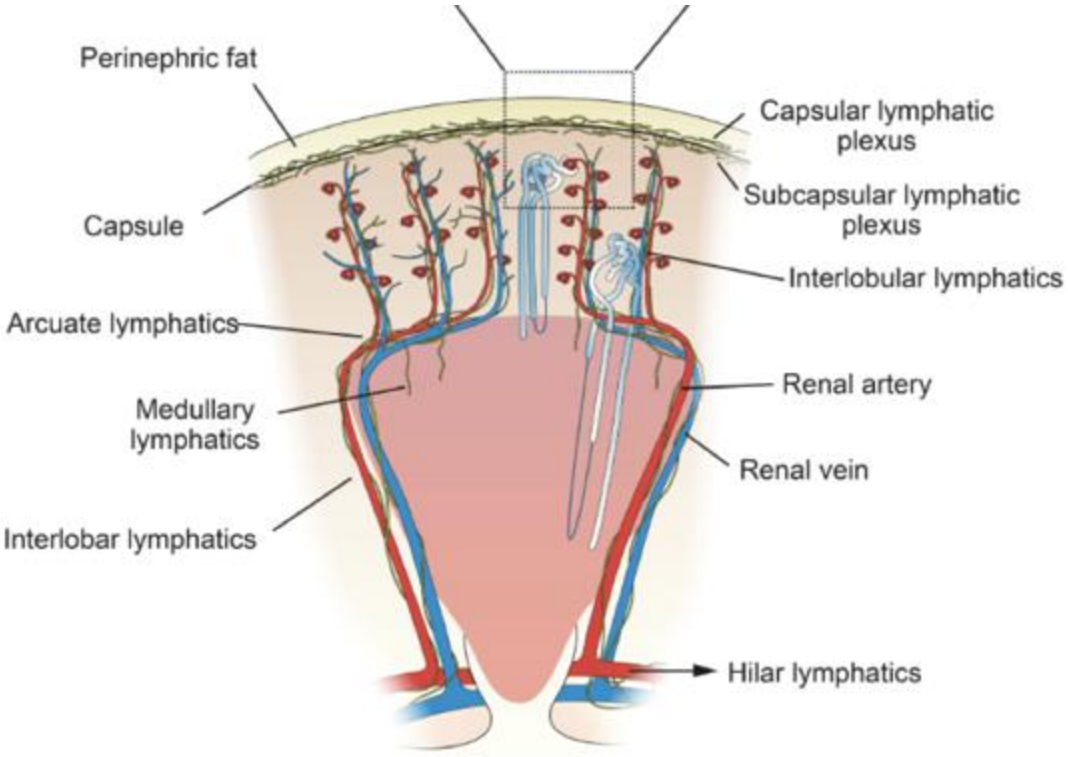

The importance of renal lymphatics in fluid balance has been demonstrated as early as the 1960s. Renal lymphatic ligation was reported to result in renal edema, increased urine volume, and, surprisingly, increased blood pressure in several studies (Barer and Ward-McQuaid, 1957; Lilienfeld et al., 1967). Zhang and colleagues later demonstrated that dual renal lymphatic ligation was as detrimental to kidney function as a nephrectomy (Zhang et al., 2008). Increased pressure within the renal capsule has also been shown to reduce GFR and renal perfusion. In conditions such as chronic heart failure where systemic venous

pressure is increased, the burden on the renal lymphatic vessels is increased because of the simultaneous increase in post-glomerular filtration and decrease in thoracic drainage in the neck. This excess need for lymphatic drainage can lead to failure of lymphatic function. In such cases, generally, new vessels form in order to help clear the excess fluid and accumulated macromolecules. In the kidney, lymphangiogenesis has been reported in association with inflammation and infiltrating immune cells in chronic inflammatory kidney diseases such as diabetic nephropathy, IgA nephropathy, tubulointerstitial nephritis, and glomerulonephritis with the degree of fibrosis directly correlating to the extent of lymphatic expansion (Yazdani et al., 2014). In acute kidney injury, renal lymphangiogenesis was associated with tubulointerstitial injury and suppression of renal lymphangiogenesis reduced fibrosis in a mouse model of unilateral ureteric obstruction (UUO). VEGF-D and VEGF-D were demonstrated to be highly expressed during acute kidney injury and chronic kidney disease (Zarjou et al., 2019). Tubular epithelial cells along with macrophages were demonstrated to be sources of VEGF-C in UUO. Hasegawa and colleagues were able to reduce inflammation and subsequent fibrosis by delivering VEGF-C for two weeks during UUO (Hasegawa et al., 2017). In another study, it was reported that lymphangiogenesis might occur in parallel with the onset of proteinuria, yet prior to the development of fibrosis, with activated proximal tubular epithelial cells acting as sources of VEGF-C (Yazdani et al., 2012). Renal transplants are also associated with the formation of new lymphatic vessels; however, the

consequences of these vessels is debated. The newly formed vessels could be beneficial by draining out fluid and for immune clearance immediately after operation. In fact, low lymphatic vessel density in the first post-procedural biopsy is associated with acute rejection. The persistence of these vessels on the other hand may eventually lead to transplant rejection as these vessels help transport APCs to the lymph nodes and initiate immune responses (Kerjaschki et al., 2004; Pedersen et al., 2020).

With renal immune cell infiltration and accumulation, a part of the pathogenesis of hypertension, IAL in the kidney should be evident and necessary to remediate inflammation. Our laboratory investigated this relationship and reported that the kidneys of SHRs demonstrate increased renal lymphatic vessel density in association with inflammation and infiltration of CD68+ macrophages (Kneedler et al., 2017). Interestingly, a strain of SHRs (SHR-B2) that were hypertensive but resistant to renal injury displayed lower lymphatic vessel density than their age-matched controls. Fischer 344 rats are a strain of rats that are normotensive but display age-associated renal injury. Kidneys from these rats at 20 or 24 months of age demonstrated increased renal lymphatic vessel density accompanying age-associated renal injury compared to 4-month old controls (Kneedler et al., 2017). Thus, renal inflammation evident in hypertensive and aged kidneys is associated with an increase in renal lymphatic vessel density.

Following the SHR genetic model of hypertension, our lab also tested if this increase in renal lymphatic density occurs in two other models of hypertension,

salt-sensitive, and nitric oxide synthase inhibition-induced hypertension induced by the administration of L-NAME. In both hypertensive models, we observed a significant increase in renal lymphatic vessel density (Lopez Gelston et al., 2018). In salt-sensitive hypertension, the increase in lymphatic density was associated with renal infiltration of macrophages and Th1 cells, whereas in L-NAME-induced hypertension, this was associated with an increase in renal macrophages and DCs. Further, we hypothesized that while minimal renal lymphatic expansion may be indicative of inflammation, it is insufficient to clear infiltrating immune cells from the cortical interstitium and that further augmenting renal lymphangiogenesis should therefore be beneficial. Enhancing renal lymphatic expansion prior to the onset of hypertension using an inducible genetic model of kidney-specific lymphangiogenesis (Lammoglia et al., 2016) completely prevented the development of hypertension associated with high-salt diet and nitric oxide synthase inhibition (Lopez Gelston et al., 2018). Importantly, in both of these models augmenting renal lymphatic vessel density reduced the immune cell populations previously found to be increased suggesting increased trafficking from hypertensive kidneys.

1.13 The hypothesis and specific aims of the dissertation

The following hypotheses and specific aims will be examined in Sections 2, 3 and 4.

Hypothesis 1. Augmenting renal lymphatic vessel density will prevent the development of angiotensin II-induced hypertension in male and female mice.

Specific Aim 1a will identify whether renal lymphatic vessel density is altered in angiotensin II-induced hypertension. We hypothesize that renal lymphatic vessel density will be increased in male and female mice with angiotensin II-induced hypertension in association with renal immune cell accumulation.

Specific Aim 1b will identify the effects of angiotensin II on lymphatic endothelial cells *in vitro*. We hypothesize that angiotensin II will have direct and indirect effects on lymphatic endothelial cells to induce their proliferation and activation.

Specific Aim 1c will identify the effects of augmenting renal lymphatic vessel density on blood pressure in angiotensin II-induced hypertension. We hypothesize that augmenting renal lymphatic vessel density will prevent the development of angiotensin II-induced hypertension in male and female mice in association with a reduction in renal immune cell accumulation.

Hypothesis 2. Therapeutic augmentation of renal lymphatic vessel density will lower blood pressure in L-NAME-induced hypertension in association with a reduction in renal immune cell accumulation and an increase in urinary Na^+ excretion.

Specific Aim 2a will determine whether the therapeutic induction of renal lymphatic expansion will attenuate established hypertension. We hypothesize that augmenting renal lymphatic density in a model of

established L-NAME-induced hypertension will reduce renal immune cell accumulation and increase urinary Na^+ excretion and thereby reduce blood pressure.

Specific Aim 2b will characterize the role of renal lymphatic vessels in Na^+ homeostasis at baseline. We hypothesize that augmenting renal lymphatic vessels will not alter renal Na^+ handling during baseline conditions.

Specific Aim 2c will identify the role of renal lymphatic vessels in maintaining Na^+ homeostasis during acute and chronic salt-loaded conditions. We hypothesize that augmenting renal lymphatic vessel density will increase urinary Na^+ excretion following acute and chronic salt-loaded conditions.

Hypothesis 3. Therapeutic induction of renal lymphatic vessel expansion will lower blood pressure in angiotensin II-dependent and salt-sensitive hypertension in association with a reduction in renal immune cell accumulation and an increase in urinary Na^+ excretion.

Specific Aim 3a will determine whether the therapeutic induction of renal lymphatic expansion will attenuate angiotensin II-induced hypertension. We hypothesize that augmenting renal lymphatic density will reduce renal immune cell accumulation and increase urinary Na^+ excretion and thereby reduce blood pressure in angiotensin II-dependent hypertension.

Specific Aim 3b will determine whether the therapeutic induction of renal lymphatic expansion will attenuate salt-sensitive hypertension. We

hypothesize that augmenting renal lymphatic density will reduce renal immune cell accumulation and increase urinary Na^+ excretion and thereby reduce blood pressure in salt-sensitive hypertension.

2. AUGMENTING RENAL LYMPHATIC VESSEL DENSITY PREVENTS ANGIOTENSIN II-INDUCED HYPERTENSION IN MALE AND FEMALE MICE*

2.1 Overview

Renal inflammation and immune cell infiltration are characteristic of several forms of hypertension. Our lab has previously demonstrated that renal inflammation-associated lymphangiogenesis occurs in salt-sensitive and nitric oxide inhibition-induced hypertension. Moreover, enhancing renal lymphatic density prevented the development of these two forms of hypertension. In the current study, we determined whether augmenting renal lymphatic vessel density can prevent the development of angiotensin II-induced model of hypertension. The angiotensin II-dependent model of hypertension is characterized by high circulating and intrarenal levels of angiotensin II. Inappropriate renin-angiotensin system activation is found in the majority of patients with essential hypertension, and has been shown to be required for the development of several experimental forms of hypertension. The pressor response to infusion of angiotensin II is much higher than that achieved with nitric oxide inhibition. Moreover, sex differences in the development of hypertension in response to angiotensin II infusion have been established, and hence, we investigated male and female mice separately in this study.

Here, we investigated the effects of angiotensin II-induced hypertension on renal lymphatic vessel density in male and female mice. Wild-type and genetically engineered male and female mice were infused with angiotensin II for two or three weeks. Isolated splenocytes and peritoneal macrophages from mice, and commercially available mouse lymphatic endothelial cells were used for *in vitro* studies. Compared to vehicle controls, angiotensin II-infused male and female mice had significantly increased renal lymphatic vessel density in association with pro-inflammatory immune cells in the kidneys of these mice. Direct treatment of lymphatic endothelial cells with angiotensin II had no effect since they lack angiotensin II receptors, however angiotensin II treatment of splenocytes and peritoneal macrophages induced secretion of the lymphangiogenic growth factor VEGF-C *in vitro*. Utilizing our genetic mouse model of inducible renal lymphangiogenesis, we demonstrated that greatly augmenting renal lymphatic density prior to angiotensin II infusion prevented the development of hypertension in male and female mice and this was associated with a reduction in renal $CD11c^{+}F4/80^{-}$ monocytes. Renal lymphatics play a significant role in renal immune cell trafficking and blood pressure regulation, and represent a novel avenue of therapy for hypertension.

2.2 Introduction

With the revision of the Hypertension Clinical Guidelines in 2017, nearly half of the adult population in the United States is classified as being hypertensive, and hypertension is the leading modifiable risk factor for deaths from

cardiovascular diseases (Whelton et al., 2018). Overactivation of the renin-angiotensin-system (RAS) is a powerful mediator of high blood pressure (BP) and its accompanying risks; accordingly, angiotensin converting enzyme inhibitors and angiotensin receptor blockers remain popular for the treatment of hypertension (Case et al., 1977). Sex differences in hypertension are well documented (Boynton and Todd, 1947; Yoon et al., 2015; Mozaffarian et al., 2016); men have a higher prevalence of hypertension than women from ages 45-54, whereas from age 75, more women become hypertensive. Despite improved awareness and treatment options, roughly 30%-60% of hypertensive patients do not achieve BP targets and lowering BP by just 10 mmHg significantly reduces risks and improves health outcomes (Braam et al., 2017).

Several studies over the past years have established that renal infiltration of immune cells and inflammation is linked to hypertension in humans and experimental models; experimentally reducing inflammation reduces hypertension, thus confirming this link (Guzik et al., 2007; De Miguel et al., 2010). Renal infiltration of activated macrophages, dendritic cells, and T and B lymphocytes promote sodium retention, mediate renal injury and fibrosis, and elevate BP (De Ciuceis et al., 2005; Chan et al., 2015; Barbaro et al., 2017). Angiotensin II (Ang II), among other factors, is a powerful activator of the immune system, promoting pro-inflammatory cytokine production by activated immune cells (Satou et al., 2018). In turn, these cytokines lead to activation of RAS components, thus setting up a vicious cycle. Sex differences have also been noted

in renal immune cell infiltration during hypertension. Increased pressor responses to Ang II in males is associated with greater T cell infiltration in the kidney and perivascular adipose tissue (Ji et al., 2014; Pollow et al., 2014). The mechanisms contributing to this differential response have not been fully elucidated, and gaining a better understanding of BP control in both males and females remains important.

Lymphatic vessels transport extravasated fluid, cells, and proteins out of the tissue interstitium to the draining lymph node, eventually returning it to the circulation, thus maintaining immune surveillance and tissue fluid balance (Abouelkheir et al., 2017). Inflammation-associated lymphangiogenesis is observed in many renal inflammatory diseases including renal carcinoma, unilateral ureteral obstruction, and diabetic nephropathy (Yazdani et al., 2014). Previous studies from our lab have demonstrated that lymphangiogenesis in the kidney is associated with hypertension in spontaneously hypertensive rats, and salt-sensitive hypertension and nitric oxide inhibition-induced hypertension in mice (Kneedler et al., 2017; Lopez Gelston et al., 2018). Endogenous renal lymphangiogenesis accompanied immune cell accumulation and is likely a result of the increased physiological need for immune cell clearance during inflammation. In fact, accumulating monocytes have been identified as the source of the lymphangiogenic factor VEGF-C in the kidney upon injury. In all of these models, the extent of lymphangiogenesis, however, is limited and potentially insufficient to restore tissue homeostasis. We hypothesized that augmenting renal

lymphatic density prior to the onset of hypertensive stimuli will prevent the development of hypertension. Using a genetic mouse model of inducible renal lymphangiogenesis, we demonstrated that enhancing renal lymphatic density prevented the development of salt-sensitive and nitric oxide inhibition-induced hypertension and this was associated with a reduction in renal immune cell accumulation in both of these models (Lopez Gelston et al., 2018).

In the current study, we examined the effects of Ang II-induced hypertension (A2HTN) on renal lymphatic vessels. As mentioned above, since sex differences have been documented in the pressor response to Ang II infusion and in renal accumulation of immune cells, we independently studied the effects of A2HTN on renal lymphatic density in male and female mice. In addition, we examined the direct and indirect effects of Ang II on lymphatic endothelial cells (LECs). We also tested the effects of genetically augmenting renal lymphatic vessel density on A2HTN in male and female mice. Our hypotheses were that male and female mice with A2HTN will demonstrate an increase in renal lymphatic vessel density, and that Ang II will directly induce the activation and adhesion of LECs. We also hypothesized that the genetic augmentation of renal lymphatic density will prevent the development of A2HTN in both male and female mice.

2.3 Materials and Methods

2.3.1 Mice

2.3.1.1 C57BL/6J

Wild type C57BL/6J mice were purchased from Jackson Laboratories (Bar Harbor, ME). Male and female mice 10-14 weeks of age were anesthetized with isoflurane and subcutaneously implanted with osmotic mini-pumps (Alzet, model 1004, Cupertino, CA) filled with vehicle (saline) or Ang II (490 ng/kg/min; BACHEM, Torrance, CA). Infusion was carried out for a period of 2 or 3 weeks during which the mice had free access to normal vivarium diet and drinking water. Mice were euthanized by exsanguination under 5% inhalational isoflurane anesthesia with death confirmed by cervical dislocation before tissue collection. All procedures performed in mice were approved by the Texas A&M University IACUC in accordance with the NIH Guide for the Care and Use and Care of Laboratory Animals.

2.3.1.2 KidVD

KidVD mice backcrossed minimally 7 generations to C57BL/6J have been described previously. TRE-VEGF-D mice were crossed with mice carrying a kidney promoter-driven rtTA (Cdh16; KSP) to generate transgenic mice (KidVD) that overexpress VEGF-D specifically in the kidney following doxycycline administration. The KSP-rtTA mouse was made available by the University of Texas-Southwestern George M. O'Brien Kidney Research Core Center (P30DK079328). KidVD+ and KidVD- littermates received doxycycline (0.2 mg/mL; doxycycline hyclate, Sigma) in their drinking water for 1 week, following

which the mice were implanted with mini-pumps and infused with Ang II for 3 weeks as described above.

2.3.2 Blood pressure measures

Systolic BP (SBP) was measured to confirm hypertension using the non-invasive tail cuff method. The IITC Life Science (IITC Inc, Woodland Hills, CA) blood pressure acquisition system was used for all measurements. The restrainers and warming chamber were preheated to 34°C. Mice were placed in restrainers of appropriate size and were acclimatized in the preheated chamber for 5 minutes before beginning measurements. SBP values were recorded from the blood pressure traces by blinded investigators.

2.3.3 Renal immunofluorescence

2.3.3.1 Immunofluorescence

Kidneys were sagittally cut into halves and fixed in 10% buffered formalin solution (Sigma, St. Louis, MO) for 48 hours. Kidneys were then rinsed and stored in 70% ethanol until they were embedded in paraffin. 5 μm sections were cut, deparaffinized, rehydrated, and permeabilized with 0.1% Triton solution (BioRad, Hercules, CA). The kidney sections were blocked with 10% AquaBlock (EastCoastBio, North Berwick, ME), and were incubated at 4°C overnight with antibodies against the lymphatic endothelial cell markers markers lymphatic vessel endothelial hyaluronan receptor 1 (LYVE-1) or podoplanin (Goat polyclonal, R&D Systems, Minneapolis, MN). The sections were then incubated with corresponding Alexafluor 488 or 594 secondary antibodies (Life

Technologies, Carlsbad, CA) for 1 hour at room temperature. Samples incubated with only secondary antibody were used as negative controls. The slides were mounted with ProLong Gold antifade reagent containing DAPI (Invitrogen, Carlsbad, CA) and imaged using an Olympus BX51 fluorescence microscopy system with Olympus Q5 camera. Images were captured at 40X magnification using Olympus cellSens imaging software (Olympus, Shinjuku, Tokyo, Japan).

2.3.3.2 Quantification

All LYVE-1+, lumen-containing lymphatic vessels found around the interlobular arteries in the cortex and corticomedullary junction, excluding vessels at the hilus, were counted at 20X magnification by 2 independent, blinded investigators. For quantification of KidVD+ and KidVD- kidney sections, 4 images from pre-determined areas within the renal cortex of each kidney section were captured at 10X magnification, with efforts made to exclude tissue defects, minor calyx, and large areas of glomeruli. After exclusion of glomeruli within the captured images, the area values measuring total number of podoplanin+ pixels were determined using ImageJ software (NIH, Rockville, MD) after setting the threshold for positive endothelium. Endomucin+ pixel density was quantified in a similar manner using images captured at 10X magnification.

2.3.4 qRT-PCR

Kidneys were stored in RNAlater (Sigma, St. Louis, MO) at -80°C until use. Total RNA was isolated using RNeasy Mini (Qiagen, Germantown, MD) following the manufacturer's instructions. cDNA synthesis of 0.5 µg total RNA was

performed using RT2 First Strand Kit (Qiagen) following the manufacturer's instructions. qRT-PCR reactions were carried out using SYBR Green ROX qPCR Mastermix (Qiagen), Nuclease-free water (Invitrogen, Carlsbad, CA), and primers (10 μM) (IDT, Coralville, IA) in combination with kidney cDNA. Reactions were run in duplicate using the Applied Biosystems 7900HT Fast Real-Time PCR Thermal Cycler (Applied Biosystems, Foster City, CA). Fold changes were calculated using the comparative Ct (ΔΔCT) method with Ubiquitin (Ubc) as an endogenous control. Forward and reverse primer sequences were generated using NCBI Gene DataBase and PrimerBank and are listed in Table A1 in the Appendix.

2.3.5 Flow Cytometry

Kidneys were harvested and thoroughly minced after removing the capsules. The minced tissues were digested in buffer containing 2.5 mg/mL Collagenase D (Roche Sigma, St. Louis, MO) and 1 mg/mL Dispase II (Sigma) at 37°C for 1 hour. Single cell suspensions were obtained by filtering the digested tissue through sterile 100 μm and 40 μm strainers. The cellular components were isolated by centrifugation, and red blood cells were lysed in NH4Cl/EDTA. Splenocytes were isolated by a similar protocol for use as antibody controls and for forward versus side scatter gating of immune cell size and shape. Cells were resuspended in 0.1% FBS solution and nonspecific Fc binding was blocked with an anti-mouse CD16/CD32 antibody (BD Pharmingen, San Jose, CA) for 10 minutes on ice. Following the blocking step, cells were incubated with fluorescent-conjugated antibodies against CD45, F4/80, CD11c, and CD3e for 10 minutes on

ice and were filtered through a sterile 40 μm strainer. All antibodies were purchased from either BD Pharmingen or eBiosciences. Data was acquired on a BD LSR Fortessa X-20 flow cytometer using FACS DIVA software (BD Biosciences, San Jose, CA) and analyzed using Flow Jo v7.6.2 (FlowJo, LLC, Ashland, OR). CD3e+, CD3e-, F4/80+, and CD11c+ populations were quantified within the CD45+ gate. Results are expressed as a percentage of CD45+ cells per kidney.

2.3.6 Cells

2.3.6.1 Splenocytes

For collection of splenocyte-conditioned media, splenocytes were isolated as described above and plated in 24-well plates at a concentration of 1 X 10_6 cells/mL using RPMI media containing 10% FBS. The splenocytes were treated with either vehicle (saline) or 1 μM Ang II for 48 hours. At the end of treatment, the conditioned media from each treatment was collected and spun down to remove any cellular components or debris.

2.3.6.2 Peritoneal CD11b+ Cells

To isolate CD11b+ peritoneal macrophages, peritoneal fluid was collected from mice and the cellular components were separated by centrifugation. Following red blood cell lysis, CD11b+ cells were isolated using the Dynabeads M-280 Streptavidin magnetic beads (Thermo Fisher Scientific, Waltham, MA) coupled to biotinylated CD11b monoclonal antibody (Thermo Fisher) according to

the manufacturer's protocol. Isolated CD11b+ cells were resuspended to 1 X 106 cells/mL concentration using DMEM/F-12 media containing 10% FBS.

2.3.6.3 Lymphatic endothelial cells

Primary mouse LECs were purchased from Cell Biologics (Chicago, IL) and cultured using mouse endothelial cell medium (Cell Biologics) containing 5% FBS in a 37°C incubator with 5% CO2. The cells were plated in 12-well plates at 90% confluence and starved overnight in media containing 1% FBS. The cells were then treated with either vehicle (saline) or Angiotensin II (1 μM) for 24 hours. For conditioned media experiments, the cells were incubated with a 1:1 ratio of endothelial cell media and conditioned media derived from vehicle- or Angiotensin II-treated splenocytes. At the end of 24 hours, cells were lysed using RNA lysis buffer (RNeasy Mini, Qiagen), total RNA isolated, and cDNA synthesized as described above. All experiments were conducted within passages 4-6. Primer sequences used in qRT-PCR are listed in Table A1 in the Appendix.

2.3.6.4 ELISA

Splenocytes and peritoneal CD11b+ cells were isolated as described above. Splenocytes and peritoneal CD11b+ cells were treated with saline, 1 μM Ang II, 1 μM Ang II + 1 μM Losartan (AT1aR inhibitor, Sigma), 1 μM Ang II + 1 μM PD123319 (AT2R inhibitor, Sigma), or 1 μM Ang II + 1 μM Losartan + 1 μM PD123319 for 48 hours. The conditioned media was collected from each treatment and VEGF-C was measured in the conditioned media using Mouse VEGF-C ELISA kit (LSBio, Seattle, WA).

2.3.7 Statistical Analysis

Data are presented as mean ± SEM. Statistical analysis were performed using GraphPad Prism, version 7.0e. Two-tailed Student's t test was used for analysis of data between 2 groups. One-way ANOVA followed by Tukey or Student–Newman–Keuls post-hoc analysis was used for testing significant differences between more than 2 groups. Significance was denoted at $P < 0.05$.

2.4 Results

2.4.1 Renal lymphatic vessel density is increased in male mice with Angiotensin II-induced hypertension

To examine changes in renal lymphatic density induced by A2HTN, male mice were infused with saline (control) or Ang II for 2 or 3 weeks. As expected, Ang II-infused mice were hypertensive at weeks 2 and 3 (Fig 2.1A; $P < 0.05$). Cross-sections of kidneys isolated from these mice were stained with antibodies against the lymphatic vessel markers LYVE-1 (Fig 2.1B) and podoplanin (not shown). Compared to controls, A2HTN male mice at 2 and 3 weeks had a visible increase in the number of lymphatic lumina (Fig 2.1B). This was then quantified by counting every LYVE-1+, lumen-containing vessel found around the cortical interlobular arteries in each kidney section. The mean number of lymphatic vessels per kidney section and per artery were significantly increased in A2HTN male mice at 2 and 3 weeks compared to controls (Fig 2.1C and 2.1D; $P < 0.01$).

Figure 2.1 Renal lymphatic vessel density is increased in male mice with angiotensin II-induced hypertension: (A) Systolic blood pressure measures in male mice infused with saline (Control) or Angiotensin II for 2 (M-ANGII-2wk) or 3 (M-ANGII-3wk) weeks. (B) LYVE-1 (lymphatic vessel endothelial hyaluronan receptor 1) immunofluorescence on kidney sections from Control, M-ANGII-2wk, and M-ANGII-3wk mice. Scale bars = 50 μm. Renal interlobular lymphatic density as determined by mean number of LYVE-1+, lumen-containing lymphatic vessels (RLVs) (C) per kidney section and (D) per artery. (E) Gene expression changes in lymphatic vessel markers in kidneys from Control, M-ANGII-2wk, and M-ANGII-3wk mice. (F) Immune cell populations expressed as percentage of $CD45_+$ cells in kidneys of Control, M-ANGII-2wk, and M-ANGII-3wk mice as determined by flow cytometry. Results are expressed as mean±SEM (n= 6 per group) and statistical analyses were performed with Student's *t* test. **P*<0.05 vs Control mice.

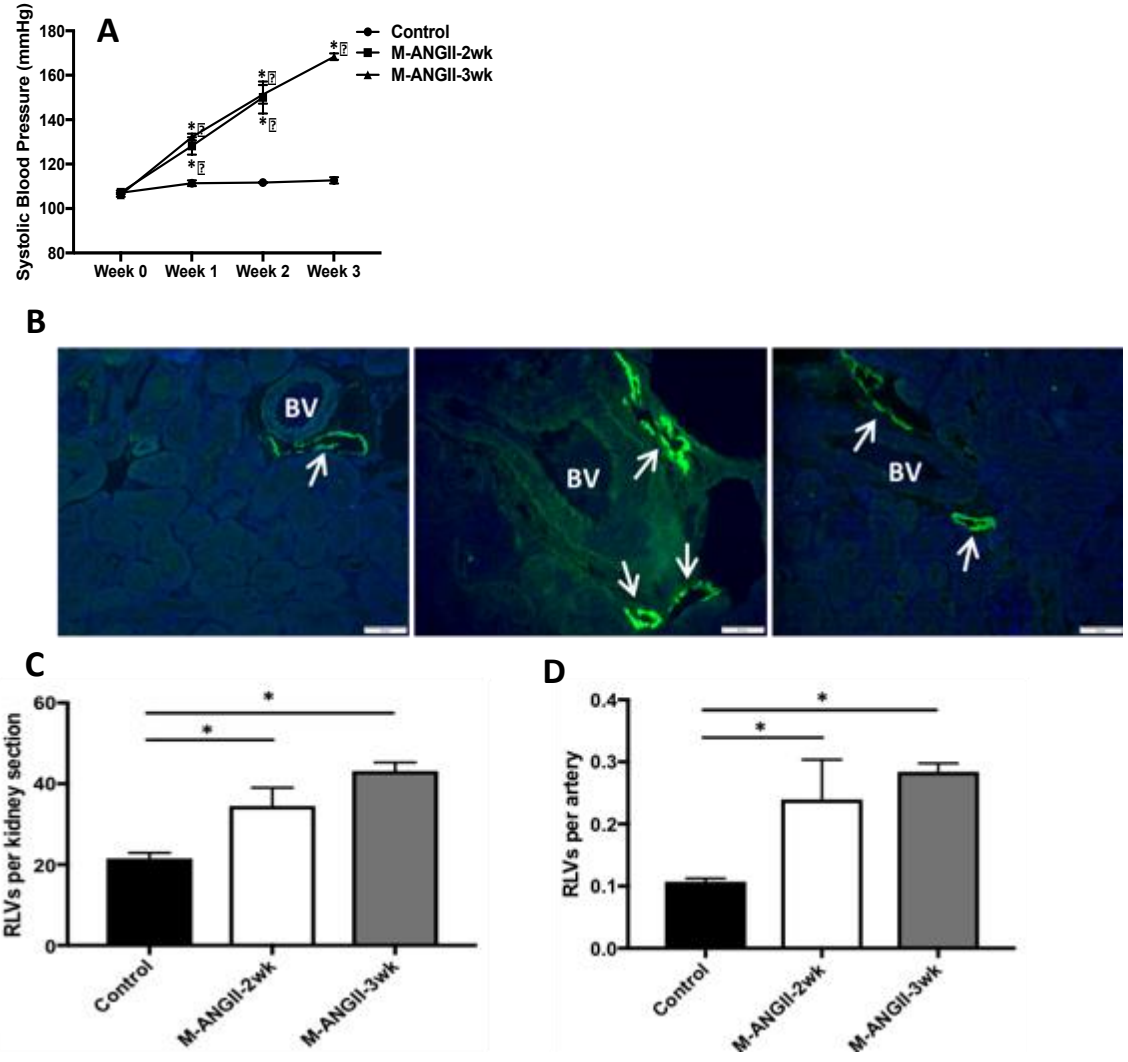

Figure 2.1 Continued

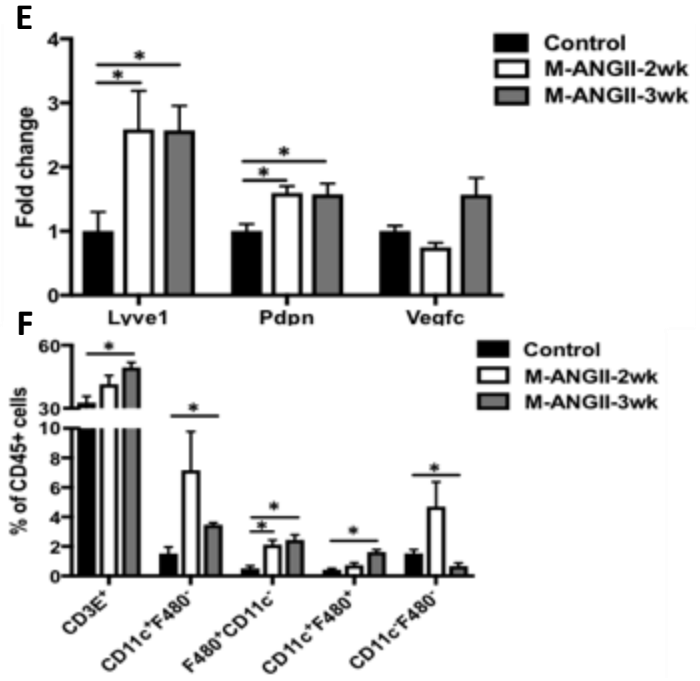

A corresponding increase in renal gene expression of *Lyve1* and *Pdpn* ($P < 0.05$) further supported these data, however there was no significant change in gene expression of the lymphangiogenic signal *Vegfc* (Fig 2.1E, $P = 0.28$). We hypothesized that this increase in renal lymphatic vessel density was an inflammation response and thereby associated with renal immune cell accumulation. To test this hypothesis, we performed flow cytometry analysis on the kidneys of these mice. The gating strategy used is provided in Fig 2.2. A2HTN male mice had significant increases in F4/80+CD11c- monocytes at 2 weeks, and CD3E+ T cells, CD11c+F4/80-, F4/80+CD11c-, and CD11c+F4/80+ monocyte populations at 3 weeks, while CD11c-F4/80- cells were decreased at week 3 (Fig 2.1F; $P < 0.05$). Renal mRNA expression of the pro-inflammatory markers *Tnfa*,

and *Il1b* were also increased in A2HTN male mice at 2 and 3 weeks (Fig 2.3; $P < 0.01$).

Figure 2.2: Flow cytometry gating strategy and representative plot. (A) Gating strategy for flow cytometry, and (B) Representative scatter plot for CD3e+ cells from Control and M-ANGII-3wk mice. Percentages are calculated out of CD45+ cells.

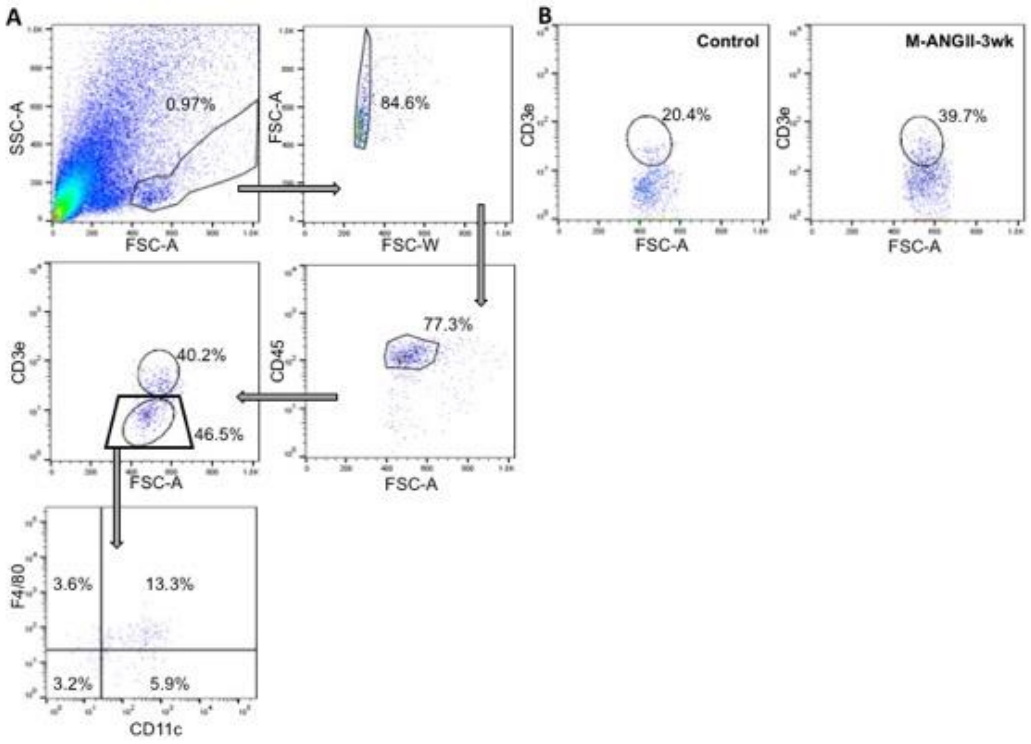

Together, these results suggest that A2HTN male mice demonstrate an increase in renal lymphatic vessel density in association with renal accumulation of pro-inflammatory immune cells and a corresponding increase in renal gene expression of pro-inflammatory cytokines.

Figure 2.3: Renal mRNA expression of pro-inflammatory cytokine markers in male mice with angiotensin II-induced hypertension: Gene expression changes in pro-inflammatory cytokine markers in kidneys of Control, M-ANGII-2wk, and M-ANGII-3wk mice (n=6 per group). Results are expressed as mean ±SEM. Statistical analyses were performed using one-way ANOVA with Tukey post-hoc. #0.05<*P*<0.1 vs Control mice; *P<0.05 vs Control mice.

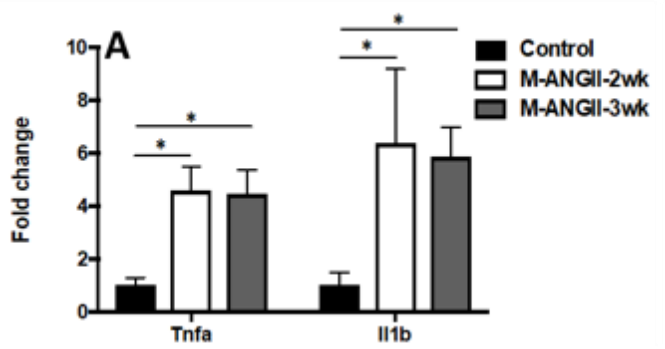

2.4.2 Renal lymphatic vessel density is increased in female mice with Angiotensin II-induced hypertension

As noted earlier, A2HTN females exhibit differences in immune activation and inflammatory milieu. Hence, we determined whether A2HTN in female mice was associated with an increase in renal lymphatic vessel density. Female mice were similarly infused with saline or Ang II for 2 or 3 weeks, and as expected, these mice were hypertensive although to a lesser degree than males (Fig 2.4A; $P < 0.05$).

Figure 2.4: Renal lymphatic vessel density is increased in female mice with angiotensin II-induced hypertension: (A) Systolic blood pressure measures in female mice infused with saline (Control) or Angiotensin II for 2 (F-ANGII-2wk) or 3 (F-ANGII-3wk) weeks. (B) LYVE-1 (lymphatic vessel endothelial hyaluronan receptor 1) immunofluorescence on kidney sections from Control, F-ANGII-2wk, and F-ANGII-3wk mice. Scale bars = 50 μm. Renal interlobular lymphatic density as determined by mean number of LYVE-1+, lumen-containing lymphatic vessels (C) per kidney section and (D) per artery. (E) Gene expression changes in

lymphatic vessel markers in kidneys from Control, F-ANGII-2wk, and F-ANGII-3wk mice. (F) Immune cell populations expressed as percentage of CD45+ cells in kidneys of Control, F-ANGII-2wk, and F-ANGII-3wk mice as determined by flow cytometry. Results are expressed as mean±SEM (n= 6 per group) and statistical analyses were performed with Student's t test. #0.05<P<0.1 vs Control mice; *P<0.05 vs Control mice.

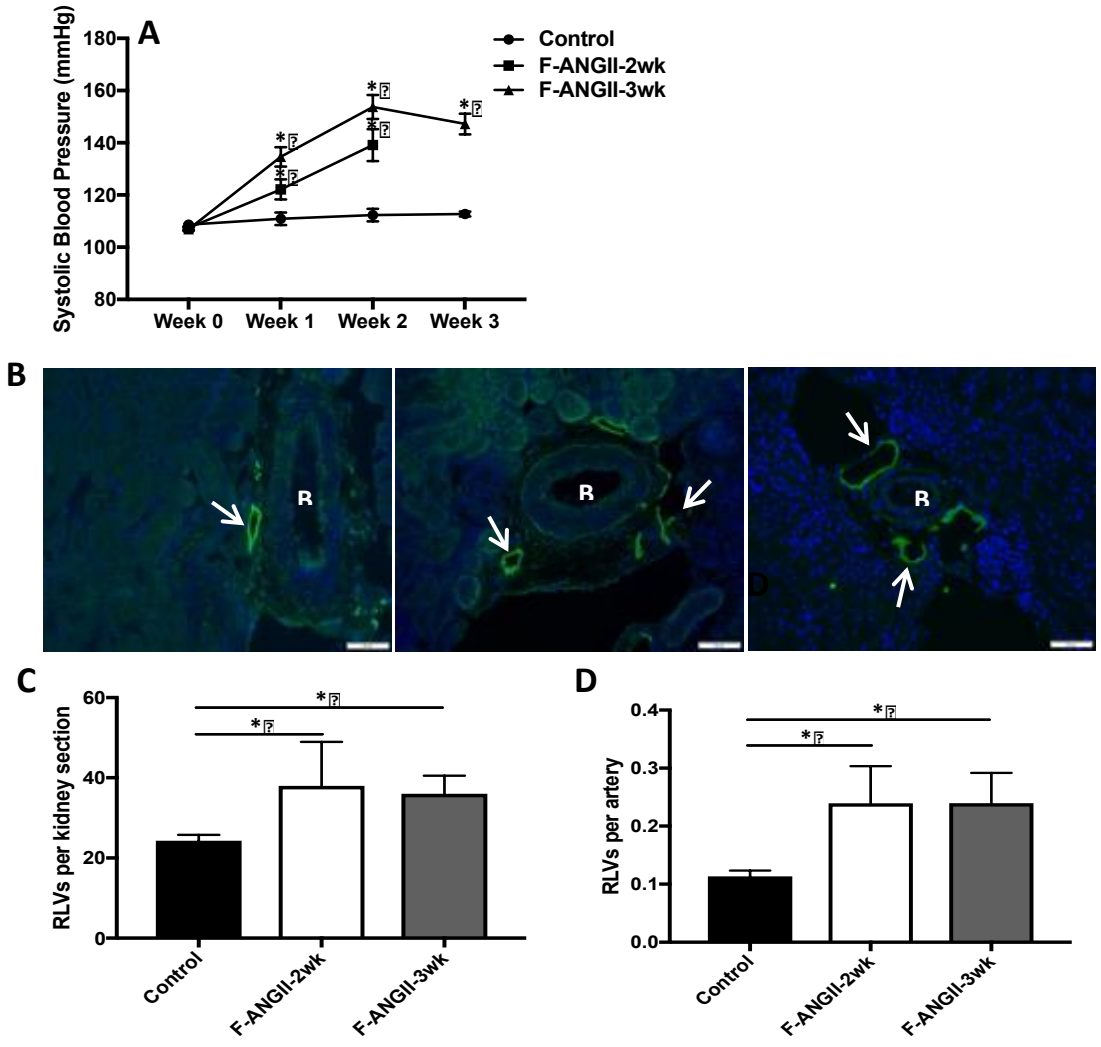

Figure 2.4 Continued

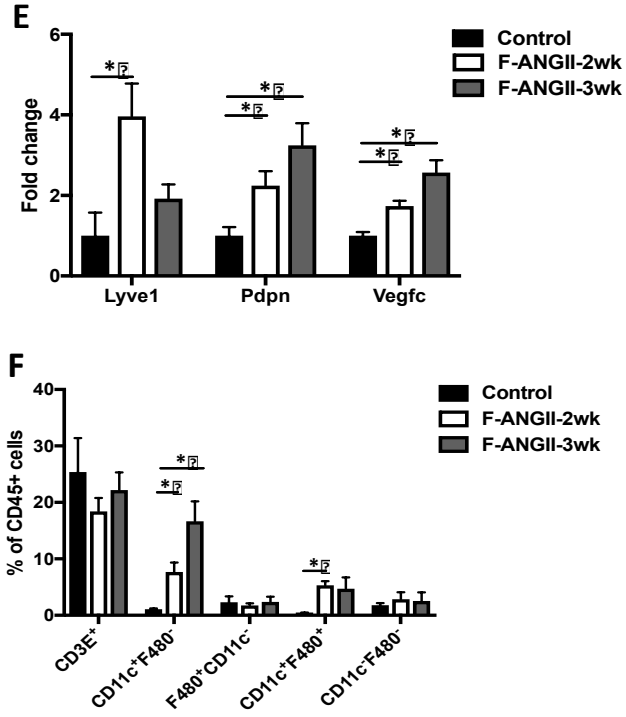

Similar to males, females with A2HTN had an increase in renal lymphatic vessel staining as demonstrated by immunofluorescence for LYVE-1 (Fig 2.4B) and podoplanin (not shown). Quantification of these vessels demonstrated that the mean number of lymphatic vessels per kidney section and per artery were significantly higher in A2HTN females at 2 and 3 weeks compared to controls (Figs 2.4C and 2.4D; $P < 0.05$). In addition to the increased mRNA expression of *Lyve1* and *Pdpn*, A2HTN females also upregulated their expression of *Vegfc* in the kidney (Fig 2.4E; $P < 0.05$). Upon analysis of renal immune cell populations, we noted that A2HTN females had significantly increased renal CD11c+F4/80- and CD11c+F4/80+ monocytes at 2 weeks, and that the CD11c+F4/80- monocytes

remained elevated at 3 weeks (Fig 2.4F; P < 0.05). The renal immune cell accumulation was also associated with a significant increase in gene expression of *Tnfa* and *Il1b* in the kidneys (Fig 2.5; P < 0.05). These data collectively suggest that A2HTN female mice demonstrate an increase in renal lymphatic vessel density in association with renal accumulation of CD11c+ monocytes and pro-inflammatory cytokines.

Figure 2.5: Renal mRNA expression of pro-inflammatory cytokine markers in female mice with angiotensin II-induced hypertension: Gene expression changes in pro-inflammatory cytokine markers in kidneys of Control, F-ANGII-2wk, and F-ANGII-3wk mice (n=6 per group). Results are expressed as mean ±SEM. Statistical analyses were performed using one-way ANOVA with Tukey post-hoc. #0.05<*P*<0.1 vs Control mice; **P*<0.05 vs Control mice.

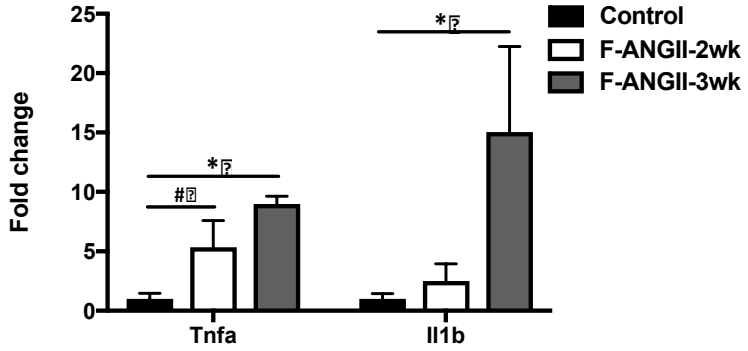

2.4.3 Angiotensin II-activated splenocytes induce LEC activation and inflammation

It has been reported that the concentration of Ang II in the renal interstitium is several folds higher than in the plasma. Since this interstitial fluid comes in direct contact with LECs, we first tested whether Ang II could directly act on LECs to induce their activation. Primary mouse LECs treated with vehicle or Ang II for 24 hours demonstrated no difference in gene expression for various markers

involved in LEC activation, adhesion, and proliferation (Fig 2.6A). Furthermore, no detectable transcript levels of the Ang II receptors *Agtr1a* or *Agtr2* were found in these LECs (Fig 2.6B), suggesting that interstitial Ang II does not directly act on LECs. Since there were no direct effects of Ang II on LECs, we then determined the effects of Ang II-treated immune cells on LECs. Splenocytes were treated with vehicle control (saline) or Ang II for 48 hours and conditioned media (CM) was collected. In order to elicit an acute response to Ang II treatment in vitro, and since females are known to have a dampened immune response to Ang II, only splenocytes isolated from male mice were used. Compared to control CM-treated

Figure 2.6: Angiotensin II-activated immune cells induce lymphatic endothelial cell activation and inflammation: (A) Gene expression changes in LECs treated with vehicle (saline) or Angiotensin II for 24 hours. (B) Gel electrophoresis of PCR products from mouse kidney (positive control) and primary mouse LECs amplified for *Agtr1a* and *Agtr2*. *Rn18s* was used as housekeeping gene. (C) Gene expression changes in LECs treated for 24 hours with conditioned media from saline-treated or Angiotensin II-treated splenocytes. VEGF-C levels in conditioned media derived from (D) splenocytes or (E) peritoneal CD11b+ cells treated with saline, Angiotensin II, Angiotensin II + Los, Angiotensin II + PD, or Angiotensin II + Los + PD for 48 hours as measured by ELISA. All experiments were performed in triplicate. Results are expressed as mean±SEM and statistical analyses were performed with Student's *t* test. **P*<0.05 vs Control or Control CM.

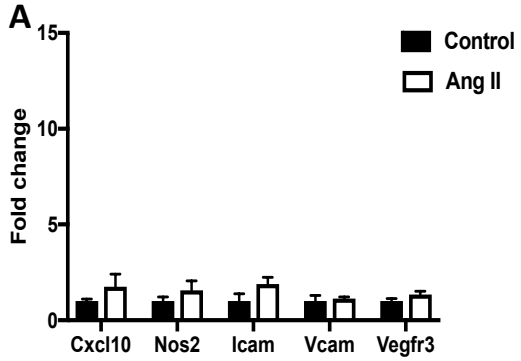

Figure 2.6 Continued

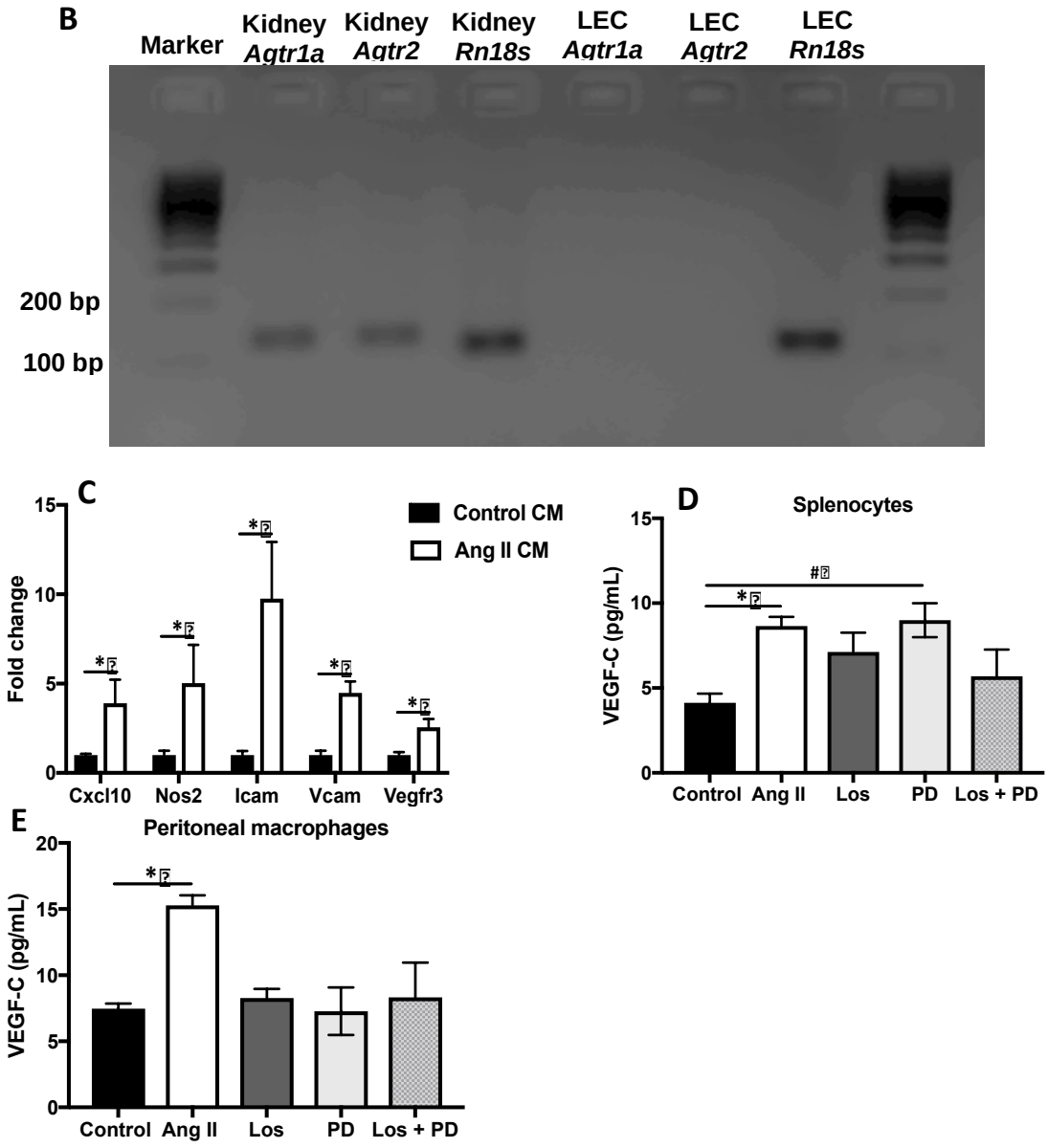

LECs, Ang II CM-treated LECs had increased gene expression of the inflammatory markers *Cxcl10* and *Nos2*, the adhesion molecules *Icam* and *Vcam*, and the VEGF-C/VEGF-D receptor *Vegfr3* (Fig 2.6C; $P < 0.01$). To identify whether Ang II induces immune cells to secrete VEGF-C, splenocytes and

peritoneal CD11b+ cells were isolated and treated with Ang II. Treatment with Ang II induced elevated secretion of the VEGFR-3 ligand VEGF-C as measured by ELISA (Fig 2.6D and 2.6E; $P < 0.05$). Furthermore, inhibition of the Ang II receptors AT1aR and AT2R with Losartan (Los) and PD123319 (PD), respectively, blocked the secretion of VEGF-C (Fig 2.6D and 2.6E). These results demonstrate that while interstitial Ang II does not directly act on LECs, it induces activation of LECs through its effects on immune cells and primarily CD11b+ cells.

2.4.4 Genetic augmentation of renal lymphatic vessel density prevents the development of angiotensin II-induced hypertension in male mice

We used our genetic mice that undergo doxycycline (DOX)-inducible, kidney-specific VEGF-D overexpression (KidVD) that leads to massive lymphangiogenesis to determine the effects of enhanced renal lymphatic density on A2HTN (Lammoglia et al., 2016). Administration of DOX a week before Ang II infusion induced the overexpression of the VEGFR-3 specific ligand VEGF-D and lead to augmentation of renal lymphatic density in KidVD+ male mice. KidVD- male mice infused with Ang II became hypertensive starting at week 1 and remained hypertensive throughout the 3-week Ang II infusion.

Figure 2.7: Genetic augmentation of renal lymphatic vessel density prevents the development of angiotensin II-induced hypertension in male mice: (A) Systolic blood pressure measures in KidVD(-) and KidVD(+) male mice infused with Angiotensin II for 3 weeks (KidVD(-) M-ANGII and KidVD(+) M-ANGII). (B) Podoplanin immunofluorescence on kidney sections from KidVD(-) M-ANGII and KidVD(+) M-ANGII mice. Scale bars = 50 μm. (C) Renal lymphatic density in KidVD(-) M-ANGII and KidVD(+) M-ANGII mice as measured by podoplanin+ pixel density. (D) Gene expression changes in lymphatic vessel markers in kidneys

from KidVD(-) M-ANGII and KidVD(+) M-ANGII. (E) Renal microvessel density in KidVD(-) M-ANGII and KidVD(+) M-ANGII mice measured by endomucin+ pixel density. (F) Immune cell populations expressed as percentage of CD45+ cells in kidneys of KidVD(-) M-ANGII and KidVD(+) M-ANGII mice as determined by flow cytometry. Results are expressed as mean±SEM (n= 5 per group) and statistical analyses were performed with Student's *t* test or one-way ANOVA. #0.05<*P*<0.1 vs KidVD(-) M-ANGII mice; *P<0.05 vs KidVD(-) M-ANGII mice.

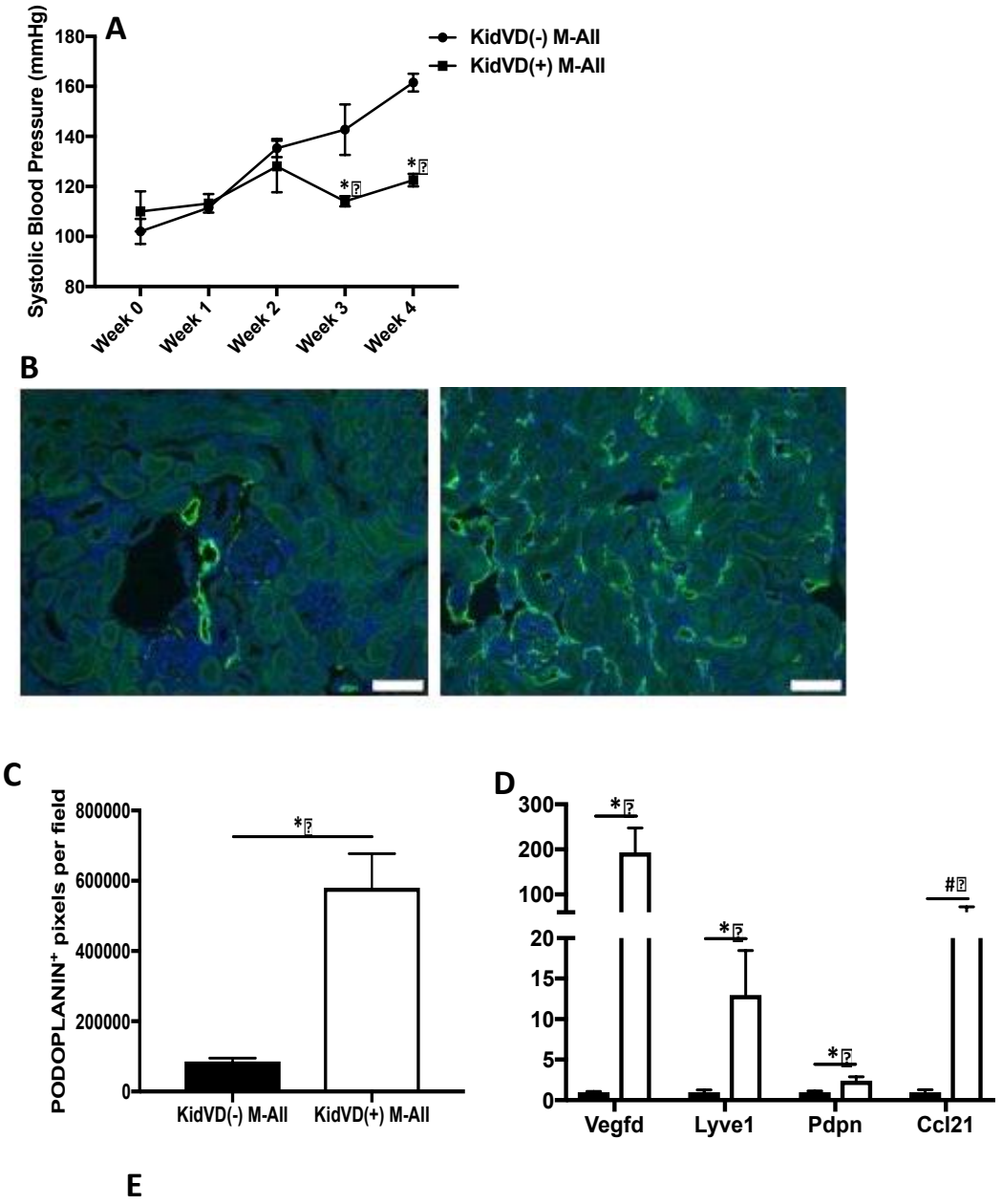

Figure 2.7 Continued

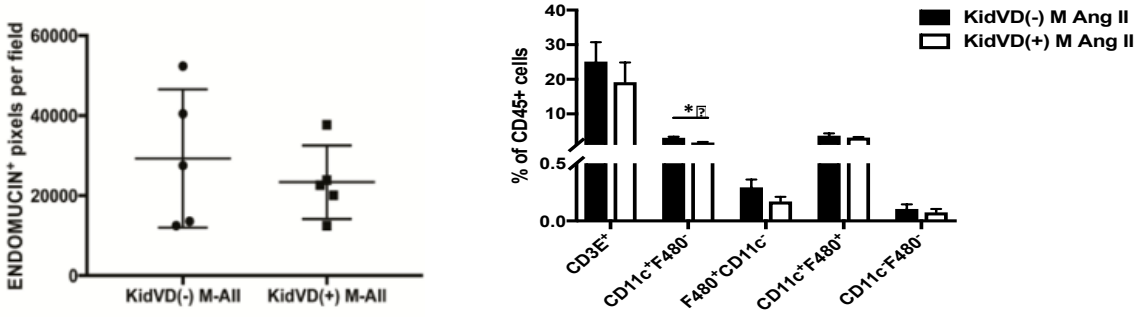

Renal immunofluorescence for podoplanin (Fig 2.7B), podoplanin+ pixel density (Fig 2.7C; $P < 0.001$), and gene expression of associated lymphatic vessel markers (Fig 2.7D; $P < 0.05$) supported the augmented renal lymphatic density. Gene expression of the LEC-derived immune cell trafficking chemokine *Ccl21* also tended to be increased in KidVD+ males (Fig 2.7D; $P = 0.08$). The observed BP response was not due to alterations in microvessel density, as identified by quantification of endomucin+ pixel density (Fig 2.7E). In association with the attenuation of BP, KidVD+ male mice demonstrated a significant decrease in renal CD11c+F4/80- monocytes (Fig 2.7E; $P < 0.05$). Gene expression of *Tnfa* and *Il1b* that were previously elevated in the A2HTN males were normalized in Ang II-treated KidVD+ males (Fig 2.8A). Additionally, while wild-type male mice given Ang II had significantly elevated levels of the injury markers *Fn1* and *Lcn2*, these were normalized in KidVD+ mice (Fig 2.8B). These data demonstrate that augmentation of renal lymphatic vessel density in male KidVD+ mice prevented the development of A2HTN and this was associated with a reduction in renal CD11c+F4/80- monocytes.

Figure 2.8: Renal mRNA expression of pro-inflammatory cytokine and injury markers in male mice: (A) Gene expression changes in pro-inflammatory cytokine markers in kidneys of KidVD(-) M-AII and KidVD(+) M-AII (n=5-6 per group). (B) Gene expression changes in kidney injury markers of (A) Control, M-ANGII-3wk, and KidVD(+) M-ANGII (n=5-6 per group). Results are expressed as mean ±SEM. Statistical analyses were performed using Student's *t* test or one-way ANOVA followed by Tukey post-hoc as appropriate. #0.05<*P*<0.1 vs Control mice; **P*<0.05 vs Control mice.

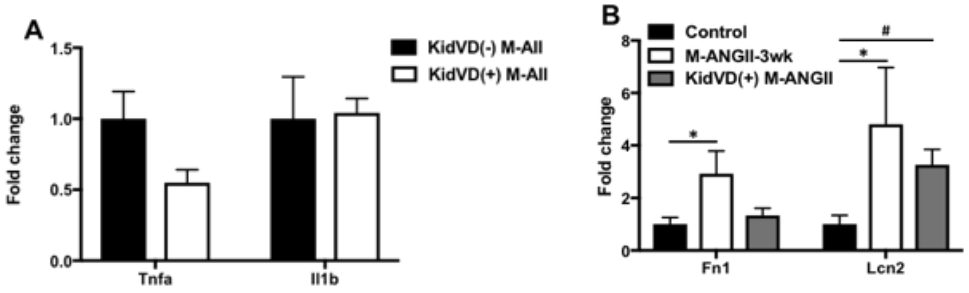

2.4.5 Genetic augmentation of renal lymphatic vessel density prevents the development of angiotensin II-induced hypertension in female mice

Given the possible contribution of different immune mechanisms to hypertension and associated lymphangiogenesis in male and female mice, we determined if augmented renal lymphatic vessel density could prevent A2HTN in female mice. DOX was administered to female KidVD- and KidVD+ mice for a week, following which these mice received DOX and Ang II for 3 weeks. Similar to males, KidVD- female mice developed hypertension, but KidVD+ female mice did not develop A2HTN (Fig 2.9A). The expansion of renal lymphatic density in KidVD+ females was confirmed by immunofluorescence for podoplanin (Fig 2.9B), podoplanin+ pixel quantification across kidney sections (Fig 2.9C; $P < 0.001$), and qPCR for *Vegfd*, *Lyve1*, and *Pdpn* (Fig 2.9D; $P < 0.01$). KidVD+ females also had significantly increased renal mRNA expression of *Ccl21* (Fig 2.9D; $P < 0.01$).

Quantification of endomucin+ pixel density revealed no changes in microvasculature density between these mice (Fig 2.9E). We hypothesized that the enhanced renal lymphatic density would aid in the exfiltration of immune cells. Indeed, similar to KidVD+ males, KidVD+ female mice had a significant reduction in renal CD11c+F4/80- monocytes ($P < 0.05$), however, there were no changes in the other immune cell populations analyzed (Fig 2.9F).

Figure 2.9: Genetic augmentation of renal lymphatic vessel density prevents the development of angiotensin II-induced hypertension in female mice: (A) Systolic blood pressure measures in KidVD(-) and KidVD(+) female mice infused with Angiotensin II for 3 weeks (KidVD(-) F-ANGII and KidVD(+) F-ANGII). (B) Podoplanin immunofluorescence on kidney sections from KidVD(-) F-ANGII and KidVD(+) F-ANGII mice. Scale bars = 50 μm. (C) Renal lymphatic density in KidVD(-) F-ANGII and KidVD(+) F-ANGII mice as measured by podoplanin+ pixel density. (D) Gene expression changes in lymphatic vessel markers in kidneys from KidVD(-) F-ANGII and KidVD(+) F-ANGII. (E) Renal microvessel density in KidVD(-) F-ANGII and KidVD(+) F-ANGII mice measured by endomucin+ pixel density. (F) Immune cell populations expressed as percentage of $CD45_+$ cells in kidneys of KidVD(-) F-ANGII and KidVD(+) F-ANGII mice as determined by flow cytometry. Results are expressed as mean±SEM (n= 5 per group) and statistical analyses were performed with Student's *t* test or one-way ANOVA. #0.05<*P*<0.1 vs KidVD(-) F-ANGII mice; *$P<0.05$ vs KidVD(-) F-ANGII mice.

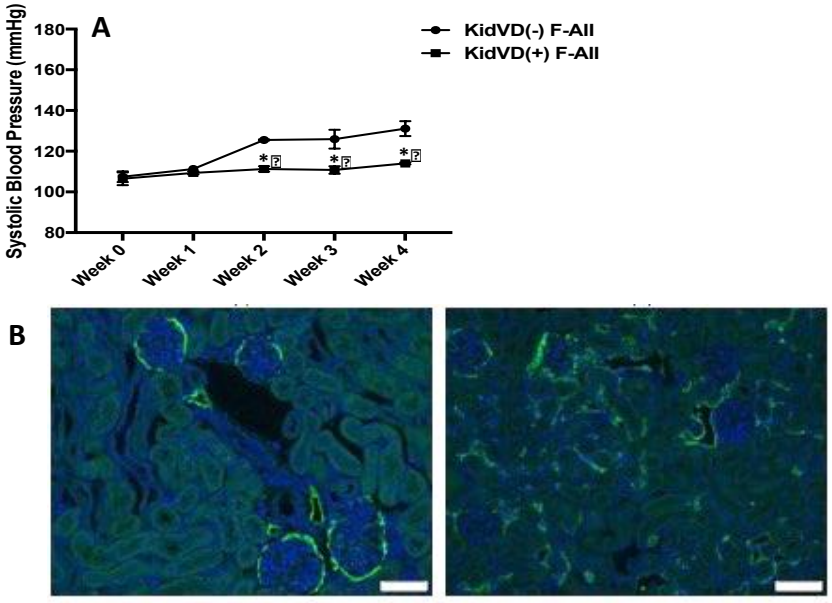

Figure 2.9 Continued

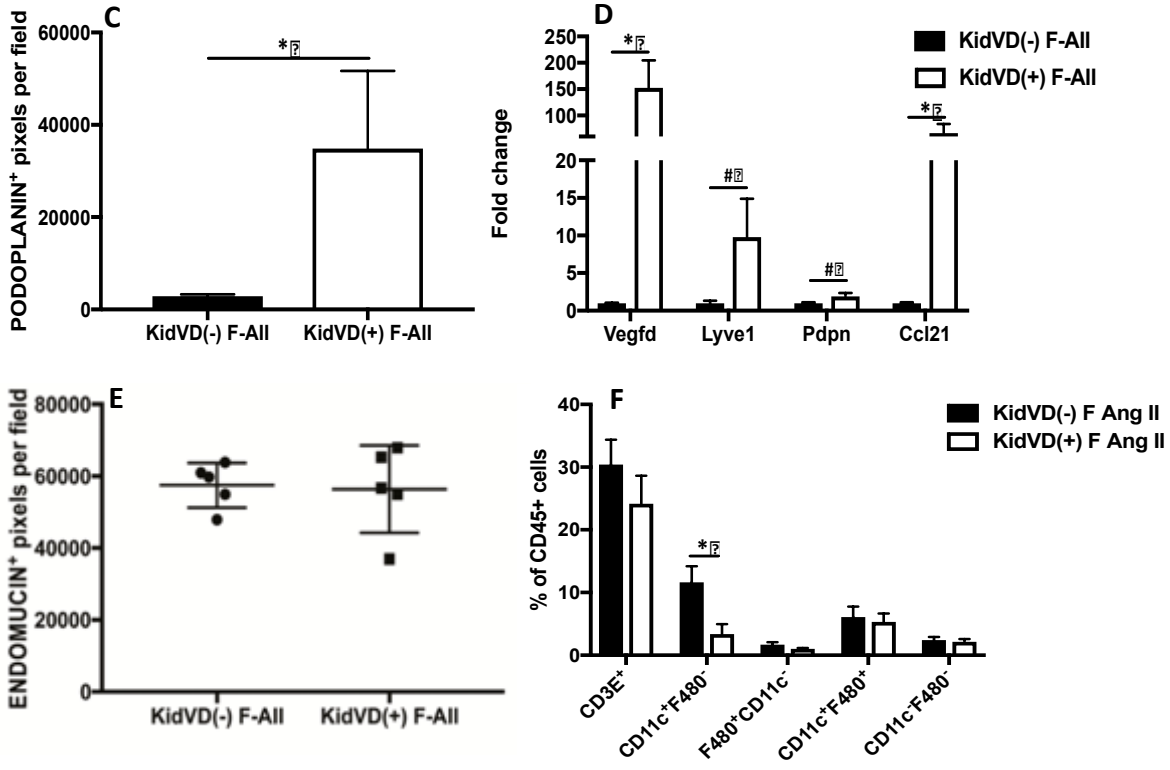

Furthermore, mRNA levels of *Tnfa* and *Il1b* were normalized in Ang II-treated KidVD+ female mice compared to wild-type mice given Ang II (Fig 2.10A). As expected, although wild-type female mice given Ang II did not have significantly increased gene levels of *Fn1* and *Lcn2*, they tended towards an increase, whereas mRNA levels of these renal injury markers were not elevated in KidVD+ female mice (Fig 2.10B). Thus, augmentation of renal lymphatic vessel density in female mice prevented the development of A2HTN in association with a reduction in renal CD11c+F4/80- monocytes.

Figure 2.10: Renal mRNA expression of pro-inflammatory cytokine and injury markers in female mice: (A) Gene expression changes in pro-inflammatory cytokine markers in kidneys of KidVD(-) M-AII and KidVD(+) M-AII (n=5-6 per group). (B) Gene expression changes in kidney injury markers of (A) Control, M-ANGII-3wk, and KidVD(+) M-ANGII (n=5-6 per group). Results are expressed as mean ±SEM. Statistical analyses were performed using Student's *t* test or one-way ANOVA followed by Tukey post-hoc as appropriate. #0.05<*P*<0.1 vs Control mice; **P*<0.05 vs Control mice.

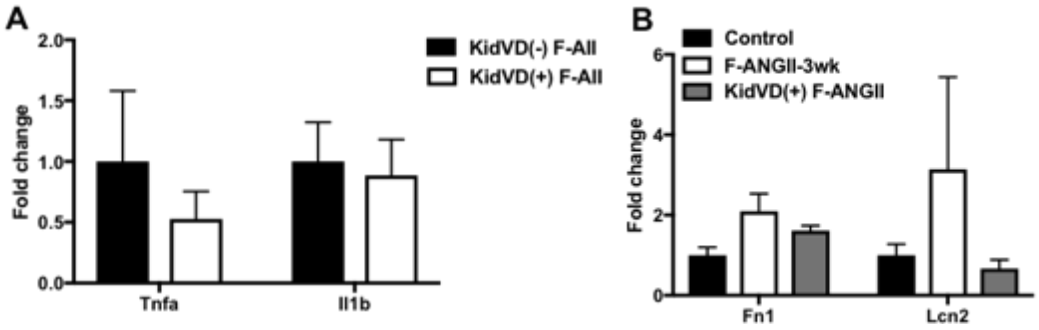

2.5. Discussion

In this study, we demonstrated that renal lymphatic vessel density and immune cell numbers are increased in kidneys of male and female mice with A2HTN. We also demonstrated that Ang II does not have direct effects on LECs since they lack Ang II receptors, but acts on immune cells, primarily CD11b+ cells, to induce the secretion of the lymphangiogenic growth factor VEGF-C, and this process is Ang II receptor-dependent. Additionally, CM from Ang II-activated immune cells induced the transcription of the lymphangiogenic growth factor receptor *Vegfr3*, adhesion molecules *Icam* and *Vcam*, and inflammatory markers *Cxcl10* and *Nos2* in LECs. Lastly, we demonstrated that augmenting renal lymphatic density prevented the development of A2HTN in male and female mice,

and in both cases, we observed a reduction in renal CD11c+F4/80- monocyte accumulation.

In general, female mice have a greater expression and activation of the nonclassical RAS (Ang type II receptor, Mas receptor, ACE2) which is thought to underlie their differential response to Ang II (Ramirez and Sullivan, 2018). The kidneys in particular might play an essential role in mediating these differences as kidney transplant from female to male mice attenuated Ang II-induced increases in BP (Wang et al., 2017). In our study, although associative, we noted differences in renal immune cell accumulation between males and females. While males showed significant increases in T cell and CD11c+F4/80-, F4/80+CD11c-, and CD11c+F4/80+ monocytes after 3 weeks of Ang II, females only exhibited an increase in CD11c+F4/80-monocytes at this time point. Studies have demonstrated that females have attenuated renal T cell accumulation and have been shown to be partially protected from the pro-hypertensive effects of T cells in A2HTN. The female hormonal milieu has been suggested to suppress T cell mediated reactions, although this remains unclear. Once activated, monocytes secrete pro-inflammatory cytokines and activate T cells. Naïve T cells polarize to Th1 or Th17 cells, which in turn secrete cytokines and cause sodium retention and hypertension (Norlander and Madhur, 2017). While *Tnfa* and *Il1b* gene expression in the kidneys was upregulated by 2 weeks of Ang II infusion in males, these cytokines were increased mostly only by the 3rd week in females. The mechanisms behind this discrepancy are currently unknown; nevertheless, our

study further corroborates the existence of sex-specific regulation of immune mechanisms during A2HTN.

Figure 2.11: Sex-specific differences in blood pressure but not in renal lymphatic density in mice: (A) Systolic blood pressure measures after 3 weeks of saline or angiotensin II treatment in wild-type and KidVD male and female mice. (B) Renal interlobular lymphatic density as determined by mean number of LYVE-1+, lumen-containing lymphatic vessels (RLVs) per kidney section after 3 weeks of saline or angiotensin II treatment in wild-type and KidVD male and female mice. Results are expressed as mean±SEM (n= 5-6 per group) and statistical analyses were performed with Student's *t* test. **P*<0.05 vs same treatment/genotype male mice.

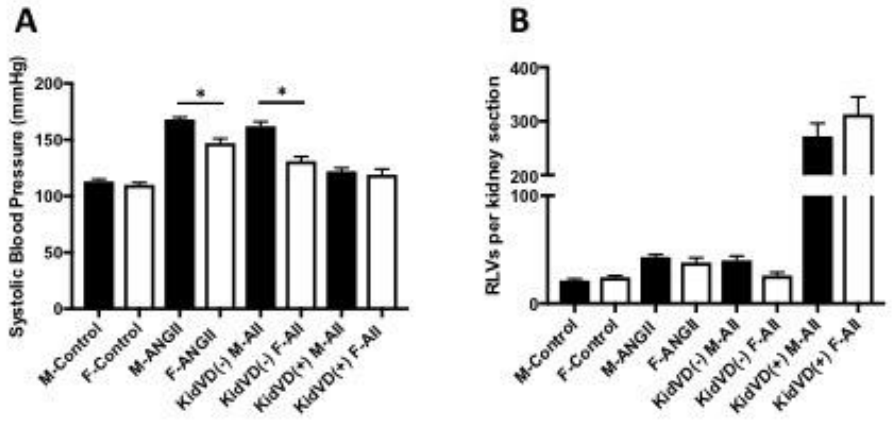

Regardless of the difference in pressor response to Ang II infusion, A2HTN male and female mice both had an almost 2-fold increase in the number of renal lymphatic vessels per artery (Fig 2.11), suggesting that the lymphangiogenesis is caused by other stimuli and not the blood pressure itself. In the kidney, activated macrophages and tubular epithelial cells could secrete VEGF-C and contribute to lymphangiogenesis (Suzuki et al., 2012). Since renal interstitial Ang II levels are several fold higher than in the plasma (Navar, 2014), we determined whether Ang

II has direct effects on LECs in vitro. The lack of changes in gene expression indicates that Ang II does not directly act on LECs, likely due to the absence of its receptors on LECs. However, conditioned media from Ang II-stimulated splenocytes induced the transcription of *Cxcl10*, *Nos2*, *Icam*, and *Vcam* in LECs. Ang II has been shown to induce immune cell proliferation and their secretion of pro-inflammatory cytokines (Hahn et al., 1994; Nataraj et al., 1999). When activated by these cytokines, LECs increase their expression of adhesion molecules and chemokines and this has been shown to aid leukocyte transmigration across the lymphatic endothelium (Johnson et al., 2006; Sawa et al., 2007). In addition, LECs also increased their transcription of the VEGF-C receptor *Vegfr3* when treated with Ang II CM. Inflammatory stimuli have been shown to induce VEGF-C secretion by immune cells, and hence, to identify whether Ang II stimulates immune cells to secrete VEGF-C, splenocytes and peritoneal CD11b+ cells were stimulated with Ang II *in vitro*. Treatment with Ang II induced VEGF-C secretion by both splenocytes and peritoneal CD11b+ cells. Inhibiting AT1R or both AT1R and AT2R, but not AT2R alone, on splenocytes diminished this response, whereas blocking either of the receptors or both prevented the increase in VEGF-C secretion by CD11b+ cells. Whether Ang II receptor stimulation directly induces VEGF-C secretion or activates the TGFß or connective tissue growth factor (CTGF) pathway to induce VEGF-C will be examined.

Although inflammation-associated lymphangiogenesis is a common event in chronic inflammation, the consequences of these newly grown vessels seem to be tissue- and context-dependent (Kerjaschki et al., 2004; Huggenberger et al., 2011). In the context of hypertension, our lab has previously demonstrated that renal inflammation induces lymphangiogenesis and that further augmenting renal lymphatic density prevents the development of nitric oxide inhibition-induced and salt-sensitive hypertension (Kneedler et al., 2017; Lopez Gelston et al., 2018). Besides immune activation, sex differences may also exist in the regulation of lymphatic responses. Recently, it was shown that estradiol promotes the transcriptional upregulation of *Vegfd*, *Vegfr3*, and *Lyve1*, and confers a protective effect against lymphedema (Morfoisse et al., 2018). Here, we report that females, but not males, have an increased gene expression of *Vegfc* in the kidney during Ang II infusion. Whether females have a more robust lymphangiogenic response to Ang II-induced renal inflammation and whether this underlies their different susceptibilities to Ang II-induced responses remains to be determined. Overall, these differences highlight the need to independently investigate BP regulation in both males and females. Nonetheless, augmenting renal lymphatic density using our genetic mouse model was able to prevent the development of A2HTN in both male and female mice. It should be noted that while the tail-cuff method is sufficient to detect large differences in BP as seen in this study, it would be beneficial to obtain more accurate BP values using the telemetry approach. The enhanced lymphatics could aid in the clearance of interstitial immune cells, as

evidenced by reduced accumulation of renal CD11c+F4/80- monocytes in both males and females.

Figure 2.12 Augmenting renal lymphatic density prevents angiotensin II-dependent hypertension: A) Hypertensive stimuli such as angiotensin II induce renal inflammation and immune cell accumulation, which lead to the development of hypertension. In this study, we demonstrated that renal lymphatic vessel density is increased in angiotensin II-induced hypertension in association with renal inflammation. Other factors such as sodium retention or high blood pressure that could potentially contribute to increased renal lymphatic vessel density have not been determined. B) Genetically augmenting renal lymphatic vessel density before exposure to hypertensive stimuli such as angiotensin II reduces renal inflammation and prevents the development of hypertension. Whether augmenting renal lymphatic vessels also reduces blood pressure by reducing sodium retention remains unknown. Dashed lines indicate hypothesized mechanisms that have not been proved.

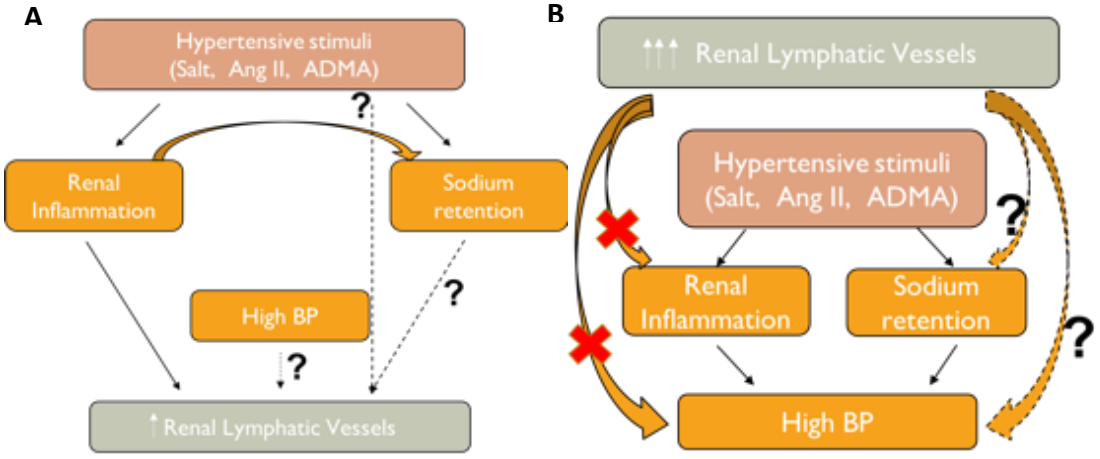

In conclusion, A2HTN induces an increase in renal lymphatic vessel density in male and female mice (Fig 2.12). Ang II induces secretion of the lymphangiogenic growth factor VEGF-C by activated immune cells *in vitro* and could potentially aid lymphangiogenesis. Further augmentation of renal lymphatic density beyond pathological levels prevents the development of A2HTN in males and females and might represent a novel mechanism of regulation of BP.

3. KIDNEY-SPECIFIC LYMPHANGIOGENESIS INCREASES SODIUM EXCRETION AND LOWERS BLOOD PRESSURE IN MICE*

3.1 Overview

Hypertension is associated with renal immune cell accumulation and sodium retention. Lymphatic vessels provide a route for immune cell trafficking and fluid clearance. Our lab has previously demonstrated that genetically augmenting renal lymphatic vessel density can prevent salt-sensitive, L-NAME-induced and angiotensin II-dependent hypertension in mice. In these models, we demonstrated that the prevention of hypertension was associated with a reduction in immune cell accumulation in the kidneys of these mice. However, while these models demonstrate proof-of-concept for the role of renal lymphatics in blood pressure regulation, a more clinically relevant model would be to determine whether augmenting renal lymphatic vessels after hypertension is established would attenuate hypertension. Moreover, while we demonstrated the reduction in renal immune cell accumulation and renal inflammation in these mice, the exact mechanisms by which blood pressure was reduced were not determined. In the current study, we investigated whether augmenting renal lymphatic vessel density can reduce blood pressure in a model of established hypertension induced by nitric oxide inhibition. Based on previous studies from our lab, we determined whether augmenting renal lymphatic vessels reduces renal immune cell

*Reprinted from Balasubbramanian, D., Baranwal, G., Clark, M. C. C., Goodlett, B. L., Mitchell, B. M., & Rutkowski, J. M. (2020). Kidney-specific lymphangiogenesis increases sodium excretion and lowers blood pressure in mice. *Journal of Hypertension*.

accumulation in these mice. We also investigated whether augmenting renal lymphatic vessels affects sodium homeostasis, since sodium retention is a hallmark of human and several experimental forms of hypertension.

Here, we tested the hypothesis that augmenting renal lymphatic density can attenuate blood pressure in established hypertension. Transgenic mice with inducible kidney-specific overexpression of VEGF-D ("KidVD+" mice) and KidVD- controls were administered a nitric oxide synthase inhibitor, L-NAME, for 4 weeks, with doxycycline administration beginning at the end of week 1. To identify mechanisms by which renal lymphatics alter renal Na^+ handling, Na^+ excretion was examined in KidVD+ mice during acute and chronic salt loading conditions. Renal VEGF-D induction for 3 weeks enhanced lymphatic density and significantly attenuated blood pressure in KidVD+ mice while KidVD- mice remained hypertensive. No differences were identified in renal immune cells, however, the urinary Na^+ excretion was increased significantly in KidVD+ mice. KidVD+ mice demonstrated normal basal sodium handling, but following chronic high salt loading, KidVD+ mice had a significantly lower blood pressure along with increased urinary fractional excretion of Na^+. Mechanistically, KidVD+ mice demonstrated decreased renal abundance of total NCC and cleaved ENaCα Na^+ transporters, increased renal interstitial fluid volume, and increased plasma ANP. Our findings demonstrate that therapeutically augmenting renal lymphatics increases natriuresis and reduces blood pressure under sodium retention conditions.

3.2 Introduction

Hypertension, or high blood pressure (BP), affects more than 45% of U.S. adults, and is the largest contributing factor to mortality in the U.S and the world. While many factors contribute to the pathogenesis of hypertension, inappropriate activation of the immune system and renal infiltration of pro-inflammatory immune cells have been identified in several experimental models and in patients with hypertension. The specific mechanisms that activate the immune system are still being discovered, however, once activated, immune cells infiltrate the kidney and inflammatory cytokines alter renal sodium (Na^+) transport, affect renal blood flow, and aggravate hypertensive damage to the kidney.

Lymphatic vessels shape immune responses through their varied roles in immune function including trafficking of antigens and leukocytes from peripheral sites to lymph nodes, antigen presentation, modulation of immune cell function, and expression of immunomodulatory factors (Breslin et al., 2018). Lymphatic vessels are thus implicated in an increasing number of chronic inflammatory diseases (Baluk et al., 2005),(Huggenberger et al., 2010), including obesity (Chakraborty et al., 2019),(Nores et al., 2016), and hypertension (Lopez Gelston et al., 2018), and therapeutically manipulating lymphatic vessel growth and function positively alters the course of disease and improves outcomes (Abouelkheir et al., 2017),(Aspelund et al., 2016). We have previously demonstrated that renal lymphatic vessel density increases during aging- and hypertension-associated renal inflammation and injury in a compensatory manner

(Kneedler et al., 2017). Using our mouse model of inducible kidney-specific overexpression of the lymphangiogenic factor VEGF-D (KidVD), we demonstrated that selectively augmenting lymphatic density in the kidney reduced renal immune cell accumulation and prevented the development of salt-sensitive, nitric oxide-inhibition-induced, and angiotensin II-induced hypertension (Lopez Gelston et al., 2018). Similarly, stimulating cardiac lymphangiogenesis decreased macrophage infiltration and lowered BP in rats fed a high salt diet (Yang et al., 2014).

Na^+ retention is a hallmark of human (Endre et al., 1994),(Kawasaki et al., 1978) and experimental hypertension (Zhang et al., 2016),(Giani et al., 2015b). Evidence obtained from studies of renal transplantation, mutations in renal Na^+ transporters, and diuretic actions demonstrate that renal fractional Na^+ reabsorption is an essential regulator of effective extracellular volume and BP (Rossier et al., 2013),(Crowley and Coffman, 2014). In 2009, Titze and colleagues outlined a novel concept in demonstrating that dermal lymphatic vessels regulate BP by undergoing hyperplasia in response to the interstitial accumulation of Na^+ in mice fed a high salt diet (Machnik et al., 2009). Blocking lymphangiogenesis resulted in electrolyte accumulation and significantly elevated BP with no reported changes to the renal lymphatics. Past studies in dogs and rats have demonstrated that ligating the extrarenal collecting lymphatic vessels transiently increased BP and induced natriuresis via extracellular volume expansion (Lilienfeld et al., 1967),(Wilcox et al., 1984). The specific mechanisms by which lymphatic vessels within the kidney potentially regulate Na^+ homeostasis thus remain undetermined.

In this study, we investigated the effects of renal lymphatic augmentation on the attenuation of BP in established hypertension. We hypothesized that the therapeutic induction of increased renal lymphatic density will lower BP in mice with nitric oxide-inhibition-induced hypertension by reducing renal immune cell accumulation and increasing urinary Na^+ excretion. We also characterized the effects of augmenting renal lymphatic density on the physiological regulation of renal Na^+ excretion during acute and chronic salt loading conditions.

3.3 Materials and Methods

3.3.1 Animal Care

All animal use protocols were approved by the Texas A&M University IACUC and were performed in accordance with the NIH Guide for the Care and Use and Care of Laboratory Animals.

3.3.2 Mice

The generation of transgenic KidVD mice has been described previously (Lammoglia et al., 2016). TRE-VEGF-D mice were crossed with mice carrying a kidney promoter-driven rtTA (Cdh16; KSP) to generate KidVD mice that overexpress VEGF-D specifically in the kidney following doxycycline administration. The KSP-rtTA mouse was made available by the University of Texas-Southwestern George M. O'Brien Kidney Research Core Center (P30DK079328). KidVD mice were backcrossed minimally 7 generations to C57BL/6J. All mice were hemizygous for the TRE-VEGF-D transgene, and were either wild-type or hemizygous for the KSP-rtTA transgene. All experiments were

conducted with littermates, and doxycycline was administered to all mice for the same duration within each experiment to control for the effects of doxycycline. Mice were housed in a 12-hour light/12-hour dark cycle. Male and female mice were equally assigned to experimental groups. All mice used in this study were between 12-16 weeks of age and had ad libitum access to diets and water. At the end of treatment protocols, mice were euthanized by exsanguination under deep isoflurane anesthesia and death was confirmed by cervical dislocation.

3.3.3 Experimental design

3.3.3.1 L-NAME hypertension

KidVD+ mice and KidVD- littermates were made hypertensive by providing L-arginine methyl ester hydrochloride (L-NAME) (0.5 mg/mL; Sigma, St. Louis, MO) in their drinking water. After a week of L-NAME treatment, KidVD- and KidVD+ mice were administered doxycycline (0.2 mg/mL; doxycycline hyclate, Sigma) concurrent with L-NAME in their drinking water for 3 weeks. All mice received normal Na^+ diet containing 1% NaCl. Weekly systolic blood pressures (SBP) were determined in these mice using the tail-cuff method as described below. At the end of 4 weeks, mice were placed in diuresis cages and allowed to acclimatize for 24 hours, following which urine was collected from individual mice over a period of 24 hours. If <100 µL was collected in 24 hours, urine analysis was excluded.

3.3.3.2 Baseline

KidVD+ mice and KidVD- littermates received normal Na_+ diet containing 1% NaCl and 0.2 mg/mL doxycycline in their drinking water for 3 weeks. Mice were then placed in diuresis cages and acclimatized for 24 hours, and urine was collected from individual mice over the next 24 hours. SBP was measured by tail-cuff at the end of 3 weeks.

3.3.3.3 Acute salt loading

KidVD- and KidVD+ mice received regular diet (1% NaCl) and 0.2 mg/mL doxycycline drinking water for 3 weeks. Mice were fasted overnight for 12 hours and were given 5% body weight 0.9% saline (9 mg/mL) intraperitoneally the following day. Immediately after injection, mice were placed in diuresis cages and hourly urine was collected from individual mice over the next 4 hours. Only collected urine volumes at each hourly time point were included in the calculations.

3.3.3.4 Chronic salt loading

KidVD- and KidVD+ mice received a 4% high salt diet (Teklad Envigo, Huntingdon, United Kingdom) along with 0.2 mg/mL doxycycline and 1% saline (10 mg/mL NaCl) in their drinking water for 3 weeks. Following a 24-hour acclimatization period, 24-hour urine was collected from individual mice placed in diuresis cages. SBP values were recorded at the end of 3 weeks by tail-cuff.

3.3.4 Blood pressure determination

SBP was determined using the IITC Life Science noninvasive tail-cuff blood pressure acquisition system. Mice were acclimatized in a designated quiet area where all procedures were performed. Mice were handled gently and placed in prewarmed (34°C) restrainers and allowed to acclimatize in the warming chamber for 5 minutes prior to beginning any recordings. SBP readings were determined by 2 independent, blinded investigators.

3.3.5 Flow Cytometry

Kidneys were harvested and minced following decapsulation. The minced kidneys were digested in buffer containing enzymes Collagenase D (Roche Sigma, St. Louis, MO) and Dispase II (Sigma) at 37°C for 1 hour, and filtered through 100 μm and 40 μm strainers to obtain single cell suspensions. Red blood cells were lysed in NH_4Cl/EDTA. Splenocytes were similarly isolated and used as antibody controls. Non-specific Fc binding was blocked using an anti-mouse CD16/CD32 antibody (BD Pharmingen, San Jose, CA), following which cells were incubated with fluorescent-conjugated antibodies against CD45, F4/80, CD11c, and CD3e for 10 minutes on ice. All antibodies were purchased from either BD Pharmingen or eBiosciences. Data was acquired on a BD LSR Fortessa X-20 flow cytometer using FACS DIVA software (BD Biosciences) and analyzed using Flow Jo v7.6.2 (FlowJo, LLC, Ashland, OR). CD3e+, CD3e-, F4/80+, and CD11c+ populations were quantified within the CD45+ gate. Results are expressed as a percentage of CD45+ cells per kidney. Antibodies used in this study are listed in

Table A2 in the Appendix. The gating strategy for flow cytometry is demonstrated in Fig 3.1.

Figure 3.1: Flow cytometry gating strategy: (a) Gating strategy for flow cytometry, and (b) Representative scatter plot for CD3e+ cells from KidVD- and KidVD+ mice during L-NAME hypertension. Percentages are calculated out of CD45+ cells or parent population.

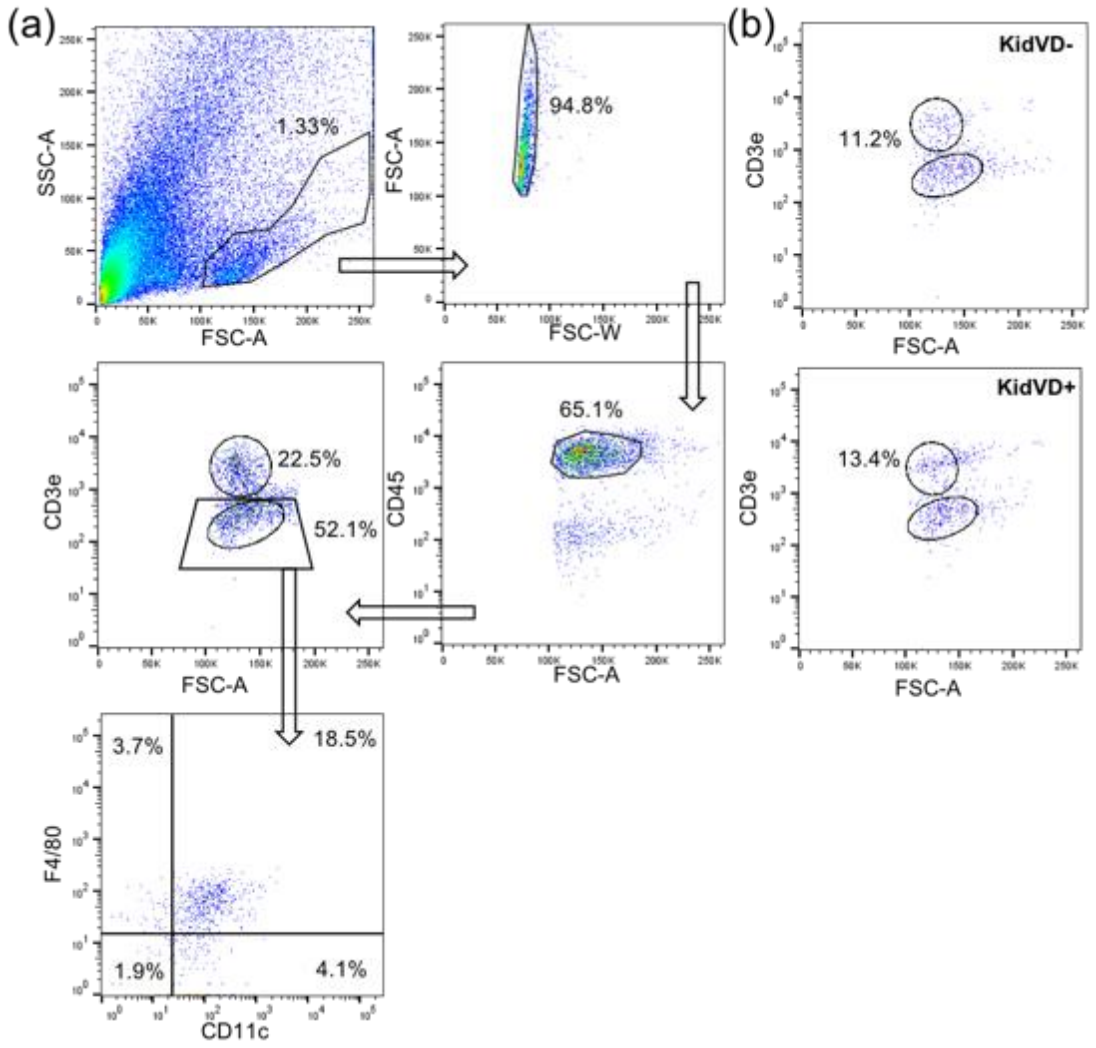

3.3.6 Urine and serum analysis

Serum and 24-hour urine samples were analyzed for creatinine by capillary electrophoresis and for Na^+ concentration using a Beckman AU400 Autoanalyzer

at the University of Texas-Southwestern George M. O'Brien Kidney Research Core Center. For hourly urine samples from the acute salt loading study, urinary Na^+ levels were measured using the LAQUAtwin Na^+ meter (Horiba Scientific, Minami-ku Kyoto, Japan) following the manufacturer's protocol. GFR was calculated using the creatinine clearance (ClCr) method. Urine was assessed for blood urea nitrogen (BUN) levels using the QuantiChrom Urea Assay Kit (BioAssay Systems, Hayward, CA). Atrial natriuretic peptide (ANP) levels were measured in the plasma using the Atrial Natriuretic Peptide EIA Kit (Sigma) following the manufacturer's protocol.

3.3.7 Renal immunofluorescence analysis

Kidney sections were cut 5 µm sagittally and were de-paraffinized, rehydrated, and permeabilized with 0.1% Triton solution. The sections were blocked with 10% AquaBlock (EastCoastBio, North Berwick, ME) for 1 hour at room temperature and were then incubated with the following primary antibodies at 4°C overnight: goat polyclonal Podoplanin (R&D Systems, Minneapolis, MN), and rat monoclonal Endomucin (Santa Cruz Biotechnology, Dallas, TX). Alexa Flour 488 or 594 secondary antibodies (Life Technologies, Carlsbad, CA) were used for visualization. Antibodies used are listed in Table A2 in the Appendix. Slides were mounted with Prolong Gold antifade reagent with DAPI (Thermo Fisher Scientific, Waltham, MA) and imaged using an Olympus BX51 fluorescence microscope with Olympus Q5 camera. Images were captured at 20X

magnification using the Olympus CellSens software (Olympus, Shinjuku, Tokyo, Japan).

3.3.8 Quantitative real-time PCR analysis

Mouse kidneys were homogenized and total RNA was isolated using the Quick-RNA mini prep kit (Zymo Research, Irvine, CA). 0.5 µg RNA was used to synthesize cDNA using the Qiagen RT_2 First Strand kit (Germantown, MD). To measure gene expression, 10 µL reactions were prepared using SYBR Green ROX qPCR Mastermix (Qiagen), nuclease-free water (Invitrogen, Carlsbad, CA), and primers (10 µM) (IDT, Coralville, IA) in a 384 well plate in duplicate and run using the AB 7900HT Fast Real-Time PCR Thermal Cycler (Applied Biosystems, Foster City, CA). All data were normalized to the expression levels of *Rps18* and fold changes were calculated using the $2^{-\Delta\Delta CT}$ method. All primer sequences used in this study are listed in Table A1 in the Appendix.

3.3.9 Immunoprecipitation and protein immunoblot analysis

Mouse kidneys were homogenized in Cell Lysis buffer (Cell Signaling, Danvers, MA) and the supernatant was separated by centrifugation at 14000g for 10 minutes at 4°C. Protein concentrations were determined using the BCA assay (Thermo Fisher). In order to efficiently capture and detect phosphorylated NCC and NKCC2 from whole kidney lysate, 30 µg protein was first immunoprecipitated with antibodies against the total protein using Dynabeads Protein G (Thermo Fisher) according to manufacturer's protocol. Following this, the precipitated protein was resolved by gel electrophoresis and probed for the corresponding

antibodies against NCC and NKCC2, followed by pThr/Ser/Tyr. For detection of other proteins, 30 µg of the total kidney homogenate was mixed with SDS sample buffer and boiled at 95°C for 5 minutes. The proteins were separated by electrophoresis using 4-20% NuPage gels (Thermo Fisher), and then transferred onto a nitrocellulose membrane (Biorad, Hercules, CA). Immunoblotting was performed by incubating the membrane at 4°C overnight with the following primary antibodies: ENaCα, ENaCß, ENaCϒ, NHE3, pNHE3. Proteins were normalized to corresponding ß-actin. Secondary antibodies used were anti-rabbit and anti-mouse IgGs conjugated to Alexa-Flour 680 or IR800Dye (LI-COR Biosciences, Lincoln, NE). All antibodies used in this study are listed in Table A2 in the Appendix. The bands were detected using infrared visualization (Odyssey System, LI-COR Biosciences), and quantified by densitometry performed on the Odyssey software.

3.3.10 Isolation of renal interstitial fluid

Interstitial fluid from the kidney was isolated by a centrifugation technique adapted from protocols described previously.(Wiig et al., 2003) The left kidney from each mouse was decapsulated, sagittally halved, and careful incisions were made restricted to the kidney cortex in one half of the kidney. Samples were suspended on 15 µm nylon mesh filters in pre-weighed centrifugal filter tubes. The tubes were spun at 6500g for 40 minutes at 4°C, following which the tubes along with the kidney and isolated interstitial fluid were weighed again. The difference in weights served as the weight of the excised kidney. The interstitial fluid was

immediately collected from the bottom of the tube and the volumes were measured using a micropipette.

3.3.11 Dermal Lymphatic Quantification

Ear samples were peeled in half, separating the anterior and posterior sides. The posterior half was fixed in 10% formalin solution (Sigma, St. Louis, MO) for 2 hours, rinsed with 1X PBS with 0.3% Triton. Samples were then incubated in a 1:400 dilution of LYVE-1 antibody (R&D Systems, Minneapolis, MN) for 3 days at 4°C. Following rinsing, the samples were similarly incubated in donkey anti-goat 488 IgG (Life Technologies, Carlsbad, CA) for 3 days. The interior portion of the ear (from edge to center of ear) was imaged using a Zeiss Discovery fluorescence stereoscope (Zeiss, Oberkochen, Germany) and Zeiss MRc camera at 5X magnification. Length and total number of branches were analyzed for a standardized area using ImageJ software.

3.3.12 Skin Na^+ quantification

Back skin samples (30-200 mg) isolated from mice were weighed and boiled for 12 days at 110°C to remove water content. Dried skin samples were weighed and then oxidized in 500 µL of 12N HCl at 82°C for 5 days. The samples were resuspended in 500 µL of deionized water and sonicated for 10 minutes. Samples were analyzed for Na^+ concentration using the LAQUAtwin Na^+ meter (Horiba Scientific, Minami-ku Kyoto, Japan).

3.3.13 Statistical methods

All results are presented as bar graphs displaying mean ± SD except time-dependent graphs that display SE for visual clarity. Blood pressures for the L-NAME hypertension study were analyzed by ANOVA for repeated measures. The 2-tailed unpaired Student's *t* test was used for comparison of means between genotypes. The criterion for significance was set at $P < 0.05$. All analysis was performed using the GraphPad Prism 7 software (La Jolla, CA).

3.4 Results

3.4.1 Selective renal lymphatic expansion in KidVD+ mice attenuates BP during L-NAME-hypertension

Chronic L-NAME administration has been shown to induce mild glomerulosclerosis, increase in glomerular afferent arteriole thickness, tubulointerstitial inflammation and injury, intrarenal angiotensin II upregulation, memory T cell response induction, and endothelial dysfunction, all of which contribute to renal sodium retention and hypertension (Ribeiro et al., 1992),(Itani et al., 2016),(Quiroz et al., 2001). We have previously demonstrated that inducing kidney-specific lymphatic network expansion in the renal cortex of KidVD+ mice (Fig. 3.2A) prevents a rise in SBP and reduces renal immune cell accumulation during L-NAME hypertension (Lopez Gelston et al., 2018). To determine if renal lymphangiogenesis could therapeutically lower BP in established hypertension, we made KidVD- and KidVD+ mice equally hypertensive by L-NAME administration (Fig 3.2B). To allow for VEGF-D induction to elicit sufficient renal

lymphangiogenesis, doxycycline was then administered concurrent with L-NAME for an additional 3 weeks. While KidVD- mice continued to be hypertensive throughout this period, SBP in KidVD+ mice was significantly attenuated following 3 weeks of VEGF-D induction (Fig 3.2C). Flow cytometry analysis of kidneys from these mice did not, however, detect any significant changes in CD3e+ T-cells, CD11c+ cells, or F4/80+ monocytes, populations that were reduced when expanded lymphatics were present prior to the hypertensive stimuli (Fig 3.2C) (Lopez Gelston et al., 2018). L-NAME hypertension also causes Na^+ retention (Giani et al., 2014a),(Bech et al., 2007), and thus, we investigated whether the enhanced renal lymphatics in KidVD+ mice might affect Na^+ excretion as an alternative anti-hypertensive mechanism. Indeed, KidVD+ mice displayed a significant increase in 24-hour urinary Na^+ excretion (Fig 3.2D), accompanied by an increase in 24-hour urine output. Urinary fractional excretion of Na^+ was also significantly increased in KidVD+ mice (Fig 3.2E) with equivalent ClCr between groups (Fig 3.2F). mRNA levels determined by qPCR analysis did not reveal any However, by protein immunoblot, we detected a significant reduction in cleaved (cl-) ENaCα (Fig 3.2H and 3.2I), suggesting reduced ENaC-dependent Na^+ reabsorption in KidVD+ mice differences in the expression of renal Na^+ transporters (Fig 3.2G).

Figure 3.2: Selective renal lymphatic expansion in KidVD+ mice attenuates BP during L-NAME-hypertension: A) Immunofluorescent labeling of podoplanin (green) and endomucin (red) in the cortex of KidVD- and KidVD+ mice during L-NAME hypertension. “G” indicates glomeruli. Arrowheads identify sparse native

renal lymphatics. Blue=DAPI. Scale bars = 50 µm. B) Weekly systolic blood pressure) in KidVD- and KidVD+ mice during L-NAME hypertension. C) Flow cytometry quantitation of renal immune cells in KidVD- and KidVD+ mice during L-NAME hypertension. Results are expressed as percentages of CD45+ cells. D) 24-hour urinary Na^+ excretion, E) Fractional excretion of Na^+ (FENa), and F) ClCr in KidVD mice during L-NAME hypertension. G) mRNA expression of renal Na^+ transporters in KidVD mice. H) Protein immunoblot analysis, and I) relative abundance of renal Na^+ transporters and their phosphorylation during L-NAME hypertension. n=5/6 mice for each group, except western blots n=4. * indicates $P<0.05$ compared to KidVD-.

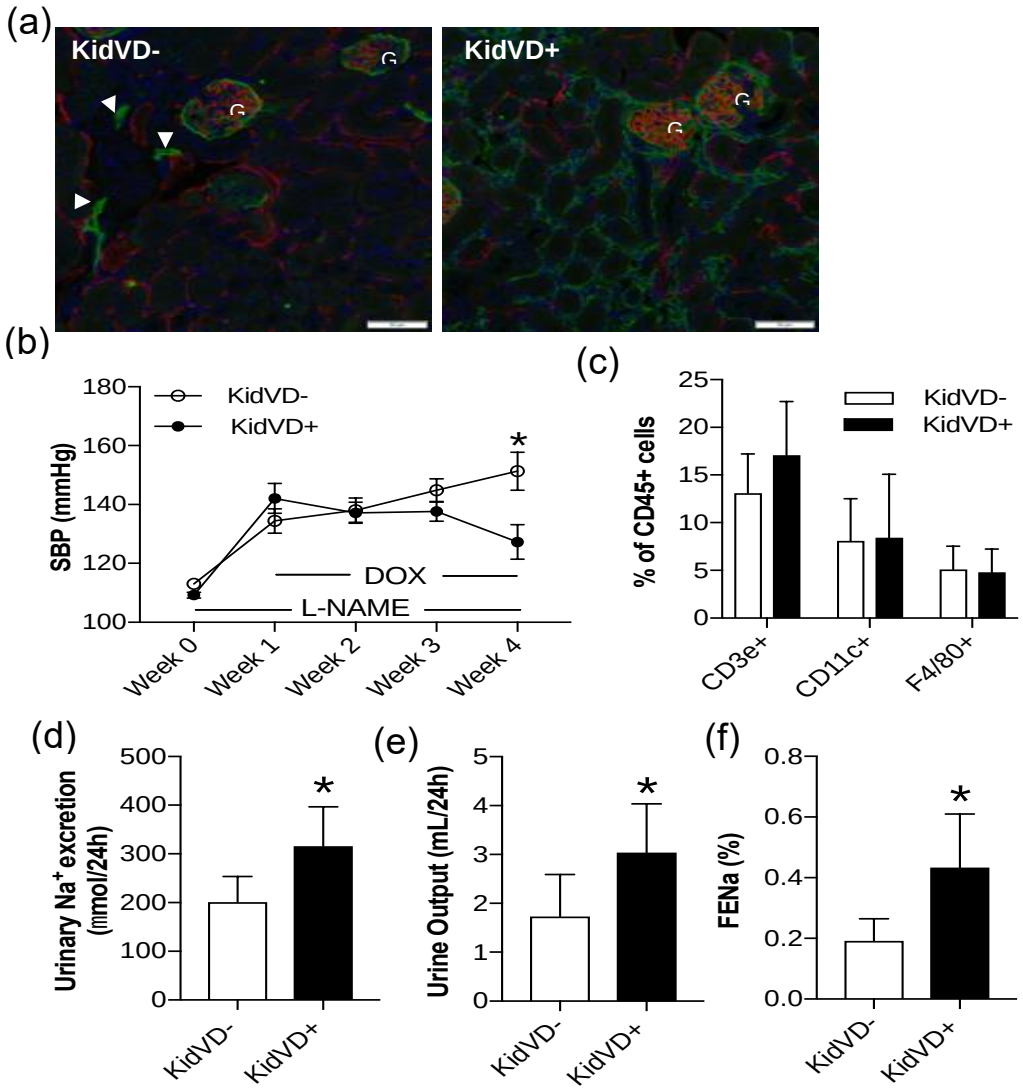

Figure 3.2 Continued

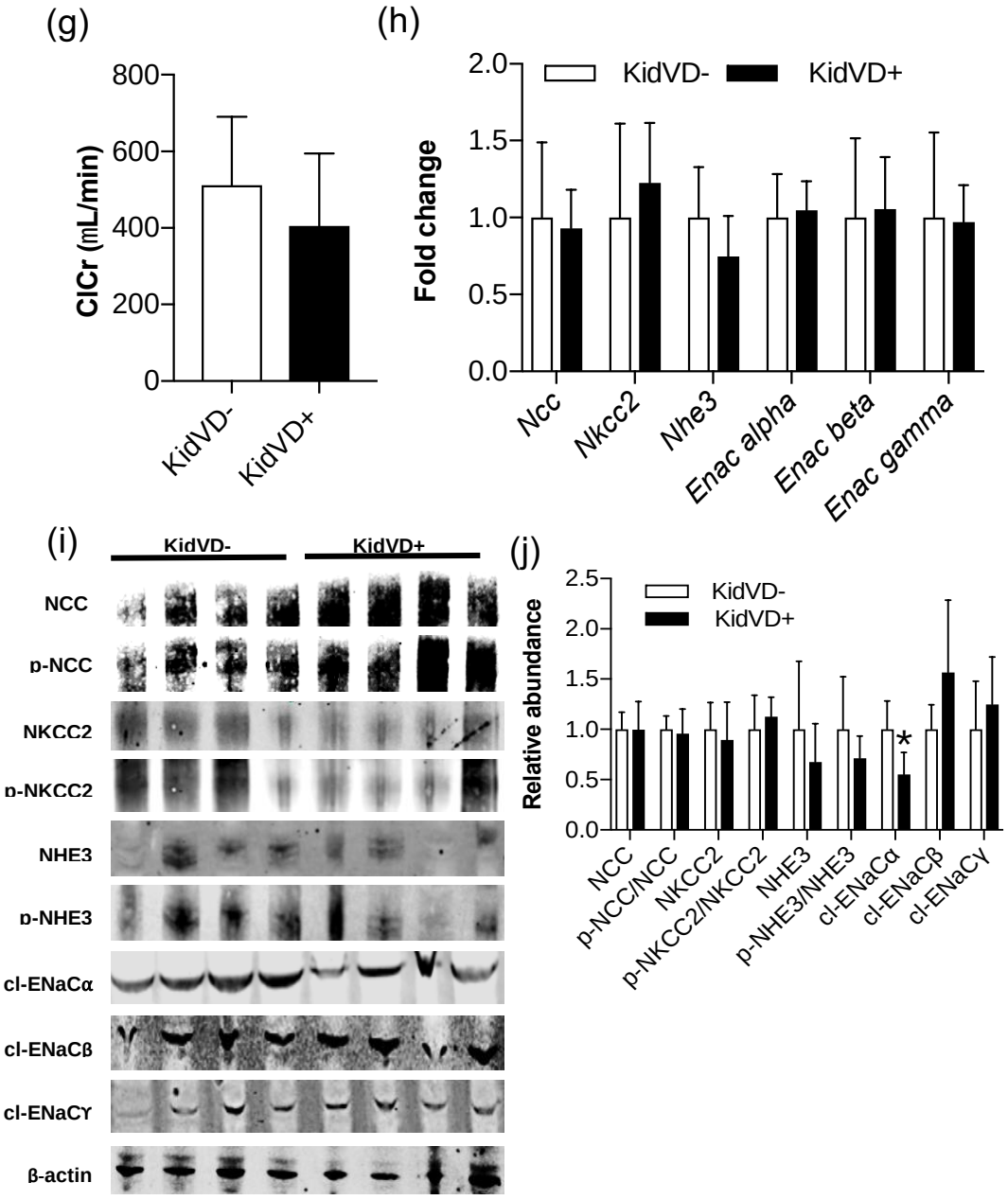

Table 3.1: Characteristics of KidVD- and KidVD+ mice at baseline and under chronic salt load:

	Baseline		Chronic Salt Load	
	KidVD-	KidVD+	KidVD-	KidVD+
Body weight (BW) (g)	23.6 ± 4.1	22.1 ± 3.1	23.8 ± 1	20.2 ± 0.8*
Kidney weight / BW	0.48 ± 0.1	0.55 ± 0.1	0.58 ± 0.1	0.7 ± 0.1*
Heart weight / BW	0.52 ± 0.1	0.51 ± 0.1	0.49 ± 0.04	0.54 ± 0.1
Urine Creatinine (mg/dL)	34.5 ± 10.6	34.5 ± 10.5	27.8 ± 9.8	22.8 ± 9.2
Blood Urea Nitrogen (mg/dL)	30.5 ± 4.1	34 ± 9.9	28.5 ± 2.3	33.3 ± 4.9
Serum Creatinine (mg/dL)	0.09 ± 0.01	0.11 ± 0.01*	0.09 ± 0.01	0.08 ± 0.003
Urine Na^+ (mmol/L)	97.4 ± 26.8	95.8 ± 35.3	613.6 ± 118	1003.6 ± 406.4*
Serum Na^+ (mmol/L)	148.2 ± 2.3	149.7 ± 3.1	152.9 ± 3.9	146.5 ± 3.5*

Values are indicated as mean + SD. Student's *t*-test was used for comparison of means. $P < 0.05$. * indicate significance against respective KidVD- .

3.4.2 Renal sodium handling Is not altered in KidVD+ mice at baseline

Following our observations, we characterized renal sodium handling in KidVD- and KidVD+ mice at baseline in the absence of hypertension. While renal lymphatic density was greatly augmented in KidVD+ mice at the end of 3 weeks of doxycycline (Fig 3.3A); there were no visible changes in renal blood capillary density (Fig 3.3A). No differences in SBP were detected between KidVD- and KidVD+ mice (Fig 3.3B) and other baseline renal characteristics were unchanged between groups (Table 3.1). KidVD+ mice did not exhibit changes in urinary Na^+ excretion (Fig 3.3C), fractional excretion of Na^+ (Fig 3.3D), or ClCr (Fig 3.3E) compared to KidVD- mice. No changes were detected in the mRNA expression of renal Na^+ transporters (Fig 3.3F). Similarly, protein abundance and activity as measured by phosphorylation or cleavage of these transporters were not different between the groups (Fig 3.3G and 3.3H). These results demonstrate that renal Na^+ handling is unaltered in KidVD+ mice at baseline.

Figure 3.3: Renal sodium handling is not altered in KidVD+ mice at baseline: Immunofluorescent labeling of podoplanin (green) and endomucin (red) in the cortex of KidVD- and KidVD+ mice administered doxycycline for 3 weeks. “G” indicates glomeruli. Arrowheads identify sparse native renal lymphatics. Blue=DAPI. Scale bars = 50 µm. B) Terminal systolic blood pressure (SBP) in KidVD- and KidVD+ mice. C) 24-hour urinary Na^+ excretion, D) Fractional excretion of Na^+ (FENa), and E) eGFR in KidVD- and KidVD+ mice. F) mRNA expression of renal Na^+ transporters in KidVD- and KidVD+ kidneys. G) Protein immunoblot analysis, and H) relative abundance of renal Na^+ transporters and

their phosphorylation in KidVD- and KidVD+ mouse kidneys. n=5/6 mice for each group, except western blots n=4.

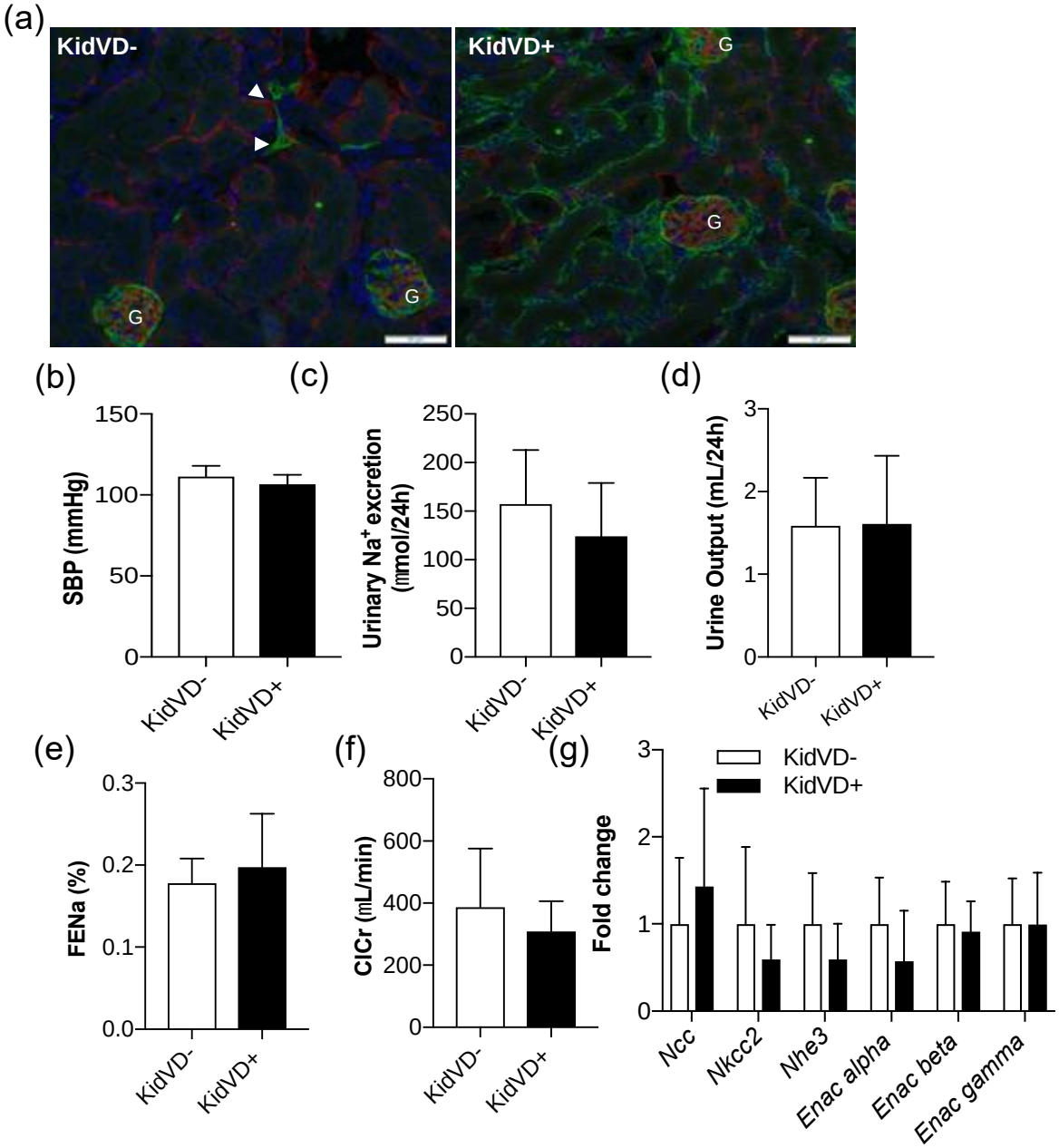

Figure 3.3 Continued

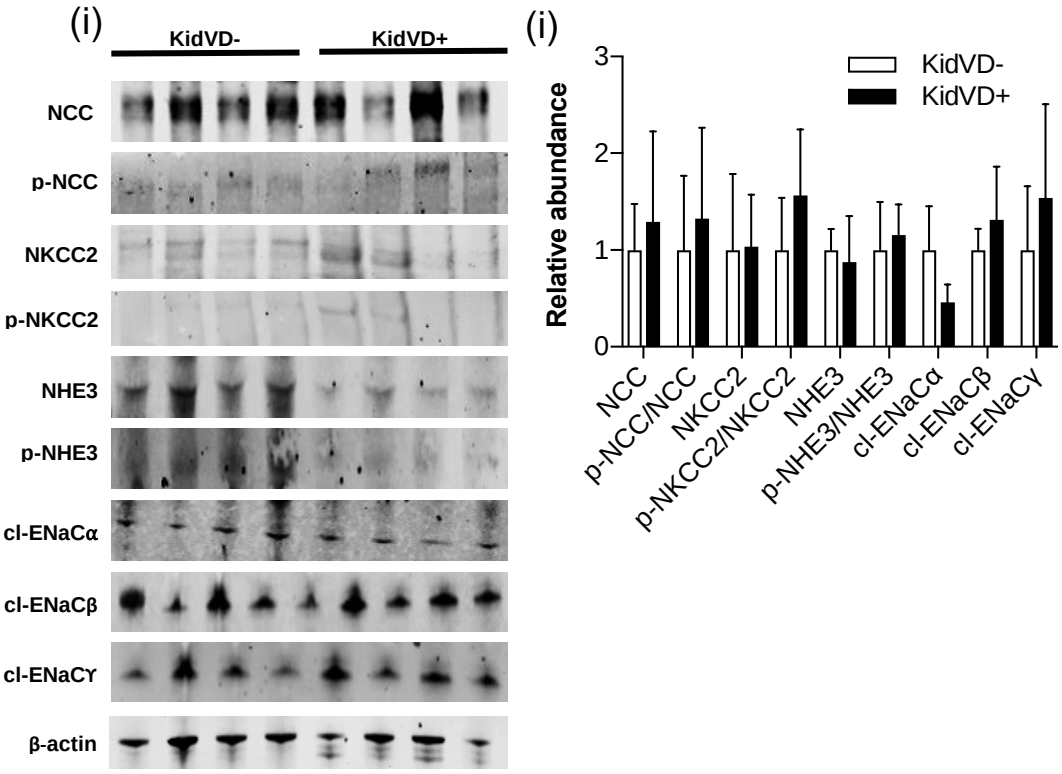

3.4.3 Renal sodium handling Is not altered in KidVD+ mice following an acute sodium load

At the end of 3 weeks of doxycycline, KidVD- and KidVD+ mice were administered a single 5% body weight saline bolus and hourly urinary Na^+ excretion was measured for 4 hours. Hourly urinary total Na^+ excretion was not different between KidVD- and KidVD+ mice (Fig 3.4A), and similarly, there were no detectable changes in urine output (Fig 3.4B). Since the peak urinary Na^+ excretion occurred at 2 hours following the bolus, gene and protein expression of Na^+ transporters were analyzed from kidneys of KidVD- and KidVD+ mice at this

time point. However, no changes were detected in the mRNA (Fig 3.4C), protein abundance or activity (phosphorylation or cleavage) (Fig 3.4D and 3.4E) of these transporters. An acute sodium loading is therefore handled equally by chow fed KidVD- and KidVD+ mice.

Figure 3.4: Renal sodium handling is not altered in KidVD+ mice following an acute sodium load: A) Hourly urinary Na^+ excretion, B) urinary Na^+ concentration, and C) urine output in fasted KidVD- and KidVD+ given an acute salt load following 3 weeks of doxycycline administration. D) mRNA expression of renal Na^+ transporters in KidVD- and KidVD+ mice. E) Protein immunoblot analysis, and F) relative abundance of renal Na^+ transporters in KidVD- and KidVD+ mouse kidneys following an acute salt load. n=5/6 mice for each group, except western blots n=4.

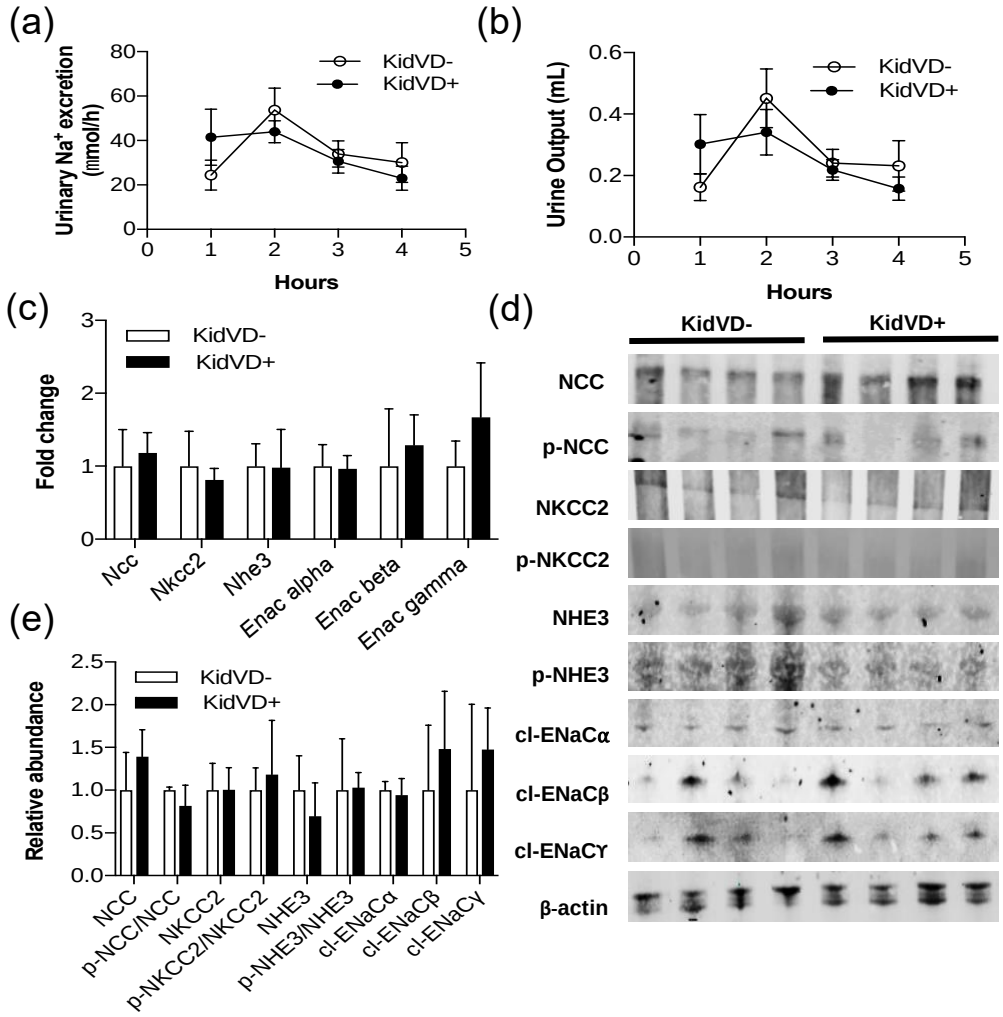

3.4.4 KidVD+ mice exhibit increased urinary fractional excretion of Na^+ during a chronic salt load

We then tested the effects of augmenting renal lymphatics on Na^+ excretion in mice during chronic salt loading. We first confirmed the augmented lymphatic density in KidVD+ mice by immunofluorescent labeling for podoplanin (Fig 3.5A). KidVD+ mice exhibited significantly lower SBP compared to KidVD- mice in response to chronic salt loading (Fig 3.5B). No change in 24-hour urinary Na^+ excretion was identified in KidVD+ mice (Fig 3.5C); however, urinary fractional excretion of Na^+ was significantly increased in KidVD+ mice (Fig 3.5D), while GFR was unchanged between the groups (Fig 3.5E). KidVD+ mice also demonstrated a significant increase in urinary Na^+ concentration along with a significant reduction in serum Na^+ concentration. At the mRNA level, KidVD+ mice had significantly downregulated expression of the renal Na^+ transporters *Ncc*, *Nkcc2*, and *Nhe3* (Fig 3.5F). Mirroring the reduced sodium reabsorption in KidVD+ L-NAME-treated mice, we again observed a significant reduction in the abundance of cl-ENaCα as well as total NCC in KidVD+ mice (Fig 3.5G and 3.5H) by immunoblot.

We then analyzed possible mechanisms by which augmenting renal lymphatics increases natriuresis to lower BP. We hypothesized that inducing extensive renal lymphatic expansion expands the interstitial space and thus measured renal interstitial fluid volume as a surrogate. While unchanged at

baseline or with an acute bolus, KidVD+ mice on chronic salt load had significantly more renal interstitial fluid volume (Fig 3.5l).

Figure 3.5: KidVD+ mice exhibit increased urinary fractional excretion of Na+ during a chronic salt load: (a) Immunofluorescent labeling of podoplanin (green) and endomucin (red) in the cortex of KidVD- and KidVD+ mice given a chronic high salt diet and water for 3 weeks. “G” indicates glomeruli. Arrowheads identify sparse native renal lymphatics. Blue=DAPI. Scale bars = 50 µm. (b) Systolic blood pressure (SBP) in KidVD- and KidVD+ mice. (c) 24-hour urinary Na+ excretion, (d) 24-hour urine output, (e) Fractional excretion of Na+ (FENa), and (f) ClCr in high salt diet-fed KidVD- and KidVD+ mice. (g) mRNA expression of renal Na+ transporters in KidVD- and KidVD+ mice. (h) Protein immunoblot analysis, and (i) relative abundance and phosphorylation of renal Na+ transporters in KidVD- and KidVD+ mouse kidneys under chronic high salt loading. (j) renal tissue fluid volume, and (k) plasma ANP levels in KidVD- and KidVD+ mice during baseline, acute salt loaded or chronic salt loaded conditions. n=5 male (m), 1 female (f) KidVD- mice, and 2m, 4f KidVD+ mice, except western blots n=3m, 1f KidVD- mice and 2m, 2f KidVD+ mice. * indicates P<0.05 compared to KidVD-.

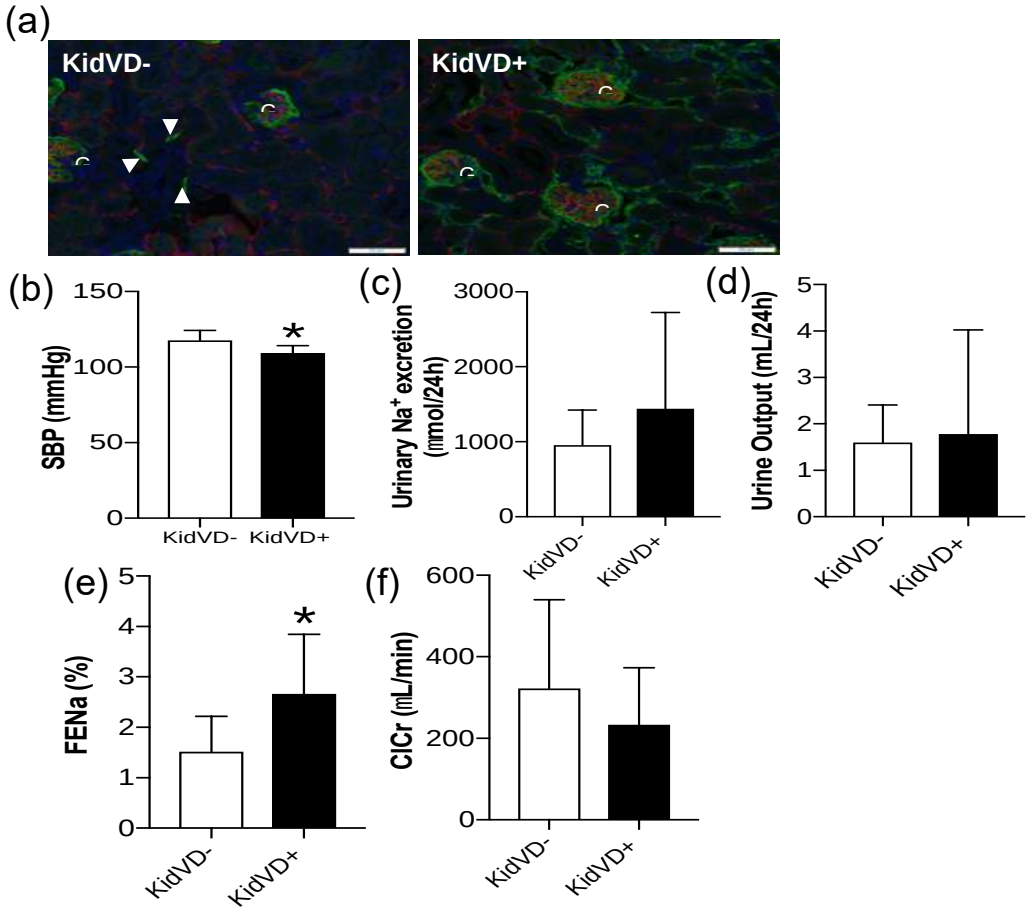

Figure 3.5 Continued

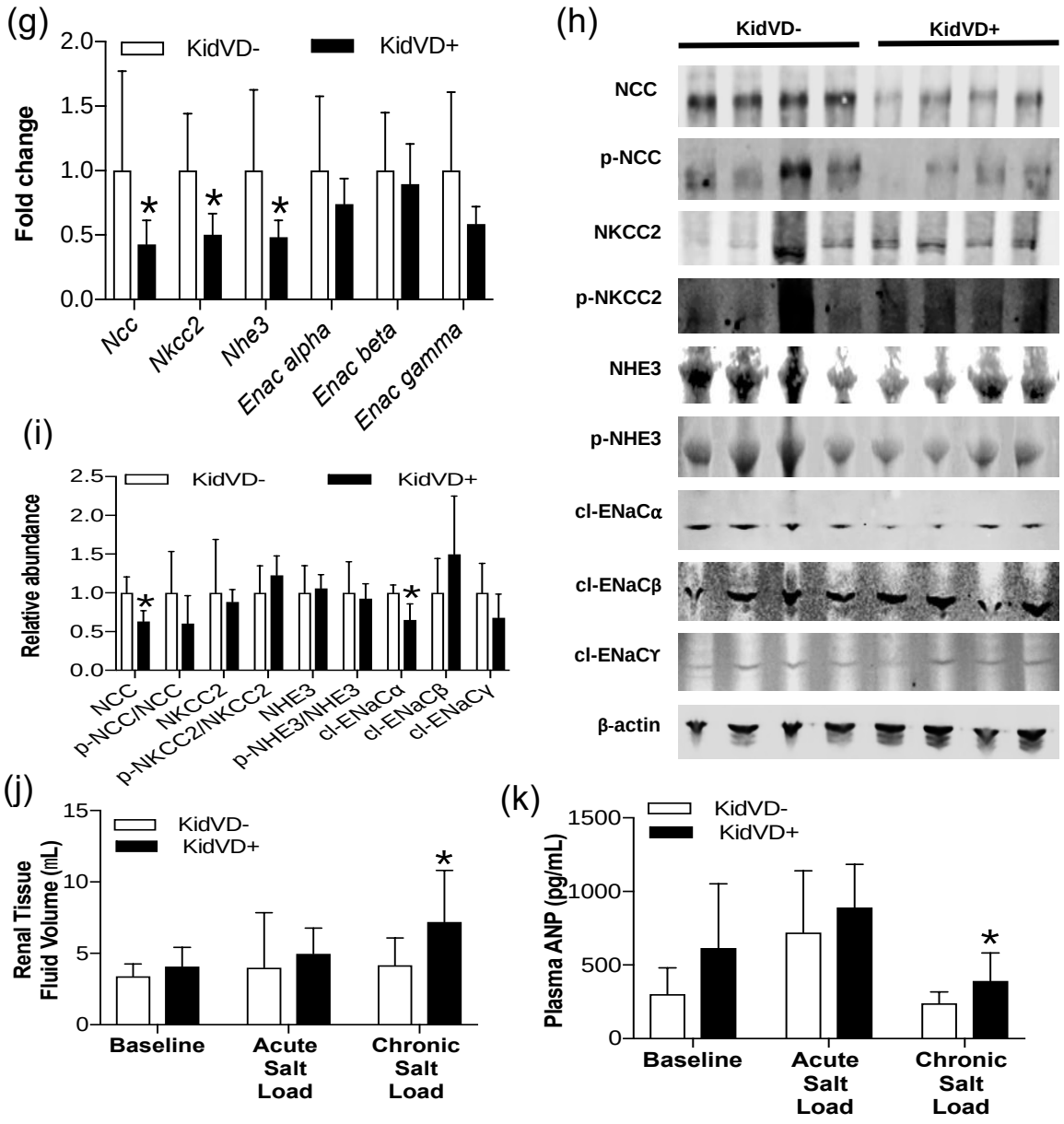

We hypothesized that changing renal hydrodynamics would result in increased venous return through venous capillary resorption or through lymphatics via the thoracic duct, leading to myocardial stretching and atrial natriuretic peptide (ANP)

release. While no significant increase in cardiac mass was measured, KidVD+ mice had a significant increase in plasma ANP levels, only when challenged with chronic sodium (Fig 3.5J).

3.5 Discussion

The major findings of the current study are that: 1) therapeutic induction of kidney-specific lymphangiogenesis increases natriuresis and attenuates BP during L-NAME-induced hypertension, 2) inducing renal lymphangiogenesis does not alter renal Na^+ handling at baseline or following an acute salt load, and 3) augmenting renal lymphatics increases urinary fractional excretion of Na^+ and lowers BP in mice given a chronic high salt loading.

The contribution of renal inflammation to the development of hypertension is well-established. Cytokines secreted by activated T cells, dendritic cells, and macrophages induce sodium retention and proteinuria, and deteriorate renal function (Norlander et al., 2016). Our group has demonstrated that enhancing renal lymphatic density before the onset of hypertension reduces renal accumulation of immune cells and prevents the development of L-NAME-induced, salt-sensitive, and angiotensin II-induced hypertension (Lopez Gelston et al., 2018). Here, we tested the effects of therapeutically enhancing renal lymphatic density to attenuate established hypertension. Inducing renal lymphangiogenesis during established hypertension attenuated BP in KidVD+ mice; however, populations of immune cells that were previously identified to be reduced during the prevention of hypertension were not altered in this study. While leading us to

investigate Na^+ handling, this finding does not exclude a role for lymphatic vessels in modulating immune responses during hypertension. In addition to regulating immune cell trafficking, lymphatic vessels influence immune outcomes by directly affecting dendritic cell and T cell maturation and activation, and thus balance protective effector immune responses (Lane et al., 2018),(Lund et al., 2016). Particularly during hypertension, certain types of immune cells, namely T regulatory cells and M2 macrophages, protect against hypertensive injury by secreting anti-inflammatory cytokines (Barhoumi et al., 2011),(Harwani, 2018). Detailed studies characterizing how renal lymphatics shape immune responses during hypertension are underway.

Altered renal Na^+ handling has a major pathogenic role in hypertension. In this study, we have demonstrated that an augmented renal lymphatic network induces natriuresis and lowers BP during L-NAME-induced hypertension and following a non-hypertensive chronic high salt challenge, thus establishing that renal lymphatics participate in maintaining Na^+ homeostasis. Previous studies have identified roles for lymphatic vessels in Na^+ homeostasis and BP regulation; for example, dermal lymphatics have been reported to play a role in electrolyte clearance from the skin and lower BP (Machnik et al., 2009). In rats given a high salt diet, overexpression of VEGF-C induced cardiac lymphangiogenesis and lowered BP (Yang et al., 2014). Similarly, VEGF-C administered subcutaneously induced renal and skin lymphangiogenesis and lowered BP in mice fed a high salt diet (Beaini et al., 2019). However, it is crucial to note that the route of VEGF-C

administration was systemic in these studies, and thus potential cross-effects on renal lymphatic vessels cannot be excluded. We have demonstrated that in our inducible, transgenic mouse model approach, lymphangiogenesis is restricted to the kidney and is not observed in other organs including the skin, heart, lung, and liver (Lopez Gelston et al., 2018). More importantly, augmenting renal lymphatics does not affect intrinsic renal Na^+ handling, as evidenced by a lack of change in urinary Na^+ excretion at baseline. In the acute saline bolus studies, urinary Na^+ excretion in these mice prior to receiving the saline challenge would be similar to baseline conditions. Following the saline bolus, peak urinary Na^+ excretion was achieved two hours after i.p. injection, similar to results from previous studies (Veiras et al., 2017). Since interstitial Na^+ accumulation and dermal lymphatics have been shown to alter Na^+ homeostasis, we measured skin Na^+ concentration in our study; however, we did not observe dermal interstitial Na^+ accumulation during basal or high salt conditions (Fig 3.6A). In addition, there were no changes in dermal lymphatic density in these mice (Fig 3.6B and 3.6C), confirming that our lymphatic modulation was confined to the kidney.

Figure 3.6: Extra-renal effects of VEGFR-3 signaling: (a) Skin Na^+ concentration [Na^+] per total tissue water (TTW) from KidVD- and KidVD+ mice during baseline, acute and chronic salt loaded conditions; Quantification of dermal lymphatic vessel density as represented by (b) length/area, and (c) Number of branches/area in KidVD- and KidVD+ mice during baseline and chronic salt loaded conditions; (d) Protein immunoblot analysis, and (e) relative abundance of cardiac VEGFR-3 and phospho-VEGFR-3 from KidVD- and KidVD+ mice given a chronic high salt diet. n=5-6 mice for each group, except western blot n=4.

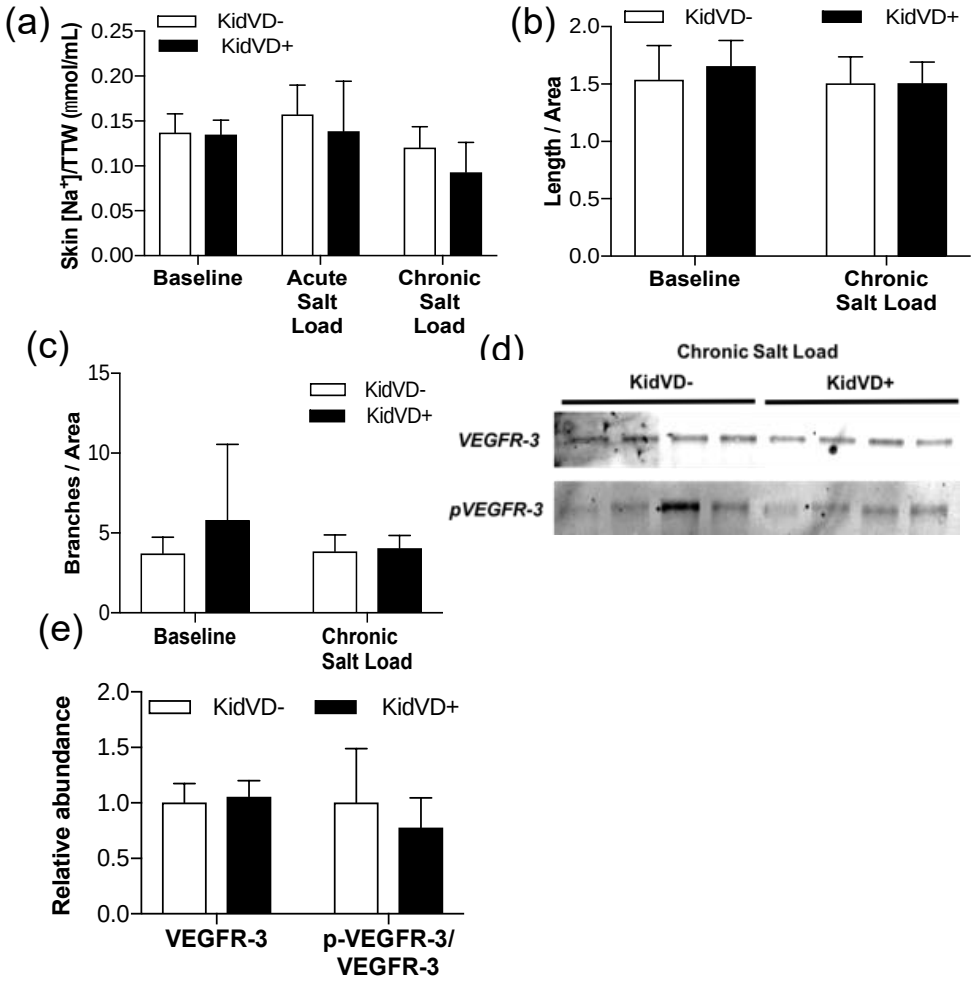

The exact mechanisms by which augmented renal lymphatics induce natriuresis are still being determined. While the proximal tubule segments are involved in reabsorbing the bulk of Na^+ from glomerular filtrate, the distal nephron is involved in fine tuning sodium excretion to match intake (Palmer and Schnermann, 2015). L-NAME hypertension increases renal vascular resistance, and reduces renal blood flow and GFR, however, the magnitude of reduction of renal blood flow is usually larger, resulting in a rise in filtration fraction (Ribeiro et al., 1992). In this study, L-NAME was administered to both KidVD- and KidVD+

mice. Although not specifically tested, renal blood flow is likely to be reduced similarly in both groups, and hence a difference in filtration fraction would not be expected to contribute to the natriuretic response. In this study, we observed a reduction in the abundance of cl-ENaCα during L-NAME-induced hypertension, and a reduction in total NCC and cl-ENaCα following a chronic high salt in KidVD+ mice. We observed a trend towards reduction in cl-ENaCα abundance in KidVD+ mice at baseline, and thus it is likely that augmenting renal lymphatics primes the kidney towards more efficiently excreting excess salt load. However, functional measures of urinary Na^+ excretion were altered only when KidVD+ mice were challenged with Na^+ retaining conditions such as a chronic high salt diet or L-NAME administration. Inappropriate activation of the major distal nephron transporters NCC and ENaCα has been implied in mediating increased Na^+ reabsorption under a high salt diet, (Mu et al., 2011),(Hoorn et al., 2011),(Aoi et al., 2007) suggesting that the downregulation of these transporters or their activity may contribute to the increased natriuresis in KidVD+ mice. These measures of transporter phosphorylation or ENaC subunit cleavage thus serve as our measure of activity, however, direct activity was not measured and other mechanisms such as membrane trafficking and endocytosis also regulate renal Na^+ transporter activity (Riquier-Brison et al., 2010),(Haque and Ortiz, 2019).

An intriguing finding of this study is that augmenting renal lymphatics increases renal interstitial fluid volume by almost 2-fold specifically during a chronic salt load. The marked lymphatic expansion in KidVD+ mice thus appears

to be a reservoir for fluid. Given the low compliance of the renal interstitium, this increase in renal interstitial fluid would be expected to raise interstitial hydrostatic pressure and induce natriuresis, as has been shown in previous studies (Khraibi, 1991),(Granger and Scott, 1988). It is interesting that during L-NAME hypertension, natriuresis occurs at the end of week 4 when BP is attenuated. While a reduction in BP and hence a reduction in renal perfusion pressure could be expected to result in antinatriuresis, we interpret these findings as that an increase in renal interstitial fluid volume and natriuresis mediate the effect on BP, and not vice versa; however, a specific cause-and-effect relationship has not been tested in this study. An increase in renal interstitial fluid volume in KidVD+ mice at the end of week 4 is likely to have been initiated between weeks 3 and 4 when lymphatic vessels are fully formed. It is important to note that the hypertensive stimuli such as L-NAME or high salt, and VEGF-C/D exposure are also likely to have effects on the native lymphatic architecture in KidVD- mice and the expanded lymphatic network in the KidVD+ mice. For example, nitric oxide inhibition has been shown to reduce lymph flow velocity in initial lymphatics, and increase contraction frequency of collecting lymphatic vessels (Hagendoorn et al., 2004),(Gashev et al., 2002). Similarly, a high salt diet enhances lymphatic pump efficiency and lymph flow (Mizuno et al., 2014). The expanded lymphatic network in KidVD+ mice might augment this response, leading to increased renal lymph flow and increased return to the heart, and causing increased plasma ANP levels during chronic salt load. VEGF-C stimulation of myocardial VEGFR-3 has been

shown to promote ANP release (Zhao et al., 2015), however, we ruled out this possibility in our study, as there was no increase in cardiac total or phospho-VEGFR3 in chronic salt-loaded KidVD+ mice (Fig 3.6D and 3.6E). Changes in renal renin or angiotensin II levels, other vasoactive or natriuretic hormones, glomerular function, and degree of tubuloglomerular feedback activation have not been measured in this study and may play a role in lymphatics effects on tubular Na^+ handling (Cervenka et al., 1999).

In this study, we measured BP by the tail-cuff method and while we acknowledge the limitations of the technique in obtaining sensitive BP measurements, the technique has proven sufficient in detecting large differences in BP such as seen in our study (Kurtz et al., 2005). Attenuation of BP in both models occurred after 3 weeks of doxycycline administration, which coincided with the timing by which extensive lymphangiogenesis occurs in the model; nevertheless, possible effects of VEGF-D within the kidney cannot be completely excluded. A recent study reported that podocyte-specific overexpression of VEGF-C reduced glomerular permeability and albuminuria during diabetic nephropathy (Onions et al., 2019). Unlike VEGF-C, murine VEGF-D is specific for VEGFR-3, limiting direct blood vascular effects via VEGFR-2 (Baldwin et al., 2001). Additionally, ascending vasa recta have been suggested to be lymphatic-like vessels and express VEGFR-3 in development (Kenig-Kozlovsky et al., 2018). Possible effects of VEGF-D signaling in other VEGFR-3 expressing cells within the kidney, therefore, cannot be fully excluded (Mu et al., 2009).

Figure 3.7 Augmenting renal lymphatic density treats nitric oxide inhibition-induced hypertension: Hypertension induced by nitric oxide inhibition is associated with renal immune cell accumulation and sodium retention. Genetically augmenting renal lymphatic vessel density after hypertension is established attenuated hypertension. The reduction in blood pressure was associated with a reduction in sodium retention. While renal immune cell accumulation was unchanged in this study, detailed investigations of various immune cell subtypes will offer insight into how augmenting renal lymphatic density alters the immune microenvironment. Dashed lines indicate hypothesized mechanisms that have not been proved.

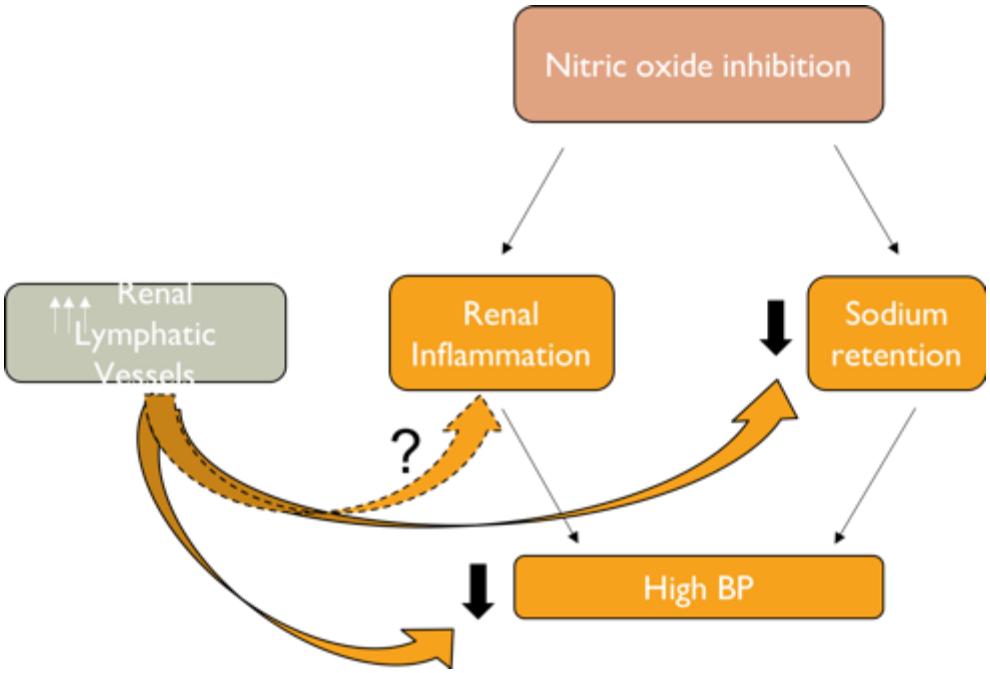

In conclusion, our study establishes that renal lymphatics help to maintain Na^+ homeostasis during conditions of renal Na^+ retention (Fig 3.7). At least in part by increasing natriuresis, the therapeutic induction of renal lymphangiogenesis lowers BP during established hypertension providing a new potential target in the worldwide hypertension epidemic.

4. THERAPEUTIC AUGMENTATION OF RENAL LYMPHATIC DENSITY ATTENUATES BLOOD PRESSURE IN ANGIOTENSIN II-DEPENDENT AND SALT-SENSITIVE HYPERTENSION IN MICE

4.1 Overview

Renal immune cell accumulation and sodium retention are well-known mechanisms in the pathogenesis of hypertension. We have previously demonstrated that augmenting renal lymphatic vessels prior to the onset of hypertension prevents the development of hypertension, in association with a reduction in renal immune cell accumulation. Using a more clinically relevant model of established hypertension induced by nitric oxide inhibition, we have demonstrated that augmenting renal lymphatic vessels after hypertension is established attenuates hypertension. While immune cell accumulation was not reduced in this model, we observed that the reduction in blood pressure was associated with an increase in natriuresis, and characterized the roles of renal lymphatic vessels in sodium homeostasis during conditions of sodium retention. The L-NAME model of hypertension is a model of low circulating angiotensin II, and as such, provides an ideal model to study the effects of renal lymphatic augmentation on sodium homeostasis without the confounding effects of elevated circulating angiotensin II. However, the angiotensin II-induced and salt-sensitive models of hypertension are characterized by highly elevated circulating and intrarenal angiotensin II. Whether augmenting renal lymphatic density in these models of hypertension can attenuate established hypertension, and whether the

increased vessel density can alter sodium homeostasis in these models remain undetermined.

We hypothesized that enhancing renal lymphatic density will lower blood pressure in angiotensin II-dependent and salt-sensitive hypertension. To test our hypothesis, we utilized our genetic mouse model of doxycycline-inducible, kidney-specific overexpression of VEGF-D ("KidVD"+) mice. Doxycycline was administered to KidVD- and KidVD+ mice after 1 week of angiotensin II infusion, or 1 week of high salt diet following nitric oxide synthase inhibition. At the end of four weeks of angiotensin II infusion or high salt diet administration, renal immune cell accumulation and urinary Na^+ excretion were analyzed in these mice. Renal VEGF-D overexpression in KidVD+ mice significantly enhanced renal lymphatic density and lowered blood pressure during angiotensin II-dependent and salt-sensitive hypertension. Renal immune cell accumulation was not reduced in these mice, however, urinary fractional Na^+ excretion was significantly increased in KidVD+ mice during angiotensin II-dependent hypertension. Overall, our findings demonstrate the potential therapeutic role of renal lymphatic vessels in manipulating Na^+ homeostasis and regulating blood pressure during hypertension.

4.2 Introduction

Systemic arterial hypertension is the most important modifiable risk factor for morbidity and mortality worldwide, and the increasing global prevalence of hypertension points to the importance of improvement in medical therapies for

hypertension. In several forms of experimental hypertension including angiotensin II-dependent and salt-sensitive hypertension, renal immune cell infiltration is a known contributing factor to the development of hypertension (Quiroz et al., 2001; Mattson et al., 2006). Inflammatory cytokines released by activated immune cells cause glomerular and tubular injury, activate renal sodium (Na^+) transporters, and result in impaired Na^+ excretion thereby increasing blood volume and blood pressure (BP) (Rodriguez-Iturbe et al., 2013; Norlander and Madhur, 2017). Studies have demonstrated that approaches to reduce renal immune cell infiltration lower BP, thus further corroborating the link between renal inflammation and hypertension (Herrera et al., 2006).

Lymphatic vessels play integral roles in maintaining immune and fluid homeostasis. More than just a passive conduit for fluid and macromolecules, it is now recognized that lymphatic vessels actively respond to inflammatory stimuli by secreting immunomodulatory cytokines and chemokines, archiving and presenting antigen to immune cells, or otherwise coordinating immune responses in peripheral tissues (Card et al., 2014)(Randolph et al., 2017). Thus, not surprisingly, lymphatic vessels have been implicated in several diseases such as chronic inflammatory conditions of the skin, gut, and airway tract, obesity, metabolic syndrome and atherosclerosis (Kim et al., 2014)(Abouelkheir et al., 2017). With regard to hypertension, a role for lymphatic vessels in electrolyte clearance from the skin was first demonstrated by Titze and colleagues. Their study identified that dermal lymphatic vessels undergo hyperplasia in response to

Na+ accumulation in the skin interstitium. These vessels act as a temporary depot for excess electrolytes thus removing them from circulation, and eventually aiding in their removal by the kidney (Machnik et al., 2009; Wiig et al., 2013).

We have recently identified a novel role for renal lymphatic vessels in the regulation of Na^+ homeostasis during hypertension and conditions of sodium retention. We demonstrated that augmenting renal lymphatic vessels increases fractional Na excretion and reduces BP in mice fed a chronic high salt diet. We also demonstrated that the selective augmentation of renal lymphatic vessels during established hypertension increases urinary Na^+ excretion and lowers blood pressure in a model of nitric oxide inhibition-induced hypertension. The increase in sodium excretion observed in KidVD+ mice was associated with a decrease in abundance of the renal Na^+ transporters NCC and ENaC when fed a chronic high salt diet, and a reduction in αENaC abundance during the L-NAME treatment. Importantly, these changes in Na^+ excretion were not associated with a reduction in renal immune cell accumulation in the L-NAME treated mice, as we have demonstrated previously. However, whether augmenting renal lymphatic vessels lowers blood pressure in other models of hypertension is unknown.

In this study, we investigated whether augmenting renal lymphatic vessel density can lower blood pressure in established angiotensin II-dependent and salt-sensitive models of hypertension. Our hypotheses were that the selective expansion of renal lymphatic vessels will attenuate both angiotensin II-dependent and salt-sensitive hypertension, and that this reduction in blood pressure will be

associated with an increase in fractional Na^+ excretion in association with a reduced abundance of renal Na^+ transporters.

4.3 Materials and Methods

4.3.1 Animal Care

All animal use protocols were approved by the Texas A&M University IACUC and were performed in accordance with the NIH Guide for the Care and Use and Care of Laboratory Animals.

4.3.2 Mice

The generation of transgenic KidVD mice has been described previously. TRE-VEGF-D mice were crossed with mice carrying a kidney promoter-driven rtTA (Cdh16; KSP) to generate KidVD mice that overexpress VEGF-D specifically in the kidney following doxycycline administration. The KSP-rtTA mouse was made available by the University of Texas-Southwestern George M. O'Brien Kidney Research Core Center (P30DK079328). KidVD mice were backcrossed minimally 7 generations to C57BL/6J. All mice had ad libitum access to diets and water.

4.3.3 Experimental design

4.3.3.1 Angiotensin II-dependent hypertension

KidVD+ mice and KidVD- littermates were implanted with subdermal osmotic mini-pumps and infused with 490 ng/kg BW/min angiotensin II for 4 weeks. After 1 week of angiotensin II infusion, KidVD- and KidVD+ mice were administered doxycycline (0.2 mg/mL; doxycycline hyclate, Sigma) in their

drinking water for 3 weeks. Weekly systolic blood pressures (SBP) were determined in these mice using the tail-cuff method as described below. At the end of 4 weeks, mice were placed in metabolic cages and allowed to acclimatize for 24 hours, following which urine was collected from individual mice over a period of 24 hours.

4.3.3.2 Salt-sensitive hypertension

Salt-sensitive hypertension was induced in KidVD+ mice and KidVD- littermates by administering the nitric oxide synthase inhibitor, L-NAME for 2 weeks, followed by a washout period for 2 weeks, and a 4% high salt diet for 4 weeks. A week after the high salt diet was initiated, mice were administered 0.2 mg/mL doxycycline in their drinking water for 3 weeks. Weekly SBP was determined by tail-cuff. At the end of the 8-week protocol, mice were acclimatized for 24 hours in metabolic cages, and urine was collected from individual mice over 24 hours.

4.3.4 Blood pressure determination

Systolic blood pressure was measured by the non-invasive tail-cuff method using the IITC Life Science acquisition system. Mice were acclimatized in a designated quiet area for 30 minutes prior to SBP measurement. Mice were placed in pre-warmed restrainers (34°C) and allowed to acclimatize for 5 minutes before recordings began. SBP readings were determined from traces by 2 independent, blinded investigators.

4.3.5 Flow Cytometry

Kidneys were harvested, decapsulated and thoroughly minced. The minced tissue was placed in digestion buffer containing enzymes Collagenase D (Roche Sigma, St. Louis, MO) and Dispase II (Sigma) at 37°C for 1 hour. Following digestion, the tissue was then filtered through 100 μm and 40 μm strainers to obtain single cell suspensions. Red blood cells were lysed in NH_4Cl/EDTA. Splenocytes were similarly isolated and used as antibody controls. The single cell suspension was incubated with anti-mouse CD16/CD32 to block non-specific Fc binding, and then incubated with fluorescent-conjugated antibodies against CD45, F4/80, CD11c, and CD3e for 10 minutes on ice. Data was acquired on a BD LSR Fortessa X-20 flow cytometer using FACS DIVA software (BD Biosciences) and analyzed using Flow Jo v7.6.2 (FlowJo, LLC, Ashland, OR). CD3e+, CD3e-, F4/80+, and CD11c+ populations were quantified within the CD45+ gate. Results are expressed as a percentage of CD45+ cells per kidney.

4.3.6 Urine and serum analysis

Serum and 24-hour urine samples were analyzed for creatinine by capillary electrophoresis and for Na^+ concentration using a Beckman AU400 Autoanalyzer at the University of Texas-Southwestern George M. O'Brien Kidney Research Core Center. GFR was calculated using the creatinine clearance method. Urinary albumin concentrations were determined by ELISA using the Albuwell M kit (Ethos Biosciences, Philadelphia, PA). Atrial natriuretic peptide (ANP) levels were

measured in the plasma using the Atrial Natriuretic Peptide EIA Kit (Sigma) following the manufacturer's protocol. The characteristics of KidVD- and KidVD+ mice during angiotensin II-dependent and salt-sensitive hypertension are listed in Table 4.1.

Table 4.1 Characteristics of KidVD- and KidVD+ mice during angiotensin II-dependent and salt-sensitive hypertension:

	Angiotensin II-dependent hypertension		Salt-sensitive hypertension	
	KidVD-	KidVD+	KidVD-	KidVD+
Body weight (BW) (g)	38.4 ± 1.8	36.5 ± 1.5	30.9 ± 0.9	32.1 ± 1.8
Kidney weight / BW	0.57 ± 0.04	0.46 ± 0.02	0.55 ± 0.02	0.61 ± 0.01
Urine Creatinine (mg/dL)	38.5 ± 5.4	31.7 ± 5.6	13.2 ± 3.1	11.7 ± 2.9
Serum Creatinine (mg/dL)	0.12 ± 0.02	0.31 ± 0.03*	0.07 ± 0.003	0.1 ± 0.01*
Urine Na_+ (mmol/L)	132.8 ± 13.5	118.7 ± 16.3	471.9 ± 36.3	469.9 ± 25.8
Serum Na_+ (mmol/L)	161.7 ± 15.5	178.7 ± 10.3	153.4 ± 1.8	159.4 ± 5.9
Serum ANP (pg/mL)	223.02 ± 61.8	153.88 ± 14.89	112.5 ± 11.1	245.9 ± 84.6

Values are indicated as mean + SEM. Student's *t*-test was used for comparison of means. $P < 0.05$. * indicate significance against respective KidVD- .

4.3.7 Renal immunofluorescence analysis

Kidney sections were cut 5 µm sagittally and were de-paraffinized, rehydrated, and permeabilized with 0.1% Triton solution. The sections were blocked with 10% AquaBlock (EastCoastBio, North Berwick, ME) for 1 hour at room temperature and were then incubated with the following primary antibodies at 4°C overnight: goat polyclonal Podoplanin (R&D Systems, Minneapolis, MN), and rat monoclonal Endomucin (Santa Cruz Biotechnology, Dallas, TX). Alexa Flour 488 or 594 secondary antibodies (Life Technologies, Carlsbad, CA) were used for visualization. Antibodies used are listed in Table A2 in the Appendix. Slides were mounted with Prolong Gold antifade reagent with DAPI (Thermo Fisher Scientific, Waltham, MA) and imaged using an Olympus BX51 fluorescence microscope with Olympus Q5 camera. Images were captured at 20X magnification using the Olympus CellSens software (Olympus, Shinjuku, Tokyo, Japan).

4.3.8 Immunoprecipitation and protein immunoblot analysis

Mouse kidneys were homogenized in Cell Lysis buffer (Cell Signaling, Danvers, MA) and the supernatant was separated by centrifugation at 14000g for 10 minutes at 4°C. Protein concentrations were determined using the BCA assay (Thermo Fisher). To aid the visualization of phosphorylated NCC, 30 µg protein was first immunoprecipitated with antibodies against the total protein using Dynabeads Protein G (Thermo Fisher) according to manufacturer's protocol. Following this, the precipitated protein was resolved by gel electrophoresis and

probed for NCC followed by pThr/Ser/Tyr. For detection of ENaCα, 30 µg of the total kidney homogenate was mixed with SDS sample buffer and boiled at 95°C for 5 minutes. The proteins were separated by electrophoresis using 4-20% NuPage gels (Thermo Fisher), and then transferred onto a nitrocellulose membrane (Biorad, Hercules, CA). Immunoblotting was performed by incubating the membrane at 4°C overnight with an antibody against ENaCα. Proteins were normalized to corresponding vinculin. Secondary antibodies used were anti-rabbit and anti-mouse IgGs conjugated to Alexa-Flour 680 or IR800Dye (LI-COR Biosciences, Lincoln, NE). The bands were detected using infrared visualization (Odyssey System, LI-COR Biosciences), and quantified by densitometry performed on the Odyssey software.

4.4 Results

4.4.1 Enhancing renal lymphatic density attenuates blood pressure during angiotensin II-dependent hypertension

We tested the effects of therapeutically augmenting renal lymphatic density on attenuating BP during angiotensin II-dependent hypertension. We first confirmed that KidVD+ mice had enhanced renal lymphatic density compared to KidVD- mice by immunofluorescent staining for podoplanin (Fig 4.1A). At the end of three weeks of doxycycline administration, KidVD+ mice had significantly attenuated SBP compared to KidVD- mice (Fig 4.1B). Flow cytometry analysis of the kidneys of these mice revealed no changes in CD11c+ dendritic cells, or F4/80+ macrophages, and additionally, there was a significant increase in CD3e+

T cells (Fig 4.1C). Urinary Na^+ excretion over 24 hours was not changed (Fig 4.1D), however, KidVD+ mice demonstrated a significant increase in fractional excretion of Na^+ (FENa) (Fig 4.1E). Angiotensin II infusion also caused glomerular hyperfiltration in KidVD- mice as demonstrated by creatinine clearance, which was significantly attenuated in KidVD+ mice (Fig 4.1F). Since we have identified that the therapeutic augmentation of renal lymphatic density during L-NAME hypertension induces natriuresis along with downregulation of renal Na+ transporters NCC and cleaved (cl-) ENaCα, we measured the gene and protein levels of these transporters in this study. However, mRNA (Fig 4.1G), and protein abundance or activity as measured by phosphorylation or cleavage (Fig 4.1H and 4.1I) of these renal Na^+ transporters was unchanged between the groups.

Figure 4.1: Selective renal lymphatic expansion in KidVD+ mice attenuates blood pressure during angiotensin II-induced hypertension: A) Immunofluorescent labeling of podoplanin (green) in the cortex of KidVD- and KidVD+ mice during angiotensin II-induced hypertension. “G” indicates glomeruli. Arrowheads identify sparse native renal lymphatics. Blue=DAPI. Scale bars = 50 µm. B) Weekly SBP (systolic blood pressure) in KidVD- and KidVD+ mice during angiotensin II-induced hypertension. C) Flow cytometry quantitation of renal immune cells in KidVD- and KidVD+ mice during angiotensin II-induced hypertension. Results are expressed as percentages of CD45+ cells. D) 24-hour urinary Na^+ excretion, E) Fractional excretion of Na^+ (FENa), and F) creatinine clearance in KidVD mice during angiotensin II-induced hypertension. G) mRNA expression of renal Na^+ transporters in KidVD mice. H) Protein immunoblot analysis, and I) relative abundance of renal Na^+ transporters and their phosphorylation during angiotensin II-induced hypertension. n=5 mice for each group, except western blots n=4. * indicates $P<0.05$ compared to KidVD-.

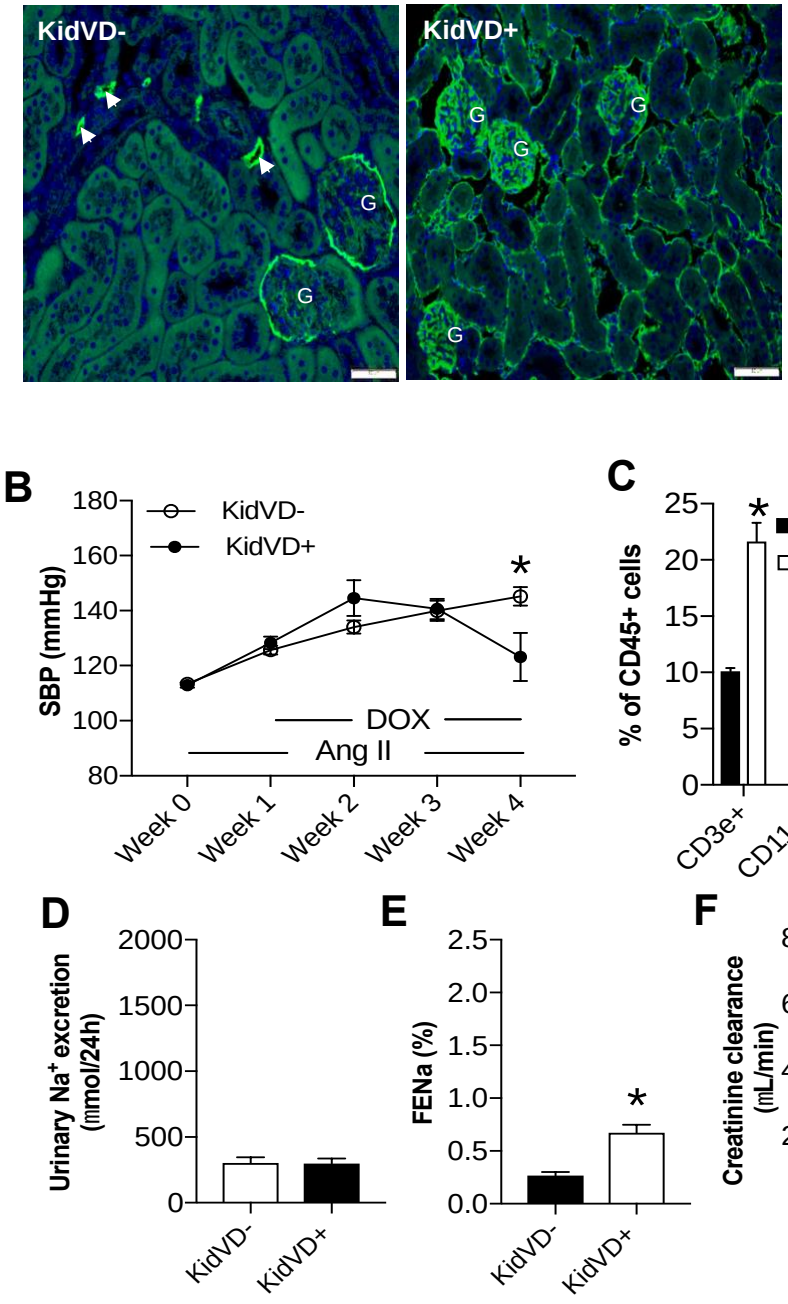
KidVD-
KidVD+
G
G
G
G
G
B
SBP (mmHg)
180
160
140
120
100
80
KidVD-
KidVD+
*
DOX
Ang II
Week 0
Week 1
Week 2
Week 3
Week 4
C
% of CD45+ cells
25
20
15
10
5
0
*
KidVD-
KidVD+
CD3e+
CD11c+
F4/80+
D
Urinary Na+ excretion (mmol/24h)
2000
1500
1000
500
0
KidVD-
KidVD+
E
FENa (%)
2.5
2.0
1.5
1.0
0.5
0.0
*
KidVD-
KidVD+
F
Creatinine clearance (mL/min)
800
600
400
200
0
*
KidVD-
KidVD+

Figure 4.1 Continued

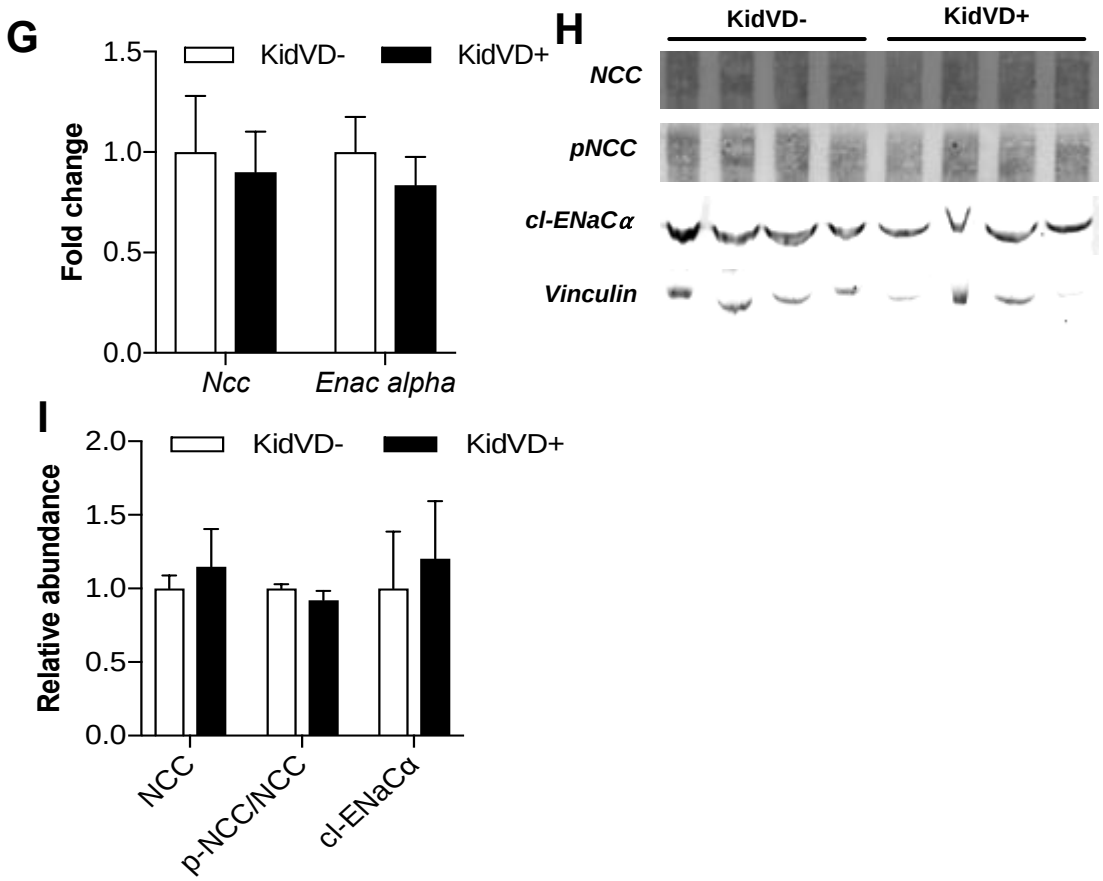

4.4.2 Therapeutic augmentation of renal lymphatic density attenuates blood pressure during salt-sensitive hypertension

We next investigated whether therapeutically augmenting renal lymphatic density attenuates salt-sensitive hypertension in mice. Immunofluorescent labeling for podoplanin revealed augmented renal lymphatic density in KidVD+ mice compared to KidVD- mice (Fig 4.2A). Following L-NAME administration for 2 weeks and a washout period for 2 weeks, KidVD- mice fed a 4% high salt diet were hypertensive (Fig 4.2B). However, KidVD+ mice had significantly attenuated BP following 3 weeks of VEGF-D induction. We analyzed renal immune cells by

flow cytometry and detected no changes in CD3e+ T cells, CD11c+ dendritic cells, or F4/80+ macrophages between the groups (Fig 4.2C). 24-hour urinary Na^+ excretion (Fig 4.2D), FENa (Fig 4.2E), and creatinine clearance (Fig 4.2F) were also not significantly altered between the groups. qPCR analysis did not detect changes in mRNA levels of NCC or ENaCα (Fig 4.2G). Similarly, protein abundance and activity of these transporters were unchanged between the groups (Fig 4.2H and 4.2I).

Figure 4.2: Selective renal lymphatic expansion in KidVD+ mice attenuates BP during salt-sensitive hypertension: A) Immunofluorescent labeling of podoplanin (green) in the cortex of KidVD- and KidVD+ mice during salt-sensitive hypertension. "G" indicates glomeruli. Arrowheads identify sparse native renal lymphatics. Blue=DAPI. Scale bars = 50 µm. B) Weekly SBP (systolic blood pressure) in KidVD- and KidVD+ mice during salt-sensitive hypertension. C) Flow cytometry quantitation of renal immune cells in KidVD- and KidVD+ mice during salt-sensitive hypertension. Results are expressed as percentages of CD45+ cells. D) 24-hour urinary Na^+ excretion, E) Fractional excretion of Na^+ (FENa), and F) creatinine clearance in KidVD mice during salt-sensitive hypertension. G) mRNA expression of renal Na^+ transporters in KidVD mice. H) Protein immunoblot analysis, and I) relative abundance of renal Na^+ transporters and their phosphorylation during salt-sensitive hypertension. n=5 mice for each group, except western blots n=4. * indicates $P<0.05$ compared to KidVD-.

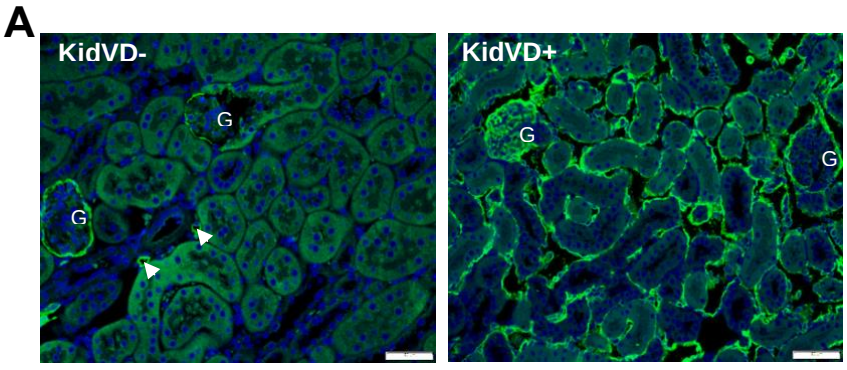

Figure 4.2 Continued

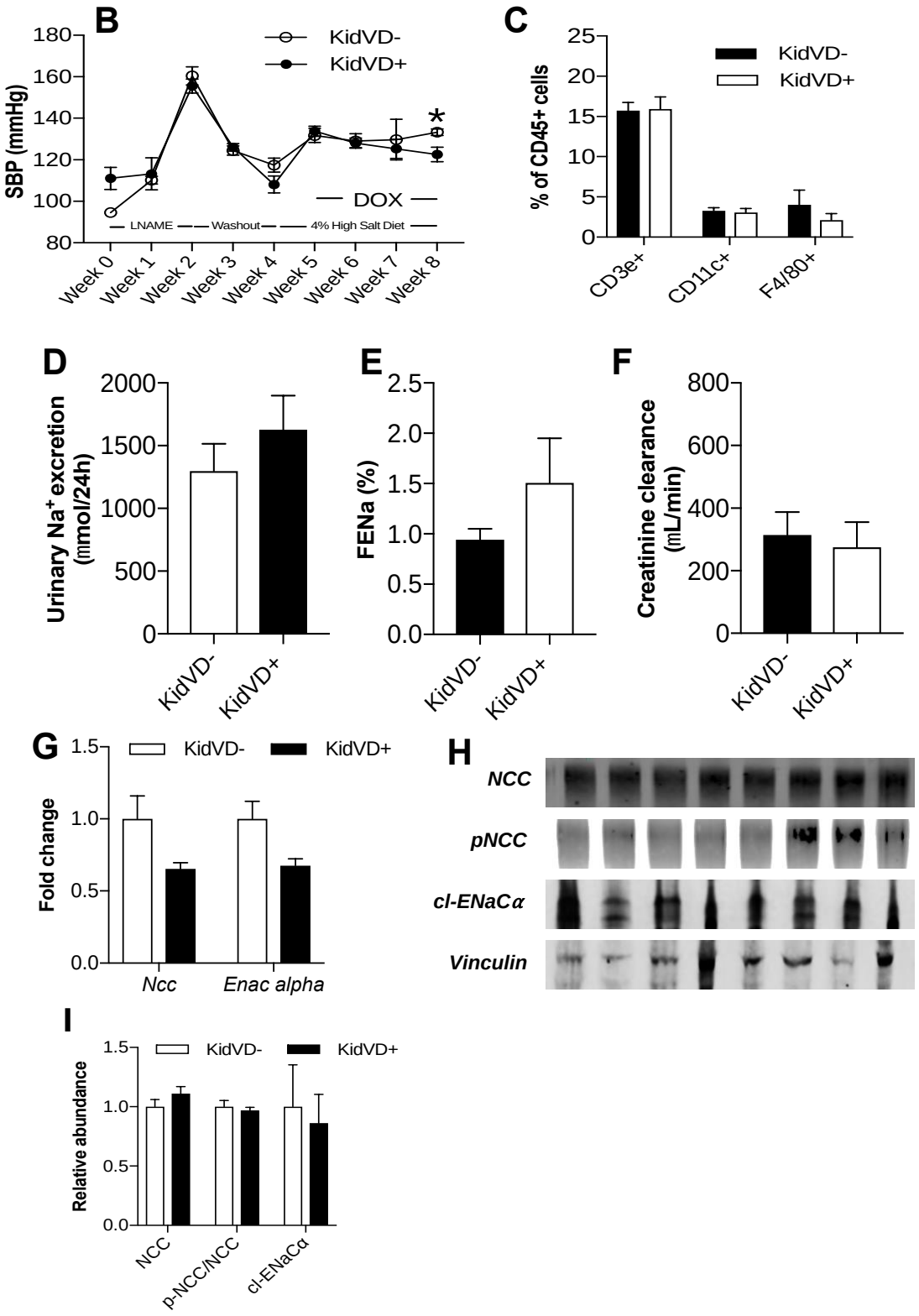

4.5 Discussion

The major results from the current study are: 1) selectively augmenting renal lymphatic vessel density attenuates BP in established angiotensin II-dependent hypertension, 2) selectively augmenting renal lymphatic vessel density attenuates BP in established salt-sensitive hypertension, 3) therapeutic augmentation of renal lymphatic vessels did not reduce renal immune cell accumulation in both models, but induced a significant increase in fractional Na^+ excretion during angiotensin II-dependent hypertension.

Renal immune cell infiltration and accumulation plays a major pathogenic role in the development of angiotensin II-dependent and salt-sensitive hypertension. Our lab has previously demonstrated that augmenting renal lymphatic density prior to the onset of angiotensin II-dependent and salt-sensitive hypertension reduces renal immune cell accumulation in both models prevents a rise in BP (Lopez Gelston et al., 2018). In this study, while the therapeutic augmentation of renal lymphatic density attenuated established hypertension, renal immune cell accumulation was not reduced in both models. These results are in accordance with our previous observations obtained during the therapeutic attenuation of L-NAME hypertension. These results suggest that the timing of induction of renal lymphangiogenesis affects the immune responses during an ongoing inflammatory reaction. In studies investigating tumor-associated lymphatic vessels, it has been shown that while lymphatic vessels are required for the recruitment of immune cells and initiation of adaptive immune response,

lymphatic endothelial cells themselves might release immunosuppressive factors that also act on immune cells (Christiansen et al., 2016; Stachura et al., 2016; Lane et al., 2018). Alterations to immune responses might be initiated with VEGF-D signaling even before the formation of lymphatic vessels, as VEGFR-3 is present on circulating and recruited immune cells and could be activated by VEGF-D (Skobe et al., 2001; Schoppmann et al., 2002). Moreover, while a reduction in T cell, dendritic cell, or macrophage numbers was not observed in this study, the specific polarization status of these immune cell subsets and their secreted cytokines were not analyzed. Several studies have demonstrated that certain subsets of immune cells, such as T regulatory cells, myeloid derived suppressor cells, and alternatively activated macrophages, play a protective role during hypertension (Barhoumi et al., 2011; Shah et al., 2015). The increase in CD3e+ T cells observed in KidVD+ mice during angiotensin II-hypertension suggests that the therapeutic augmentation of renal lymphatic vessels might confer protective effects during hypertension by inducing such beneficial polarization states of immune cells (Barhoumi et al., 2011). Moreover, this increase was not seen during salt-sensitive hypertension or L-NAME hypertension and hence it is likely that different hypertensive stimuli could participate in differentially affecting immune outcomes.

We demonstrated that during conditions of non-hypertensive chronic salt loading, augmenting renal lymphatic vessels increases renal interstitial fluid volume and plasma ANP levels, possibly due to increased lymph return. This

increased interstitial fluid volume might contribute to increased renal interstitial hydrostatic pressure, thus inducing natriuresis. However, in this study, plasma ANP levels were not increased during angiotensin II-dependent or salt-sensitive hypertension. It is possible that ANP levels were elevated at an earlier time point in KidVD+ mice, and that the ANP levels at the end of the measured time point during angiotensin II-dependent and salt-sensitive hypertension in this study reflect a time when compensatory mechanisms to lower blood pressure are in place. Impaired renal Na^+ excretion is a well-established contributing factor in both these forms of hypertension, and accordingly, increasing fractional Na^+ excretion has been shown to lower blood pressure in these models. We have identified that the therapeutic augmentation of renal lymphatic vessels induces natriuresis during L-NAME hypertension, thus establishing a role for renal lymphatic vessels in maintaining Na^+ homeostasis. In this study, we demonstrate that augmenting renal lymphatic density increases fractional Na^+ excretion during angiotensin II-dependent, but not salt-sensitive hypertension. While Na^+ retention is a common feature of experimental hypertension, the mechanisms by which Na^+ excretion is impaired might be different in varying forms of hypertension. The degree of diminution of renal blood flow and GFR, the extent of glomerular damage, renal perfusion pressure, renin-angiotensin-aldosterone system activation, activation of tubuloglomerular feedback, and activation of various renal Na^+ transporters all together contribute to Na^+ retention by the kidney (Yang et al., 2008; Nguyen et al., 2013b). Hence, the varying involvement of these mechanisms among the

different experimental models of hypertension might explain the differences in results obtained in our studies. Here, we observed that angiotensin II-hypertension induced glomerular hyperfiltration in KidVD- mice, which was significantly reduced in KidVD+ mice, suggesting that the fluid load handled by the kidneys would be different in these mice. Angiotensin II has been demonstrated to reduce renal interstitial hydrostatic pressure, and hence an increased volume of interstitial fluid might counteract the reduction in interstitial hydrostatic pressure and facilitate natriuresis (Haas et al., 1994; Yu and Khraibi, 2006). While NCC or cl-ENaC abundance that was previously reduced in L-NAME hypertension was not changed in this study, other renal Na^+ transporters known to play a role during exposure to angiotensin II or high salt load were not measured. Moreover, urinary fractional Na^+ excretion was not increased in KidVD+ mice during salt-sensitive hypertension, however, these mice demonstrated a significant reduction in BP, suggesting that renal lymphatic vessels might regulate BP through yet unidentified mechanisms.

Figure 4.3 Augmenting renal lymphatic density treats angiotensin II-induced and salt-sensitive hypertension: Hypertension induced by exposure to angiotensin II or high salt is associated with renal immune cell accumulation and sodium retention. Genetically augmenting renal lymphatic vessel density after hypertension is established attenuated hypertension. The reduction in blood pressure was not associated with a reduction in sodium retention. While renal immune cell accumulation was unchanged in this study, detailed investigations of various immune cell subtypes will offer insight into how augmenting renal lymphatic density alters the immune microenvironment. Dashed lines indicate hypothesized mechanisms that have not been proved.

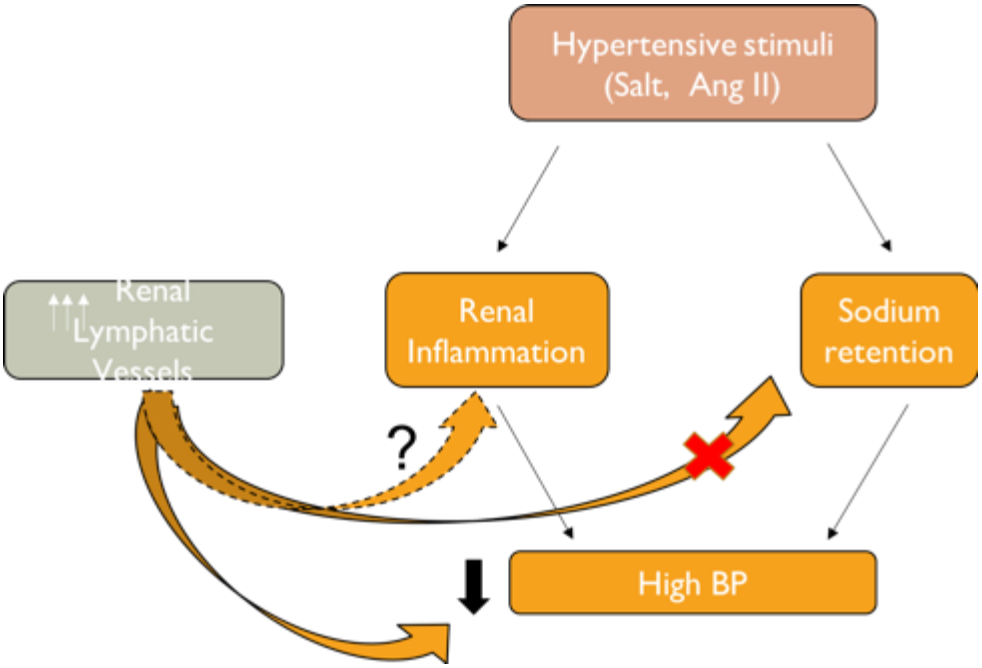

In conclusion, our study demonstrates that the therapeutic augmentation of renal lymphatic vessels attenuates blood pressure during angiotensin II-dependent and salt-sensitive hypertension (Fig 4.3). The reduction of BP is associated with an increase in urinary fractional Na^+ excretion during angiotensin II-dependent hypertension, thus establishing a role for renal lymphatic vessels in the maintenance of Na^+ homeostasis.

5. CONCLUSIONS

Despite tremendous advances in research, the death rate and the number of deaths attributable to hypertension have increased over the last 15 years. Chronic hypertension is the leading risk factor for myocardial infarction, heart failure, stroke, and kidney failure, and thus an improvement of medical therapies for hypertension is critical in order to prevent cardiovascular morbidity and mortality. The study of the key cardiovascular centers, including the vasculature, CNS, the kidney, and more recently the skin has yielded important insights into the mechanisms responsible for the pathogenesis of hypertension, and inappropriate activation of the immune system has emerged as a common pathogenic mechanism mediating several effects in these key regulatory centers.

Early observations of kidney biopsies and serum samples from patients with hypertension and transplantation studies done in experimental rats have established a link between renal inflammation and hypertension. High salt intake, sympathetic nervous stimulation, antigen stimulation have all been shown to activate the immune system. Once activated immune cells infiltrate the kidney, these cells are capable of producing several effector molecules including cytokines, free radicals and other potentially vasoactive substances that contribute to elevated BP and renal end-organ damage. Although not considered as a formal part of the immune system, the lymphatic vasculature has integral roles in immunity. Through their transport functions and immunomodulatory roles, lymphatic vessels play a major role in regulating local immunity, and

lymphangiogenesis is a hallmark of inflammatory diseases in the skin, airways, gut, and other organs. A role for lymphatic vessels in hypertension was elucidated by Titze and colleagues, demonstrating that salt-sensitive hypertension activates the immune system to coordinate lymphangiogenic responses in the skin interstitium, leading to an expansion of the dermal lymphatic vessels in an effort to store, and eventually clear excess electrolytes. With renal inflammation, fluid and electrolyte handling central to BP regulation and hence the development of hypertension, it is conceivable that the renal lymphatic vessels play a role in hypertension.

Our lab has previously demonstrated that renal inflammation that occurs with aging in spontaneously hypertensive rats is associated with an increase in renal lymphatic vessel density, and that the degree of lymphangiogenesis corresponded with the degree of renal inflammation. Following this observation, using experimental models of hypertension in mice, we demonstrated that renal immune cell accumulation and inflammation in salt-sensitive and L-NAME-induced hypertension are associated with a compensatory increase in renal lymphatic vessel density. We thus utilized a genetic mouse model of inducible, kidney-specific lymphangiogenesis and demonstrated that selectively augmenting renal lymphatic vessel density prevented the onset of salt-sensitive and L-NAME-induced hypertension. The prevention of hypertension was associated with a reduction in renal immune cell populations, thus corroborating the link between renal inflammation and hypertension.

Following these studies, the work presented within this dissertation tested three major hypotheses: 1) augmenting renal lymphatic density prevents the onset of angiotensin II-induced hypertension in male and female mice, 2) therapeutic augmentation of renal lymphatic density will lower BP in L-NAME-induced hypertension in association with a reduction in renal immune cell accumulation and increased urinary Na^+ excretion, and 3) therapeutic augmentation of renal lymphatic density will lower BP in angiotensin II-induced and salt-sensitive hypertension in association with a reduction in renal immune cell accumulation and increased urinary Na^+ excretion.

The current study demonstrates that renal inflammation in angiotensin II-induced hypertension is associated with a compensatory increase in renal lymphatic vessel density. Male and female mice with angiotensin II-induced hypertension had activated innate and adaptive immune cells; however, which cell types are involved in secreting lymphangiogenic growth factors, and the signals causing the proliferative response have not been determined. Moreover, whether the newly formed lymphatic vessels sprout from existing vessels or are formed *de novo* from progenitor cells and the functional consequences of these newly formed vessels are unknown. The pressor response, and mechanisms and degree of renal inflammation and immune cell infiltration have gender-specific differences in angiotensin II-induced hypertension. Regardless, both male and female mice demonstrated a lymphangiogenic response during hypertension and ongoing inflammation. It is possible that existing differences in renal lymphatic

density between male and female mice might affect their predisposition to developing hypertension and renal inflammation, and warrants further exploration. We demonstrated using *in vitro* studies that angiotensin II activates immune cells to secrete lymphangiogenic growth factors and other cytokines that have proliferative and pro-inflammatory effects on lymphatic endothelial cells. We demonstrated that lymphatic endothelial cells lack the receptors for angiotensin II, however, the cells used in this study were primary dermal-derived cells, which may not be entirely representative of lymphatic endothelial cells *in vivo*. Moreover, lymphatic vessels in different tissues have different properties. Immunofluorescence studies investigating the expression of angiotensin receptors in kidney sections or investigating the expression of these receptors in lymphatic endothelial cells isolated from the murine kidney might provide more insight into accurately interpreting the expression of these receptors in these cells. In addition, functional studies demonstrating proliferation and activation of these cells might corroborate gene expression analysis demonstrated in this study.

Genetically augmenting renal lymphatic vessel density reduces renal immune cell accumulation and prevents the onset of angiotensin II-induced hypertension in male and female mice. Thus, this study elucidates the role played by renal lymphatic vessels in regulating blood pressure and immune responses during angiotensin II-induced hypertension. The mechanistic details of how augmenting renal lymphatic density prevents hypertension remain to be elucidated. In addition to trafficking out immune cells from interstitium to draining

lymph nodes, lymphatic vessels are actively involved in altering the immune microenvironment during steady state and inflammatory conditions. While we demonstrated that augmenting renal lymphatic density reduced renal immune cell accumulation, whether this is through exfiltration or otherwise altering activation states of immune cells remains unknown. It is remarkable that prevention starts from week 1 of angiotensin II infusion, suggesting that immune protection mechanisms might be activated even before fully formed lymphatic vessels are in place. Lymphatic endothelial cells prime CD8+ T cells to become memory T cells that mount a rapid and robust response upon inflammatory challenge. Thus, it is possible that lymphatic endothelial cells recruited to the kidney while forming new vessels prime the kidney with memory T cell responses that prevent renal immune cell accumulation and the development of hypertension. Cytokines released during inflammation have been shown to promote sodium transport, impair glomerular function, and affect renal blood flow, all of which promote an increase in blood pressure. In this study, augmenting renal lymphatic density reduced renal inflammation, however, by reducing inflammation, which of these processes is altered to reduce blood pressure is unknown. This study has also not investigated how collecting lymphatics are affected by angiotensin II and other hypertensive stimuli such as high salt and nitric oxide inhibition, and how they could potentially affect blood pressure regulation. Unlike lymphatic endothelial cells, lymphatic muscle cells are likely to express receptors for angiotensin II, and could likely exhibit increased contractility in response to high angiotensin II levels. An

increased contractility might adversely affect lymph transport, however, how this affects blood pressure regulation during hypertension is unknown.

Altered renal Na^+ handling is a major pathogenic factor in hypertension. A key finding of our current study is that renal lymphatic vessels participate in Na^+ homeostasis during conditions of Na^+ retention. Following a chronic high salt-diet, we demonstrated that augmenting renal lymphatic vessels increases fractional Na^+ excretion and lowers blood pressure, however, renal accumulation of major immune cell populations was unchanged. The attenuation of BP was accompanied by an increase in renal interstitial fluid volume and plasma ANP levels and a decrease in renal Na^+ transporter abundance. More importantly, our study has demonstrated that the therapeutic augmentation of renal lymphatic vessels increases natriuresis and reduces BP during L-NAME-induced hypertension. Thus, our study outlines a role for renal lymphatic vessels in regulating Na^+ homeostasis during conditions of Na^+ overload. This study highlights a novel role for lymphatic vessels in BP regulation, however, the mechanistic details about how lymphatic vessels regulate Na^+ excretion remain undetermined. The expanded lymphatic network seems to act a reservoir for interstitial fluid, which could reduce reabsorption across the nephron, and promote sodium excretion. The increase in renal tissue fluid volume only after three weeks suggests that fully formed vessels are required for this response. Importantly, despite comparable extent of lymphatic expansion, the increase in renal tissue fluid or sodium excretion does not happen during basal conditions, suggesting

that increased flux across the nephron during sodium retaining conditions leads to interstitial fluid accumulation, which then reduces reabsorption. Renal immune cell accumulation was not reduced in this study, however, specific polarization states of innate and adaptive immune cells was not investigated in detail.

Finally, our current study also demonstrates that BP can be attenuated in established angiotensin II-induced and salt-sensitive hypertension by the selective induction of kidney-specific lymphangiogenesis. Unlike in the prevention studies, the reduction in BP during established hypertension was not associated with a reduction in major immune cell populations within the kidney, but rather BP was attenuated along with an increased urinary fractional Na^+ excretion in the L-NAME- and angiotensin II-induced hypertension models. The L-NAME model of hypertension has low circulating angiotensin II and intrarenal angiotensin II levels are lower than the other models. This might be a key difference, as apart from activating sodium transporters within the nephron, circulating angiotensin II can also induce aldosterone secretion, activate sympathetic outflow, all of which further augment sodium retention. The lack or the lesser effect of this phenomenon in the L-NAME model might be key to inducing natriuresis. Moreover, the hypertensive stimuli used in these models are all likely to have different effects on lymphatic vessels that are different, and how that plays into the different mechanisms of blood pressure regulation is unknown. These results have important implications in the management of hypertension, and highlight the potential of therapeutic augmentation of renal lymphatic density in BP regulation

during hypertension. Future studies aimed at investigating the detailed mechanisms by which augmenting renal lymphatic density alters Na^+ and fluid handling by the kidney, and investigating the differences in these mechanisms that might be at play in various experimental models of hypertension will yield important insights into renal lymphatic biology in the context of hypertension. Further studies are warranted to determine how the timing of induction of renal lymphatic expansion affects immune cell polarization, activation, and accumulation within the kidney in various models of hypertension, and how such events affect BP regulation and Na^+ retention. Thus, the work presented in this dissertation underscores an important role for renal lymphatic vessels in BP regulation.

REFERENCES

Abouelkheir, G.R., Upchurch, B.D., and Rutkowski, J.M. (2017). Lymphangiogenesis: fuel, smoke, or extinguisher of inflammation's fire? Exp. Biol. Med. *242*: 884–895.

Acedo, S.C., Gotardo, É.M.F., Lacerda, J.M., Oliveira, C.C. De, Oliveira Carvalho, P. De, and Gambero, A. (2011). Perinodal adipose tissue and mesenteric lymph node activation during reactivated TNBS-colitis in rats. Dig. Dis. Sci. *56*: 2545–52.

Aldrich, M.B., and Sevick-Muraca, E.M. (2013). Cytokines are systemic effectors of lymphatic function in acute inflammation. Cytokine *64*: 362–369.

Aoi, W., Niisato, N., Sawabe, Y., Miyazaki, H., Tokuda, S., Nishio, K., et al. (2007). Abnormal expression of ENaC and SGK1 mRNA induced by dietary sodium in Dahl salt-sensitively hypertensive rats. Cell Biol. Int. *31*: 1288–1291.

Aspelund, A., Robciuc, M.R., Karaman, S., Makinen, T., and Alitalo, K. (2016). Lymphatic system in cardiovascular medicine. Circ. Res. *118*: 515–530.

Aurora, A.B., Baluk, P., Zhang, D., Sidhu, S.S., Dolganov, G.M., Basbaum, C., et al. (2005). Immune complex-dependent remodeling of the airway vasculature in response to a chronic bacterial infection. J. Immunol. *175*: 6319–26.

Avraham, T., Daluvoy, S., Zampell, J., Yan, A., Haviv, Y.S., Rockson, S.G., et al. (2010). Blockade of transforming growth factor-β1 accelerates lymphatic regeneration during wound repair. Am. J. Pathol. *177*: 3202–14.

Baldwin, M.E., Catimel, B., Nice, E.C., Roufail, S., Hall, N.E., Stenvers, K.L., et

al. (2001). The specificity of receptor binding by vascular endothelial growth factor-D Is different in mouse and man. J. Biol. Chem. *276*: 19166–19171.

Baluk, P., Fuxe, J., Hashizume, H., Romano, T., Lashnits, E., Butz, S., et al. (2007). Functionally specialized junctions between endothelial cells of lymphatic vessels. J. Exp. Med. *204*: 2349–62.

Baluk, P., Tammela, T., Ator, E., Lyubynska, N., Achen, M.G., Hicklin, D.J., et al. (2005). Pathogenesis of persistent lymphatic vessel hyperplasia in chronic airway inflammation. J. Clin. Invest. *115*: 247–257.

Barbaro, N.R., Foss, J.D., Kryshtal, D.O., Tsyba, N., Kumaresan, S., Xiao, L., et al. (2017). Dendritic Cell Amiloride-Sensitive Channels Mediate Sodium-Induced Inflammation and Hypertension. Cell Rep. *21*: 1009–1020.

Barer, G.R., and Ward-McQuaid, J.N. (1957). Demonstration of renal lymphatics in vivo by intravenous injection of dye:the effect of lymphatic ligature on the blood-pressure. Br. J. Urol. *29*: 171–4.

Barhoumi, T., Kasal, D.A., Li, M.W., Shbat, L., Laurant, P., Neves, M.F., et al. (2011). T regulatory lymphocytes prevent angiotensin II-induced hypertension and vascular injury. Hypertension *57*: 469–476.

Beaini, S., Saliba, Y., Hajal, J., Smayra, V., Bakhos, J.J., Joubran, N., et al. (2019). VEGF-C attenuates renal damage in salt-sensitive hypertension. J. Cell. Physiol. *234*: 9616–9630.

Bech, J.N., Nielsen, E.H., Pedersen, R.S., Svendsen, K.B., and Pedersen, E.B. (2007). Enhanced sodium retention after acute nitric oxide blockade in mildly

sodium loaded patients with essential hypertension. Am. J. Hypertens. *20*: 287–295.

Bendich, A., Belisle, E.H., and Strausser, H.R. (1981). Immune system modulation and its effect on the blood pressure of the spontaneously hypertensive male and female rat. Biochem. Biophys. Res. Commun. *99*: 600–7.

Benigni, A., Cassis, P., and Remuzzi, G. (2010). Angiotensin II revisited: New roles in inflammation, immunology and aging. EMBO Mol. Med. *2*: 247–257.

Blum, K.S., Karaman, S., Proulx, S.T., Ochsenbein, A.M., Luciani, P., Leroux, J.C., et al. (2014). Chronic high-fat diet impairs collecting lymphatic vessel function in mice. PLoS One *9*: e94713.

Boynton, R.E., and Todd, R.L. (1947). Blood pressure readings of 75,258 university students. Arch. Intern. Med. *80*: 454–62.

Braam, B., Taler, S.J., Rahman, M., Fillaus, J.A., Greco, B.A., Forman, J.P., et al. (2017). Recognition and management of resistant hypertension. Clin. J. Am. Soc. Nephrol. *12*: 524–535.

Breslin, J.W., Yang, Y., Scallan, J.P., Sweat, R.S., Adderley, S.P., and Murfee, W.L. (2018). Lymphatic vessel network structure and physiology. Compr. Physiol. *9*: 207–299.

Card, C.M., Yu, S.S., and Swartz, M.A. (2014). Emerging roles of lymphatic endothelium in regulating adaptive immunity. J. Clin. Invest. *124*: 943–952.

Carey, R.M. (2015). The intrarenal renin-angiotensin system in hypertension. Adv. Chronic Kidney Dis. *22*: 204–210.

Case, D.B., Wallace, J.M., Keim, H.J., Weber, M.A., Sealey, J.E., and Laragh, J.H. (1977). Possible Role of Renin in Hypertension as Suggested by Renin-Sodium Profiling and Inhibition of Converting Enzyme. N. Engl. J. Med. *296*: 641–6.

Cervenka, L., Mitchell, K.D., and Navar, L.G. (1999). Renal function in mice: effects of volume expansion and angiotensin II. J. Am. Soc. Nephrol. *10*: 2631–2636.

Chabrashvili, T., Tojo, A., Onozato, M.L., Kitiyakara, C., Quinn, M.T., Fujita, T., et al. (2002). Expression and cellular localization of classic NADPH oxidase subunits in the spontaneously hypertensive rat kidney. Hypertension *39*: 269–74.

Chakraborty, A., Barajas, S., Lammoglia, G.M., Reyna, A.J., Morley, T.S., Johnson, J.A., et al. (2019). Vascular endothelial growth factor–D (VEGF-D) overexpression and lymphatic expansion in murine adipose tissue improves metabolism in obesity. Am. J. Pathol. *189*: 924–939.

Chakraborty, S., Davis, M.J., and Muthuchamy, M. (2015a). Emerging trends in the pathophysiology of lymphatic contractile function. Semin Cell Dev Biol 55–66.

Chakraborty, S., Nepiyushchikh, Z., Davis, M.J., Zawieja, D.C., and Muthuchamy, M. (2011). Substance P Activates Both Contractile and Inflammatory Pathways in Lymphatics Through the Neurokinin Receptors NK1R and NK3R. Microcirculation *18*: 24–35.

Chakraborty, S., Zawieja, S.D., Wang, W., Lee, Y., Wang, Y.J., Weid, P.Y. Von Der, et al. (2015b). Lipopolysaccharide modulates neutrophil recruitment and macrophage polarization on lymphatic vessels and impairs lymphatic function in rat mesentery. Am. J. Physiol. - Hear. Circ. Physiol. *309*: H2042-57.

Chan, C.T., Sobey, C.G., Lieu, M., Ferens, D., Kett, M.M., Diep, H., et al. (2015). Obligatory role for B cells in the development of angiotensin II-dependent hypertension. Hypertension *66*: 1023–33.

Choi, I., Lee, Y.S., Chung, H.K., Choi, D., Ecoiffier, T., Lee, H.N., et al. (2013). Interleukin-8 reduces post-surgical lymphedema formation by promoting lymphatic vessel regeneration. Angiogenesis *16*: 29–44.

Christiansen, A.J., Dieterich, L.C., Ohs, I., Bachmann, S.B., Bianchi, R., Proulx, S.T., et al. (2016). Lymphatic endothelial cells attenuate inflammation via suppression of dendritic cell maturation. Oncotarget *7*: 39421–39435.

Chyou, S., Ekland, E.H., Carpenter, A.C., Tzeng, T.-C.J., Tian, S., Michaud, M., et al. (2008). Fibroblast-Type Reticular Stromal Cells Regulate the Lymph Node Vasculature. J. Immunol. *181*: 3887–96.

Ciuceis, C. De, Amiri, F., Brassard, P., Endemann, D.H., Touyz, R.M., and Schiffrin, E.L. (2005). Reduced vascular remodeling, endothelial dysfunction, and oxidative stress in resistance arteries of angiotensin II-infused macrophage colony-stimulating factor-deficient mice: Evidence for a role in inflammation in angiotensin-induced vascular injury. Arterioscler. Thromb. Vasc. Biol. *25*: 2106–2113.

Cohen, J.N., Guidi, C.J., Tewalt, E.F., Qiao, H., Rouhani, S.J., Ruddell, A., et al. (2010). Lymph node-resident lymphatic endothelial cells mediate peripheral tolerance via Aire-independent direct antigen presentation. J. Exp. Med. *207*: 681–8.

Crowley, S.D., and Coffman, T.M. (2014). The inextricable role of the kidney in hypertension. J. Clin. Invest. *124*: 2341–2347.

Crowley, S.D., Gurley, S.B., Oliverio, M.I., Pazmino, A.K., Griffiths, R., Flannery, P.J., et al. (2005). Distinct roles for the kidney and systemic tissues in blood pressure regulation by the renin-angiotensin system. J. Clin. Invest. *115*: 1092–1099.

Davis, M.J., Davis, A.M., Ku, C.W., and Gashev, A.A. (2009). Myogenic constriction and dilation of isolated lymphatic vessels. Am. J. Physiol. - Hear. Circ. Physiol. *296*: H293-302.

Davis, M.J., Lane, M.M., Davis, A.M., Durtschi, D., Zawieja, D.C., Muthuchamy, M., et al. (2008). Modulation of lymphatic muscle contractility by the neuropeptide substance P. Am. J. Physiol. - Hear. Circ. Physiol. *295*: H587-97.

Drazner, M.H. (2011). The progression of hypertensive heart disease. Circulation *123*: 327–34.

Dubrot, J., Duraes, F. V., Potin, L., Capotosti, F., Brighouse, D., Suter, T., et al. (2014). Lymph node stromal cells acquire peptide–MHCII complexes from dendritic cells and induce antigen-specific CD4 + T cell tolerance. J. Exp. Med. *211*: 1153–1166.

Dzielak, D.J. (1991). Immune mechanisms in experimental and essential hypertension. Am. J. Physiol. - Regul. Integr. Comp. Physiol. *260*: R459-67.

Ebrahimian, T., Li, M.W., Lemarié, C.A., Simeone, S., Pagano, P.J., Gaestel, M., et al. (2011). Mitogen-activated protein kinase-activated protein kinase 2 in angiotensin II-induced inflammation and hypertension: Regulation of oxidative stress. Hypertension *57*: 245–54.

Edwards, L.A., Nowocin, A.K., Jafari, N. V., Meader, L.L., Brown, K., Sarde, A., et al. (2018). Chronic Rejection of Cardiac Allografts Is Associated with Increased Lymphatic Flow and Cellular Trafficking. Circulation *137*: 488–503.

Endre, T., Mattiasson, I., Berglund, G., and Hulthén, U.L. (1994). Insulin and renal sodium retention in hypertension-prone men. Hypertension *23*: 313–319.

Evans, R.G., Majid, D.S.A., and Eppel, G.A. (2005). Mechanisms mediating pressure natriuresis: what we know and what we need to find out. Clin. Exp. Pharmacol. Physiol. *32*: 400–409.

Feng, W., Dell'Italia, L.J., and Sanders, P.W. (2017). Novel Paradigms of Salt and Hypertension. J. Am. Soc. Nephrol. *28*: 1362–1369.

Flister, M.J., Wilber, A., Hall, K.L., Iwata, C., Miyazono, K., Nisato, R.E., et al. (2010). Inflammation induces lymphangiogenesis through up-regulation of VEGFR-3 mediated by NF-κB and Prox1. Blood *115*: 418–429.

Forrester, S.J., Booz, G.W., Sigmund, C.D., Coffman, T.M., Kawai, T., Rizzo, V., et al. (2018). Angiotensin II Signal Transduction: An Update on Mechanisms of Physiology and Pathophysiology. Physiol. Rev. *98*: 1627–1738.

Förster, R., Davalos-Misslitz, A.C., and Rot, A. (2008). CCR7 and its ligands: Balancing immunity and tolerance. Nat. Rev. Immunol. *8*: 362–71.

Foss, J.D., Kirabo, A., and Harrison, D.G. (2017). Do high-salt microenvironments drive hypertensive inflammation? Am. J. Physiol. - Regul. Integr. Comp. Physiol. *312*: R1–R4.

Garcia, A.G., Wilson, R.M., Heo, J., Murthy, N.R., Baid, S., Ouchi, N., et al. (2012). Interferon-γ ablation exacerbates myocardial hypertrophy in diastolic heart failure. Am. J. Physiol. - Hear. Circ. Physiol. *303*: H587-96.

Gąsecki, D., Kwarciany, M., Nyka, W., and Narkiewicz, K. (2013). Hypertension, brain damage and cognitive decline. Curr. Hypertens. Rep. *15*: 547–58.

Gashev, A.A., Davis, M.J., and Zawieja, D.C. (2002). Inhibition of the active lymph pump by flow in rat mesenteric lymphatics and thoracic duct. J. Physiol. *540*: 1023–1037.

Gasheva, O.Y., Gashev, A.A., and Zawieja, D.C. (2013). Cyclic guanosine monophosphate and the dependent protein kinase regulate lymphatic contractility in rat thoracic duct. J. Physiol. *591*: 4549–65.

Gashiev, A.A., Davis, M.J., Delp, M.D., and Zawieja, D.C. (2004). Regional variations of contractile activity in isolated rat lymphatics. Microcirculation *11*: 477–92.

Giani, J.F., Bernstein, K.E., Janjulia, T., Han, J., Toblli, J.E., Shen, X.Z., et al. (2015a). Salt sensitivity in response to renal injury requires renal angiotensin-converting enzyme. Hypertension *66*: 534–542.

Giani, J.F., Bernstein, K.E., Janjulia, T., Han, J., Toblli, J.E., Shen, X.Z., et al. (2015b). Salt sensitivity in response to renal injury requires renal angiotensin-converting enzyme. Hypertension *66*: 534–542.

Giani, J.F., Janjulia, T., Kamat, N., Seth, D.M., Blackwell, W.-L.B., Shah, K.H., et al. (2014a). Renal angiotensin-converting enzyme is essential for the hypertension induced by nitric oxide synthesis inhibition. J. Am. Soc. Nephrol. *25*: 2752–2763.

Giani, J.F., Janjulia, T., Taylor, B., Bernstein, E.A., Shah, K., Shen, X.Z., et al. (2014b). Renal Generation of Angiotensin II and the Pathogenesis of Hypertension. Curr. Hypertens. Rep. *16*: 1–5.

Gill, J.R., Gullner, H.G., Lake, C.R., Lakatua, D.J., and Lan, G. (1988). Plasma and urinary catecholamines in salt-sensitive idiopathic hypertension. Hypertension *11*: 312–9.

Gonzalez-Villalobos, R.A., Janjoulia, T., Fletcher, N.K., Giani, J.F., Nguyen, M.T.X., Riquier-Brison, A.D., et al. (2013). The absence of intrarenal ACE protects against hypertension. J. Clin. Invest. *123*: 2011–2023.

Gousopoulos, E., Proulx, S.T., Bachmann, S.B., Dieterich, L.C., Scholl, J., Karaman, S., et al. (2017). An Important Role of VEGF-C in Promoting Lymphedema Development. J. Invest. Dermatol. *137*: 1995–2004.

Granger, J.P., and Scott, J.W. (1988). Effects of renal artery pressure on interstitial pressure and Na excretion during renal vasodilation. Am J Physiol Renal Physiol *255*: F828-F833.

Gurley, S.B., Riquier-Brison, A.D.M., Schnermann, J., Sparks, M.A., Allen, A.M., Haase, V.H., et al. (2011). AT1A angiotensin receptors in the renal proximal tubule regulate blood pressure. Cell Metab. *13*: 469-475.

Guzik, T.J., Hoch, N.E., Brown, K.A., McCann, L.A., Rahman, A., Dikalov, S., et al. (2007). Role of the T cell in the genesis of angiotensin II–induced hypertension and vascular dysfunction. J. Exp. Med. *204*: 2449–2460.

Haas, J.A., Lockhart, J.C., Larson, T.S., Henrikson, T., and Knox, F.G. (1994). Natriuretic response to renal interstitial hydrostatic pressure during angiotensin II blockade. Am. J. Physiol. - Ren. Fluid Electrolyte Physiol. *266(1 Pt 2*: 117–9.

Hagendoorn, J., Padera, T.P., Kashiwagi, S., Isaka, N., Noda, F., Lin, M.I., et al. (2004). Endothelial nitric oxide synthase regulates microlymphatic flow via collecting lymphatics. Circ. Res. *95*: 204–209.

Hahn, A.W.A., Jonas, U., Bühler, F.R., and Resink, T.J. (1994). Activation of human peripheral monocytes by angiotensin II. FEBS Lett. *347*: 178–80.

Halin, C., Tobler, N.E., Vigl, B., Brown, L.F., and Detmar, M. (2007). VEGF-A produced by chronically inflamed tissue induces lymphangiogenesis in draining lymph nodes. Blood *110*: 3158–67.

Halin, C., Vigl, B., Aebischer, D., Nitschke, M., Iolyeva, M., Rothlin, T., et al. (2011). Tissue inflammation modulates gene expression of lymphatic endothelial cells and dendritic cell migration in a stimulus-dependent manner. Blood *118*: 205–215.

Hall, J.E. (2016). Renal Dysfunction, Rather Than Nonrenal Vascular

Dysfunction, Mediates Salt-Induced Hypertension. Circulation *133*: 894–906.

Hall, K.L., Volk-Draper, L.D., Flister, M.J., and Ran, S. (2012). New model of macrophage acquisition of the lymphatic endothelial phenotype. PLoS One *7*: e31794.

Haque, M.Z., and Ortiz, P.A. (2019). Superoxide increases surface NKCC2 in the rat thick ascending limbs via PKC. Am J Physiol Renal Physiol *317*: F99–F106.

Harwani, S.C. (2018). Macrophages under pressure: the role of macrophage polarization in hypertension. Transl. Res. *191*: 45–63.

Harwani, S.C., Chapleau, M.W., Legge, K.L., Ballas, Z.K., and Abboud, F.M. (2012). Neurohormonal modulation of the innate immune system is proinflammatory in the prehypertensive spontaneously hypertensive rat, a genetic model of essential hypertension. Circ. Res. *111*: 1190–7.

Hasegawa, S., Nakano, T., Torisu, K., Tsuchimoto, A., Eriguchi, M., Haruyama, N., et al. (2017). Vascular endothelial growth factor-C ameliorates renal interstitial fibrosis through lymphangiogenesis in mouse unilateral ureteral obstruction. Lab. Investig. *97*: 1439–1452.

Herrera, J., Ferrebuz, A., MacGregor, E.G., and Rodriguez-Iturbe, B. (2006). Mycophenolate mofetil treatment improves hypertension in patients with psoriasis and rheumatoid arthritis. J. Am. Soc. Nephrol. *17(12 Supp*: S218-25.

Hirosue, S., Vokali, E., Raghavan, V.R., Rincon-Restrepo, M., Lund, A.W., Corthésy-Henrioud, P., et al. (2014). Steady-State Antigen Scavenging, Cross-

Presentation, and CD8 + T Cell Priming: A New Role for Lymphatic Endothelial Cells . J. Immunol. *192*: 5002–5011.

Hoorn, E.J., Walsh, S.B., McCormick, J.A., Fürstenberg, A., Yang, C.L., Roeschel, T., et al. (2011). The calcineurin inhibitor tacrolimus activates the renal sodium chloride cotransporter to cause hypertension. Nat. Med. *17*: 1304–9.

Huggenberger, R., Siddiqui, S.S., Brander, D., Ullmann, S., Zimmermann, K., Antsiferova, M., et al. (2011). An important role of lymphatic vessel activation in limiting acute inflammation. Blood *117*: 4667–4678.

Huggenberger, R., Ullmann, S., Proulx, S.T., Pytowski, B., Alitalo, K., and Detmar, M. (2010). Stimulation of lymphangiogenesis via VEGFR-3 inhibits chronic skin inflammation. J. Exp. Med. *207*: 2255–2269.

Itani, H.A., Xiao, L., Saleh, M.A., Wu, J., Pilkinton, M.A., Dale, B.L., et al. (2016). CD70 exacerbates blood pressure elevation and renal damage in response to repeated hypertensive stimuli. Circ. Res. *118*: 1233–1243.

Jantsch, J., Schatz, V., Friedrich, D., Schröder, A., Kopp, C., Siegert, I., et al. (2015). Cutaneous Na+ storage strengthens the antimicrobial barrier function of the skin and boosts macrophage-driven host defense. Cell Metab. *21*: 493–501.

Ji, H., Zheng, W., Li, X., Liu, J., Wu, X., Zhang, M.A., et al. (2014). Sex-specific T-cell regulation of angiotensin II-dependent hypertension. Hypertension *64*: 573–582.

Johnson, L.A., Clasper, S., Holt, A.P., Lalor, P.F., Baban, D., and Jackson, D.G.

(2006). An inflammation-induced mechanism for leukocyte transmigration across lymphatic vessel endothelium. J. Exp. Med. *203*: 2763–2777.

Johnson, L.A., and Jackson, D.G. (2010). Inflammation-induced secretion of CCL21 in lymphatic endothelium is a key regulator of integrinmediated dendritic cell transmigration. Int. Immunol. *22*: 839–49.

Jover, B., and Mimran, A. (2001). Nitric oxide inhibition and renal alterations. J. Cardiovasc. Pharmacol. *38 Suppl 2*: S65-70.

Kajiya, K., and Detmar, M. (2006). An important role of lymphatic vessels in the control of UVB-induced edema formation and inflammation. J. Investig. Dermatology. *126*: 919–21.

Kamat, N. V., Thabet, S.R., Xiao, L., Saleh, M.A., Kirabo, A., Madhur, M.S., et al. (2015). Renal transporter activation during angiotensin-II hypertension is blunted in interferon-γ-/-and interleukin-17A-/-mice. Hypertension *65*: 569–576.

Kang, S., Lee, S.P., Kim, K.E., Kim, H.Z., Mémet, S., and Koh, G.Y. (2009). Toll-like receptor 4 in lymphatic endothelial cells contributes to LPS-induced lymphangiogenesis by chemotactic recruitment of macrophages. Blood *113*: 2605–13.

Karbach, S.H., Schönfelder, T., Brandão, I., Wilms, E., Hörmann, N., Jäckel, S., et al. (2016). Gut Microbiota Promote Angiotensin II-Induced Arterial Hypertension and Vascular Dysfunction. J. Am. Heart Assoc. *5*: e003698.

Karnik, S.S., Singh, K.D., Tirupula, K., and Unal, H. (2017). Significance of angiotensin 1–7 coupling with MAS1 receptor and other GPCRs to the renin-

angiotensin system: IUPHAR Review 22. Br. J. Pharmacol. *174*: 737–753.

Kassan, M., Wecker, A., Kadowitz, P., Trebak, M., and Matrougui, K. (2013). CD4+CD25+Foxp3 regulatory T cells and vascular dysfunction in hypertension. J. Hypertens. *31*: 1939–1943.

Kataru, R.P., Jung, K., Jang, C., Yang, H., Schwendener, R.A., Baik, J.E., et al. (2009). Critical role of CD11b ⊇ macrophages and VEGF in inflammatory acute inflammation model in skin lymphangiogenesis , antigen clearance , and inflammation resolution. Blood *113*: 5650–5660.

Kawasaki, T., Delea, C.S., Bartter, F.C., and Smith, H. (1978). The effect of high-sodium and low-sodium intakes on blood pressure and other related variables in human subjects with idiopathic hypertension. Am. J. Med. *64*: 193–198.

Kenig-Kozlovsky, Y., Scott, R.P., Onay, T., Carota, I.A., Thomson, B.R., Gil, H.J., et al. (2018). Ascending vasa recta are angiopoietin/tie2-dependent lymphatic-like vessels. J. Am. Soc. Nephrol. *29*: 1097–1107.

Kerjaschki, D., Huttary, N., Raab, I., Regele, H., Bojarski-Nagy, K., Bartel, G., et al. (2006). Lymphatic endothelial progenitor cells contribute to de novo lymphangiogenesis in human renal transplants. Nat. Med. *12*: 230–234.

Kerjaschki, D., Regele, H.M., Moosberger, I., Nagy-Bojarski, K., Watschinger, B., Soleiman, A., et al. (2004). Lymphatic Neoangiogenesis in Human Kidney Transplants Is Associated with Immunologically Active Lymphocytic Infiltrates. J. Am. Soc. Nephrol. *15*: 603–612.

Khraibi, A.A. (1991). Direct renal interstitial volume expansion causes exaggerated natriuresis in SHR. Am J Physiol Renal Physiol *261*: F567–570.

Kim, H., Kataru, R.P., and Koh, G.Y. (2014). Inflammation-associated lymphangiogenesis : a double-edged sword ? J. Clin. Invest. *124*: 1–8.

Kinashi, H., Ito, Y., Mizuno, M., Suzuki, Y., Terabayashi, T., Nagura, F., et al. (2013a). TGF- 1 Promotes Lymphangiogenesis during Peritoneal Fibrosis. J. Am. Soc. Nephrol. *24*: 1627–1642.

Kinashi, H., Ito, Y., Mizuno, M., Suzuki, Y., Terabayashi, T., Nagura, F., et al. (2013b). TGF-β1 promotes lymphangiogenesis during peritoneal fibrosis. J. Am. Soc. Nephrol. *24*: 1627–42.

Kirabo, A., Fontana, V., Faria, A.P.C. de, Loperena, R., Galindo, C.L., Jing, W., et al. (2014). DC isoketal-modified proteins activate T cells and promote hypertension. J. Clin. Invest. *124*: 4642–4656.

Kneedler, S.C., Phillips, L.E., Hudson, K.R., Beckman, K.M., Lopez Gelston, C.A., Rutkowski, J.M., et al. (2017). Renal inflammation and injury are associated with lymphangiogenesis in hypertension. Am J Physiol Renal Physiol *312*: F861–F869.

Kobori, H., Nishiyama, A., Abe, Y., and Navar, L.G. (2003). Enhancement of intrarenal angiotensinogen in Dahl salt-sensitive rats on high salt diet. Hypertension *41*: 592–7.

Kurtz, T.W., Griffin, K.A., Bidani, A.K., Davisson, R.L., and John, E. (2005). Recommendations for blood pressure measurement in part 2 : blood pressure

measurement in experimental animals. Hypertension *45*: 299–310.

Kvakan, H., Kleinewietfeld, M., Qadri, F., Park, J.K., Fischer, R., Schwarz, I., et al. (2009). Regulatory T cells ameliorate angiotensin II-induced cardiac damage. Circulation *119*: 2904–2912.

Lammoglia, G.M., Zandt, C.E. Van, Galvan, D.X., Orozco, J.L., Dellinger, M.T., and Rutkowski, J.M. (2016). Hyperplasia, de novo lymphangiogenesis, and lymphatic regression in mice with tissue-specific, inducible overexpression of murine VEGF-D. Am J Physiol Heart Circ Physiol *311*: 384–394.

Lane, R.S., Femel, J., Breazeale, A.P., Loo, C.P., Thibault, G., Kaempf, A., et al. (2018). IFNγ-activated dermal lymphatic vessels inhibit cytotoxic T cells in melanoma and inflamed skin. J. Exp. Med. *215*: 3057–3074.

Lee, A.S., Lee, J.E., Jung, Y.J., Kim, D.H., Kang, K.P., Lee, S., et al. (2012). Vascular endothelial growth factor-C and -D are involved in lymphangiogenesis in mouse unilateral ureteral obstruction. Kidney Int. *83*: 50–62.

Lee, D.L., Sturgis, L.C., Labazi, H., Osborne, J.B., Fleming, C., Pollock, J.S., et al. (2006). Angiotensin II hypertension is attenuated in interleukin-6 knockout mice. Am. J. Physiol. - Hear. Circ. Physiol. *290*: H935-40.

Lee, K.M., McKimmie, C.S., Gilchrist, D.S., Pallas, K.J., Nibbs, R.J., Garside, P., et al. (2011). D6 facilitates cellular migration and fluid flow to lymph nodes by suppressing lymphatic congestion. Blood *118*: 6220–9.

Levick, J.R., and Michel, C.C. (2010). Microvascular fluid exchange and the revised Starling principle. Cardiovasc. Res. *87*: 198–210.

Li, X.C., Hopfer, U., and Zhuo, J.L. (2012). Novel signaling mechanisms of intracellular angiotensin II-induced NHE3 expression and activation in mouse proximal tubule cells. Am. J. Physiol. - Ren. Physiol. *303*: F1617-28.

Li, X.C., Zhu, D., Zheng, X., Zhang, J., and Zhuo, J.L. (2018). Intratubular and intracellular renin-angiotensin system in the kidney: A unifying perspective in blood pressure control. Clin. Sci. *132*: 1383–1401.

Li, X.C., and Zhuo, J.L. (2008). Intracellular ANG II directly induces in vitro transcription of TGF-β1, MCP-1, and NHE-3 mRNAs in isolated rat renal cortical nuclei via activation of nuclear AT1a receptors. Am. J. Physiol. - Cell Physiol. *294*: C1034-45.

Liao, S., Cheng, G., Conner, D.A., Huang, Y., Kucherlapati, R.S., Munn, L.L., et al. (2011). Impaired lymphatic contraction associated with immunosuppression. Proc. Natl. Acad. Sci. U. S. A. *108*: 18784–9.

Lilienfeld, R.M., Friedenberg, R.M., and Herman, J.R. (1967). The effect of renal lymphatic ligation on kidney and blood pressure. Radiology *88*: 1105–1109.

Lim, H.Y., Thiam, C.H., Yeo, K.P., Bisoendial, R., Hii, C.S., McGrath, K.C.Y., et al. (2013). Lymphatic vessels are essential for the removal of cholesterol from peripheral tissues by SR-BI-Mediated transport of HDL. Cell Metab. *17*: 671–84.

Lopez Gelston, C.A., Balasubbramanian, D., Abouelkheir, G.R., Lopez, A.H., Hudson, K.R., Johnson, E.R., et al. (2018). Enhancing renal lymphatic expansion prevents hypertension in mice. Circ. Res. *122*: 1094–1101.

Lopez Gelston, C.A., and Mitchell, B.M. (2017). Recent advances in immunity

and hypertension. Am. J. Hypertens. *30*: 643–652.

Lund, A.W., Wagner, M., Fankhauser, M., Steinskog, E.S., Broggi, M.A., Spranger, S., et al. (2016). Lymphatic vessels regulate immune microenvironments in human and murine melanoma. J. Clin. Invest. *126*: 3386–3402.

Machnik, A., Neuhofer, W., Jantsch, J., Dahlmann, A., Tammela, T., Derer, W., et al. (2009). Macrophages regulate salt-dependent volume and blood pressure by a vascular endothelial growth factor-C–dependent buffering mechanism. Nat. Med. *15*: 545–553.

Maddaluno, L., Verbrugge, S.E., Martinoli, C., Matteoli, G., Chiavelli, A., Zeng, Y., et al. (2009). The adhesion molecule L1 regulates transendothelial migration and trafficking of dendritic cells. J. Exp. Med. *206*: 623–35.

Madhur, M.S., Lob, H.E., Mccann, L.A., Iwakura, Y., Blinder, Y., Guzik, T.J., et al. (2010). Interleukin 17 Promotes Angiotensin II – Induced Hypertension and Vascular Dysfunction. Hypertension *55*: 500–507.

Maisel, K., Sasso, M.S., Potin, L., and Swartz, M.A. (2017). Exploiting lymphatic vessels for immunomodulation: Rationale, opportunities, and challenges. Adv. Drug Deliv. Rev. *114*: 43–59.

Majid, D. (2002). Nitric oxide in the control of renal hemodynamics and excretory function. Am. J. Hypertens. *14*: S74–S82.

Mamenko, M., Zaika, O., Prieto, M.C., Behrana Jensen, V., Doris, P.A., Gabriel Navar, L., et al. (2013). Chronic angiotensin II infusion drives extensive

aldosterone-independent epithelial Na+ channel activation. Hypertension *62*: 1111-1122.

Maruyama, K., Ii, M., Cursiefen, C., Jackson, D.G., Keino, H., Tomita, M., et al. (2005). Inflammation-induced lymphangiogenesis in the cornea arises from CD11b-positive macrophages. J. Clin. Invest. *115*: 2363–72.

Marvar, P.J., Thabet, S.R., Guzik, T.J., Lob, H.E., McCann, L.A., Weyand, C., et al. (2010). Central and peripheral mechanisms of T-lymphocyte activation and vascular inflammation produced by angiotensin II-induced hypertension. Circ. Res. *107*: 263–270.

Mattson, D.L., James, L., Berdan, E.A., and Meister, C.J. (2006). Immune suppression attenuates hypertension and renal disease in the Dahl salt-sensitive rat. Hypertension *48*: 149–156.

Mattson, D.L., Lund, H., Guo, C., Rudemiller, N., Geurts, A.M., and Jacob, H. (2013). Genetic mutation of recombination activating gene 1 in Dahl salt-sensitive rats attenuates hypertension and renal damage. Am. J. Physiol. - Regul. Integr. Comp. Physiol. *304*: R407-14.

McDonough, A.A., and Nguyen, M.T.X. (2015). Maintaining Balance under Pressure: Integrated Regulation of Renal Transporters during Hypertension. Hypertension *66*: 450–455.

McKimmie, C.S., Singh, M.D., Hewit, K., Lopez-Franco, O., Brocq, M. Le, Rose-John, S., et al. (2013). An analysis of the function and expression of D6 on lymphatic endothelial cells. Blood *121*: 3768–77.

Medzhitov, R. (2010). Inflammation 2010: New Adventures of an Old Flame. Cell *140*: 771–6.

Miguel, C. De, Das, S., Lund, H., and Mattson, D.L. (2010). T lymphocytes mediate hypertension and kidney damage in Dahl salt-sensitive rats. Am. J. Physiol. - Regul. Integr. Comp. Physiol. *298*: R1136-42.

Miguel, C.D., Guo, C., Lund, H., Feng, D., and Mattson, D.L. (2011). Infiltrating T lymphocytes in the kidney increase oxidative stress and participate in the development of hypertension and renal disease. AJP Ren. Physiol. *300*: F734–F742.

Miteva, D.O., Rutkowski, J.M., Dixon, J.B., Kilarski, W., Shields, J.D., and Swartz, M.A. (2010). Transmural flow modulates cell and fluid transport functions of lymphatic endothelium. Circ. Res. *106*: 920–931.

Mizuno, R., Isshiki, M., Ono, N., Nishimoto, M., and Fujita, T. (2014). A high-salt diet differentially modulates mechanical activity of afferent and efferent collecting lymphatics in murine iliac lymph nodes. Lymphat. Res. Biol. *13*: 2–9.

Morfoisse, F., Tatin, F., Chaput, B., Therville, N., Vaysse, C., Métivier, R., et al. (2018). Lymphatic vasculature requires estrogen receptor-α signaling to protect from lymphedema. Arterioscler. Thromb. Vasc. Biol. *38*: 1346–1357.

Mozaffarian, D., Benjamin, E.J., Go, A.S., Arnett, D.K., Blaha, M.J., Cushman, M., et al. (2016). Executive summary: Heart disease and stroke statistics-2016 update: A Report from the American Heart Association. Circulation *133*: 447–54.

Mu, J., Worthmann, K., Saleem, M., Tossidou, I., Haller, H., and Schiffer, M.

(2009). The balance of autocrine VEGF-A and VEGF-C determines podocyte survival. Am J Physiol Renal Physiol *297*: F1656–F1667.

Mu, S.Y., Shimosawa, T., Ogura, S., Wang, H., Uetake, Y., Kawakami-Mori, F., et al. (2011). Epigenetic modulation of the renal β-adrenergic-WNK4 pathway in salt-sensitive hypertension. Nat. Med. *17*: 573–80.

Muthuchamy, M., Gashev, A., Boswell, N., Dawson, N., and Zawieja, D. (2003). Molecular and functional analyses of the contractile apparatus in lymphatic muscle. FASEB J. *17*: 920–922.

Nataraj, C., Oliverio, M.I., Mannon, R.B., Mannon, P.J., Audoly, L.P., Amuchastegui, C.S., et al. (1999). Angiotensin II regulates cellular immune responses through a calcineurin-dependent pathway. J. Clin. Invest. *104*: 1693–701.

Navar, L.G. (2014). Intrarenal renin-angiotensin system in regulation of glomerular function. Curr. Opin. Nephrol. Hypertens. *23*: 38–45.

Nguyen, H., Chiasson, V.L., Chatterjee, P., Kopriva, S.E., Young, K.J., and Mitchell, B.M. (2013a). Interleukin-17 causes Rho-kinase-mediated endothelial dysfunction and hypertension. Cardiovasc. Res. *97*: 696–704.

Nguyen, M.T.X., Lee, D.H., Delpire, E., and McDonough, A.A. (2013b). Differential regulation of Na+ transporters along nephron during ANG II-dependent hypertension: distal stimulation counteracted by proximal inhibition. AJP Ren. Physiol. *305*: F510–F519.

Nikpey, E., Karlsen, T. V., Rakova, N., Titze, J.M., Tenstad, O., and Wiig, H.

(2017). High-Salt Diet Causes Osmotic Gradients and Hyperosmolality in Skin Without Affecting Interstitial Fluid and Lymph. Hypertension *69*: 660–668.

Nishiyama, A., and Kobori, H. (2018). Independent regulation of renin–angiotensin–aldosterone system in the kidney. Clin. Exp. Nephrol. *22*: 1231–1239.

Nores, G.G., Cuzzone, D., Albano, N., Hespe, G., Kataru, R.P., Torrisi, J.S., et al. (2016). Obesity but not high-fat diet impairs lymphatic function. Int. J. Obes. *40*: 1582–1590.

Norlander, A.E., and Madhur, M.S. (2017). Inflammatory cytokines regulate renal sodium transporters: how, where, and why? Am. J. Physiol. - Ren. Physiol. *313*: F141–F144.

Norlander, A.E., Madhur, M.S., and Harrison, D.G. (2018). The immunology of hypertension. J. Exp. Med. *215*: 21–33.

Norlander, A.E., Saleh, M.A., Kamat, N. V., Ko, B., Gnecco, J., Zhu, L., et al. (2016). Interleukin-17a regulates renal sodium transporters and renal injury in angiotensin II-induced hypertension. Hypertension *68*: 167–174.

Oka, M., Iwata, C., Suzuki, H.I., Kiyono, K., Morishita, Y., Watabe, T., et al. (2008). Inhibition of endogenous TGF-beta signaling enhances lymphangiogenesis. Blood *111*: 4571–9.

Okuda, T., and Grollman, A. (1967). Passive transfer of autoimmune induced hypertension in the rat by lymph node cells. Tex. Rep. Biol. Med. *25*: 257–64.

Olsen, F. (1970). Type and course of the inflammatory cellular reaction in acute

angiotensin-hypertensive vascular disease in rats. Acta Pathol. Microbiol. Scand. Sect. A Pathol. *78*: 143–50.

Olsen, F. (1980). Transfer of arterial hypertension by splenic cells from DOCA-salt hypertensinve and renal hypertensive rats to normotensive recipients. Acta Pathol. Microbiol. Scand. Sect. C Immunol. *88*: 1–5.

Onions, K.L., Gamez, M., Buckner, N.R., Baker, S.L., Betteridge, K.B., Desideri, S., et al. (2019). VEGFC reduces glomerular albumin permeability and protects against alterations in VEGF receptor expression in diabetic nephropathy. Diabetes *68*: 172–187.

Palmer, L.G., and Schnermann, J. (2015). Integrated control of Na transport along the nephron. Clin. J. Am. Soc. Nephrol. *10*: 676–687.

Pedersen, M.S., Müller, M., Rülicke, T., Leitner, N., Kain, R., Regele, H., et al. (2020). Lymphangiogenesis in a mouse model of renal transplant rejection extends life span of the recipients. Kidney Int. *97*: 89–94.

Pegu, A., Qin, S., Fallert Junecko, B.A., Nisato, R.E., Pepper, M.S., and Reinhart, T.A. (2008). Human Lymphatic Endothelial Cells Express Multiple Functional TLRs. J. Immunol. *180*: 3399–405.

Pollow, D.P., Uhrlaub, J., Romero-Aleshire, M.J., Sandberg, K., Nikolich-Zugich, J., Brooks, H.L., et al. (2014). Sex differences in T-lymphocyte tissue infiltration and development of Angiotensin II Hypertension. Hypertension *64*: 384–390.

Quiroz, Y., Pons, H., Gordon, K.L., Rincón, J., Chávez, M., Parra, G., et al. (2001). Mycophenolate mofetil prevents salt-sensitive hypertension resulting

from nitric oxide synthesis inhibition. Am. J. Physiol. - Ren. Physiol. *281*: 38–47.

Ramirez, L.A., and Sullivan, J.C. (2018). Sex Differences in Hypertension: Where We Have Been and Where We Are Going. Am. J. Hypertens. *31*: 1247–1254.

Randolph, G.J., Ivanov, S., Zinselmeyer, B.H., and Scallan, J.P. (2017). The Lymphatic System: Integral Roles in Immunity. Annu. Rev. Immunol. *35*: 31–52.

Ribeiro, M.O., Antunes, E., Nucci, G. De, Lovisolo, S.M., and Zatz, R. (1992). Chronic inhibition of nitric oxide synthesis. A new model of arterial hypertension. Hypertension *20*: 298–303.

Riquier-Brison, A.D.M., Leong, P.K.K., Pihakaski-Maunsbach, K., and Mcdonough, A.A. (2010). Angiotensin II stimulates trafficking of NHE3, NaPi2, and associated proteins into the proximal tubule microvilli. Am J Physiol Renal Physiol *298*: F177–F186.

Rodriguez-Iturbe, B., Franco, M., and Johnson, R.J. (2013). Impaired pressure natriuresis is associated with interstitial inflammation in salt-sensitive hypertension. Curr. Opin. Nephrol. Hypertens. *22*: 37–44.

Rodriguez-Iturbe, B., Quiroz, Y., Nava, M., Bonet, L., Chavez, M., Herrera-Acosta, J., et al. (2002). Reduction of renal immune cell infiltration results in blood pressure control in genetically hypertensive rats. Am J Physiol Renal Physiol *282*: F191-201.

Rossier, B.C., Staub, O., and Hummler, E. (2013). Genetic dissection of sodium and potassium transport along the aldosterone-sensitive distal nephron:

importance in the control of blood pressure and hypertension. FEBS Lett. *587*: 1929–1941.

Russell, P.S., Hong, J., Windsor, J.A., Itkin, M., and Phillips, A.R.J. (2019). Renal Lymphatics: Anatomy, Physiology, and Clinical Implications. Front. Physiol. *10*: 1–18.

Sander, M., Hansen, P.G., and Victor, R.G. (1995). Sympathetically mediated hypertension caused by chronic inhibition of nitric oxide. Hypertension *26*: 691–5.

Satou, R., Penrose, H., and Navar, L.G. (2018). Inflammation as a Regulator of the Renin-Angiotensin System and Blood Pressure. Curr. Hypertens. Rep. *20*: 100.

Sawa, Y., Sugimoto, Y., Ueki, T., Ishikawa, H., and Sato, A. (2007). Effects of TNF- a on Leukocyte Adhesion Molecule Expressions in Cultured Human Lymphatic Endothelium The Journal of Histochemistry & Cytochemistry. *55*: 721–733.

Schlaich, M.P., Sobotka, P.A., Krum, H., Whitbourn, R., Walton, A., and Esler, M.D. (2009). Renal denervation as a therapeutic approach for hypertension: Novel implications for an old concept. Hypertension *54*: 1195–201.

Schoppmann, S.F., Birner, P., Stöckl, J., Kalt, R., Ullrich, R., Caucig, C., et al. (2002). Tumor-associated macrophages express lymphatic endothelial growth factors and are related to peritumoral lymphangiogenesis. Am. J. Pathol. *161*: 947–956.

Shah, K.H., Shi, P., Giani, J.F., Janjulia, T., Bernstein, E.A., Li, Y., et al. (2015). Myeloid Suppressor Cells Accumulate and Regulate Blood Pressure in Hypertension. Circ. Res. *117*: 858–869.

Shi, P., Diez-Freire, C., Jun, J.Y., Qi, Y., Katovich, M.J., Li, Q., et al. (2010). Brain microglial cytokines in neurogenic hypertension. Hypertension *56*: 297–303.

Shibata, S., Arroyo, J.P., Castañeda-Bueno, M., Puthumana, J., Zhang, J., Uchida, S., et al. (2014). Angiotensin II signaling via protein kinase C phosphorylates Kelch-like 3, preventing WNK4 degradation. Proc. Natl. Acad. Sci. U. S. A. *111*: 15556–61.

Skobe, M., Hamberg, L.M., Hawighorst, T., Schirner, M., Wolf, G.L., Alitalo, K., et al. (2001). Concurrent induction of lymphangiogenesis, angiogenesis, and macrophage recruitment by vascular endothelial growth factor-C in melanoma. Am. J. Pathol. *159*: 893–903.

Solak, Y., Afsar, B., Vaziri, N.D., Aslan, G., Yalcin, C.E., Covic, A., et al. (2016). Hypertension as an autoimmune and inflammatory disease. Hypertens. Res. *39*: 567–573.

Sparks, M.A., Crowley, S.D., Gurley, S.B., Mirotsou, M., and Coffman, T.M. (2014). Classical renin-angiotensin system in kidney physiology. Compr. Physiol. *4*: 1201–1228.

Sparks, M.A., Stegbauer, J., Chen, D., Gomez, J.A., Griffiths, R.C., Azad, H.A., et al. (2015). Vascular type 1A angiotensin II receptors control BP by regulating

renal blood flow and urinary sodium excretion. J. Am. Soc. Nephrol. *26*: 2953–2962.

Sprague, A.H., and Khalil, R.A. (2009). Inflammatory cytokines in vascular dysfunction and vascular disease. Biochem. Pharmacol. *78*: 539–52.

Stachura, J., Wachowska, M., Kilarski, W.W., Güç, E., Golab, J., and Muchowicz, A. (2016). The dual role of tumor lymphatic vessels in dissemination of metastases and immune response development. Oncoimmunology *5*: e1182278.

Suzuki, Y., Ito, Y., Mizuno, M., Kinashi, H., Sawai, A., Noda, Y., et al. (2012). Transforming growth factor-B induces vascular endothelial growth factor-C expression leading to lymphangiogenesis in rat unilateral ureteral obstruction. Kidney Int. *81*: 865–879.

Svendsen, U.G. (1976). The role of thymus for the development and prognosis of hypertension and hypertensive vascular disease in mice following renal infarction. Acta Pathol. Microbiol. Scand. Sect. A Pathol. *84*: 235–43.

Tamburini, B.A., Burchill, M.A., and Kedl, R.M. (2014). Antigen capture and archiving by lymphatic endothelial cells following vaccination or viral infection. Nat. Commun. *5*: 3989.

Tan, K.W., Chong, S.Z., and Angeli, V. (2014). Inflammatory lymphangiogenesis: Cellular mediators and functional implications. Angiogenesis *17*: 373–381.

Thomas, S.N., Rutkowski, J.M., Pasquier, M., Kuan, E.L., Alitalo, K., Randolph,

G.J., et al. (2012). Impaired Humoral Immunity and Tolerance in K14-VEGFR-3-Ig Mice That Lack Dermal Lymphatic Drainage. J. Immunol. *189*: 2181–2190.

Triacca, V., Güç, E., Kilarski, W.W., Pisano, M., and Swartz, M.A. (2017). Transcellular Pathways in Lymphatic Endothelial Cells Regulate Changes in Solute Transport by Fluid Stress. Circ. Res. *120*: 1440–1452.

Trott, D.W., and Harrison, D.G. (2014). The immune system in hypertension. Adv. Physiol. Educ. *38*: 20–24.

Trzewik, J., Mallipattu, S.K., Artmann, G.M., Delano, F.A., and Schmid-Schönbein, G.W. (2001). Evidence for a second valve system in lymphatics: endothelial microvalves. FASEB J. *15*: 1711–7.

Turbe, G. (2001). Mycophenolate mofetil prevents salt-sensitive hypertension resulting from angiotensin II exposure. *59*: 2222–2232.

Veiras, L.C., Girardi, A.C.C., Curry, J., Pei, L., Ralph, D.L., Tran, A., et al. (2017). Sexual dimorphic pattern of renal transporters and electrolyte homeostasis. J. Am. Soc. Nephrol. *28*: 3504–3517.

Vinh, A., Chen, W., Blinder, Y., Weiss, D., Taylor, W.R., Goronzy, J.J., et al. (2010). Inhibition and genetic ablation of the B7/CD28 T-cell costimulation axis prevents experimental hypertension. Circulation *122*: 2529–2537.

Vokali, E., Yu, S.S., Hirosue, S., Rinçon-Restrepo, M., Duraes, F. V., Scherer, S., et al. (2020). Lymphatic endothelial cells prime naïve CD8+ T cells into memory cells under steady-state conditions. Nat. Commun. *11*: 538.

Wang, L., Wang, X., Qu, H.Y., Jiang, S., Zhang, J., Fu, L., et al. (2017). Role of

kidneys in sex differences in angiotensin II-induced hypertension. Hypertension *70*: 1219–1227.

Weid, P.Y. Von Der (1998). ATP-sensitive K+ channels in smooth muscle cells of guinea-pig mesenteric lymphatics: Role in nitric oxide and β-adrenoceptor agonist-induced hyperpolarizations. Br. J. Pharmacol. *125*: 17-22.

Wenzel, P., Knorr, M., Kossmann, S., Stratmann, J., Hausding, M., Schuhmacher, S., et al. (2011). Lysozyme M-positive monocytes mediate angiotensin ii-induced arterial hypertension and vascular dysfunction. Circulation *124*: 1370–81.

Whelton, P.K., Robert Carey, C.M., Chair Wilbert Aronow, V.S., Ovbiagele, B., Donald Casey, F.E., Sidney Smith, F.C., et al. (2018). 2017 High Blood Pressure Clinical Practice Guideline.

White, F.N., and Grollman, A. (1964). Autoimmune factors associated with infarction of the kidney. Nephron *1964*: 93–102.

Wiig, H., Aukland, K., and Tenstad, O. (2003). Isolation of interstitial fluid from rat mammary tumors by a centrifugation method. Am J Physiol Heart Circ Physiol *284*: H416–H424.

Wiig, H., Luft, F.C., and Titze, J.M. (2018). The interstitium conducts extrarenal storage of sodium and represents a third compartment essential for extracellular volume and blood pressure homeostasis. Acta Physiol. *222*: 1–15.

Wiig, H., Schröder, A., Neuhofer, W., Jantsch, J., Kopp, C., Karlsen, T. V, et al. (2013). Immune cells control skin lymphatic electrolyte homeostasis and blood

pressure. J. Clin. Invest. *123*: 2803–15.

Wiig, H., and Swartz, M.A. (2012). Interstitial Fluid and Lymph Formation and Transport: Physiological Regulation and Roles in Inflammation and Cancer. Physiol. Rev. *92*: 1005–1060.

Wilcox, C.S., Sterzel, R.B., Dunckel, P.T., Mohrmann, M., and Perfetto, M. (1984). Renal interstitial pressure and sodium excretion during hilar lymphatic ligation. Am J Physiol Renal Physiol *247*: F344–F351.

Wirzenius, M., Tammela, T., Uutela, M., He, Y., Odorisio, T., Zambruno, G., et al. (2007). Distinct vascular endothelial growth factor signals for lymphatic vessel enlargement and sprouting. J. Exp. Med. *204*: 1431–1440.

Wu, J., Thabet, S.R., Kirabo, A., Trott, D.W., Saleh, M.A., Xiao, L., et al. (2014). Inflammation and mechanical stretch promote aortic stiffening in hypertension through activation of p38 mitogen-activated protein kinase. Circ. Res. *114*: 616–625.

Wuest, T.R., and Carr, D.J.J. (2010). VEGF-A expression by HSV-1-infected cells drives corneal lymphangiogenesis. J. Exp. Med. *207*: 101–15.

Yang, G.H., Zhou, X., Ji, W.J., Liu, J.X., Sun, J., Dong, Y., et al. (2017). VEGF-C-mediated cardiac lymphangiogenesis in high salt intake accelerated progression of left ventricular remodeling in spontaneously hypertensive rats. Clin. Exp. Hypertens. *39*: 740–747.

Yang, G.H., Zhou, X., Ji, W.J., Zeng, S., Dong, Y., Tian, L., et al. (2014). Overexpression of VEGF-C attenuates chronic high salt intake-induced left

ventricular maladaptive remodeling in spontaneously hypertensive rats. Am J Physiol Heart Circ Physiol *306*: H598–H609.

Yang, L.E., Sandberg, M.B., Can, A.D., Pihakaski-Maunsbach, K., and McDonough, A.A. (2008). Effects of dietary salt on renal Na+ transporter subcellular distribution, abundance, and phosphorylation status. AJP Ren. Physiol. *295*: F1003–F1016.

Yao, L.C., Testini, C., Tvorogov, D., Anisimov, A., Vargas, S.O., Baluk, P., et al. (2014). Pulmonary lymphangiectasia resulting from vascular endothelial growth factor-C overexpression during a critical period. Circ. Res. *114*: 806–22.

Yazdani, S., Navis, G., Hillebrands, J.L., Goor, H. van, and Born, J. van den (2014). Lymphangiogenesis in renal diseases: passive bystander or active participant? Expert Rev. Mol. Med. *16*: e15.

Yazdani, S., Poosti, F., Kramer, A.B., Mirković, K., Kwakernaak, A.J., Hovingh, M., et al. (2012). Proteinuria Triggers Renal Lymphangiogenesis Prior to the Development of Interstitial Fibrosis. PLoS One *7*: e50209.

Yi, B., Titze, J., Rykova, M., Feuerecker, M., Vassilieva, G., Nichiporuk, I., et al. (2015). Effects of dietary salt levels on monocytic cells and immune responses in healthy human subjects: A longitudinal study. Transl. Res. *166*: 103–10.

Yoon, S.S., Gu, Q., Nwankwo, T., Wright, J.D., Hong, Y., and Burt, V. (2015). Trends in blood pressure among adults with hypertension United States, 2003 to 2012. Hypertension *65*: 54–61.

Yu, T., and Khraibi, A.A. (2006). Renal interstitial hydrostatic pressure and

natriuretic response to high doses of angiotensin II in pregnant rats. Am. J. Hypertens. *19*: 300–5.

Zampell, J.C., Avraham, T., Yoder, N., Fort, N., Yan, A., Weitman, E.S., et al. (2012). Lymphatic function is regulated by a coordinated expression of lymphangiogenic and anti-lymphangiogenic cytokines. Am. J. Physiol. Physiol. *302*: C392–C404.

Zarjou, A., Black, L.M., Bolisetty, S., Traylor, A.M., Bowhay, S.A., Zhang, M.Z., et al. (2019). Dynamic signature of lymphangiogenesis during acute kidney injury and chronic kidney disease. Lab. Investig. *99*: 1376–1388.

Zawieja, D.C., and Ph, D. (2009). Contractile Physiology of Lymphatics. Lymphat. Res. Biol. *7*: 87–96.

Zawieja, S.D., Wang, W., Wu, X., Nepiyushchikh, Z. V., Zawieja, D.C., and Muthuchamy, M. (2012). Impairments in the intrinsic contractility of mesenteric collecting lymphatics in a rat model of metabolic syndrome. Am. J. Physiol. - Hear. Circ. Physiol. *302*: H643-53.

Zhang, J., Rudemiller, N.P., Patel, M.B., Karlovich, N.S., Wu, M., McDonough, A.A., et al. (2016). Interleukin-1 receptor activation potentiates salt reabsorption in angiotensin II-induced hypertension via the NKCC2 co-transporter in the nephron. Cell Metab. *23*: 360–368.

Zhang, T., Guan, G., Liu, G., Sun, J., Chen, B.I.N., Li, X., et al. (2008). Disturbance of lymph circulation develops renal fibrosis in rats with or without contralateral nephrectomy. Nephrology *13*: 128–138.

Zhang, W.C., Zheng, X.J., Du, L.J., Sun, J.Y., Shen, Z.X., Shi, C., et al. (2015). High salt primes a specific activation state of macrophages, M(Na). Cell Res. *25*: 893–910.

Zhao, T., Zhao, W., Meng, W., Liu, C., Chen, Y., Gerling, I.C., et al. (2015). VEGF-C/VEGFR-3 pathway promotes myocyte hypertrophy and survival in the infarcted myocardium. Am. J. Transl. Res. *7*: 697–709.

Zhuo, J.L., Li, X.C., Garvin, J.L., Navar, L.G., and Carretero, O.A. (2006). Intracellular ANG II induces cytosolic Ca2+ mobilization by stimulating intracellular AT1 receptors in proximal tubule cells. Am. J. Physiol. - Ren. Physiol. *290*: F1382-90.

Zimmerman, M.C., Lazartigues, E., Sharma, R. V., and Davisson, R.L. (2004). Hypertension caused by angiotensin II infusion involves increased superoxide production in the central nervous system. Circ. Res. *95*: 210–216.

APPENDIX

Table A1: *List of primer sequences used in this study*

Target	Forward (5' to 3')	Reverse (5' to 3')
Ccl21	CCCTGCTTCAACCATTACATCTGC	CCTGCTGTCTCCTTCCTCATTCC
Lyve-1	CTGACAAGCAGTTTCAGGCTTGGT	TTCAGCCCACACTCCGCTATACAT
Pdpn	ACCGTGCCAGTGTTGTTCTG	AGCACCTGTGGTTGTTATTTTGT
Ubc	GCCCAGTGTTACCACCAAGAAG	GCTCTTTTTAGATACTGTGGTGAG
Vegf-c	CAGTGTCAGGCAGCTAACAAG	GAA GGTCCACAGACATCATGGAA
Vegf-d	TGGCAAGACTTTTGAGCTTCAA	AAATCGCGCACTCTGAGGA
Vegfr3	ATCAGAAGATCGGGCGCTGTTGTA	TGTGTCATGTCCGCCCTTCAGTTA
Tnfa	GAGAAAGTCAACCTCCTCTCTG	GAAGACTCCTCCCAGGTATATG
Il1b	AGTTGACGGACCCCAAAAG	AGCTGGATGCTCTCATCAGG
Mcp1	ACTGAAGCCAGCTCTCTCTTCCTC	TTCCTTCTTGGGGTCAGCACAGAC
Il6	GAGGATACCACTCCCAACAGACC	AAGTGCATCATCGTTGTTCATA
Cxcl10	CCAAGTGCTGCCGTCATTTTC	GGCTCGCAGGGATGATTTCAA
Nos2	GTTCTCAGCCCAACAATACAAGA	GTGGACGGGTCGATGTCAC
Icam	GTGATGCTCAGGTATCCATCCA	CACAGTTCTCAAAGCACAGCG
Vcam	AGTTGGGGATTCGGTTGTTCT	CCCCTCATTCCTTACCACCC
Agtr1a	AACAGCTTGGTGGTGATCGTC	CATAGCGGTATAGACAGCCCA
Agtr2	AACTGGCACCAATGAGTCCG	CCAAAAGGAGTAAGTCAGCCAAG
Fn1	GCGACTCTGACTGGCCTTAC	CCGTGTAAGGGTCAAAGCAT
Lcn2	TGGCCCTGAGTGTCATGTG	CTCTTGTAGCTCATAGATGGTGC
Ncc/Slc12a3	GGAGTCATGGTGTCGTTCAC	ACCACCATCTCCTACCTTGC
Nkcc2/Slc12a1	GCTCCGGGAAATCAGGTAGT	TGGGTTGTCAACTTCTGCAA
Nhe3/Slc9a3	GCCCAGTGTTACCACCAAGAAG	GCTCTTTTTAGATACTGTGGTGAG
Enac alpha/ Scnn1a	ACTTCTCTGTGCCTTGTTTATATGTGTT	CAGACTTGGAGCTTTGACAAGGA
Enac beta/ Scnn1b	ACATGCTGAGGCAGGTCTCTCT	CAGACTGGGCCTATTGCTATCTAAA
Enac gamma/ Scnn1g	CGCTCAGCTTGAAGGATTCTG	CCGAGATCGAGACAGCAATGT
Rps18	CATGCAGAACCCACGACAGTA	CCTCACGCAGCTTGTTGTCTA

All sequences were verified through National Center for Biotechnology Information Primer-BLAST and single products were confirmed with a melting point dissociation step post-amplification.

Table A2: *List of antibodies used in this study*

Antigen	Source	RRID
CD16/CD32	BD Biosciences	AB_394656
CD45.1	BD Biosciences	AB_11152958
CD3e	BD Biosciences	AB_397063
CD11c	BD Biosciences	AB_1727422
F4/80	BD Biosciences	AB_2687527
Podoplanin	R&D Systems	AB_2268062
Endomucin (V.7C7)	Santa Cruz Biotechnology	AB_2100037
Thiazide-sensitive NaCl cotransporter (NCC)	Millipore	AB_571116
SLC12A1/NKCC2	Abcam	AB_2802126
Phosphoserine/threonine/tyrosine	Thermo Fisher	AB_2533941
alpha-ENaC	Thermo Fisher	AB_2184369
ENaCß	StressMarq Biosciences	AB_10644173
ENaCϒ	StressMarq Biosciences	AB_10640369
Na+/H+ Exchanger-3 isoform NHE3	Millipore	AB_94714
p-NHE-3	Santa Cruz	AB_831723
VEGFR-3	R&D Systems	AB_831723
Phosphotyrosine	Millipore	AB_831723
ß-actin	Cell Signaling Technology	AB_2242334